

REPORTS FOR MISSION SELECTION

THE FOUR CANDIDATE EARTH EXPLORER CORE MISSIONS

Gravity Field and Steady-State Ocean Circulation Mission
Land-Surface Processes and Interactions Mission
Earth Radiation Mission
Atmospheric Dynamics Mission



ESA SP-1233 (4)
July 1999

Reports for Mission Selection

THE FOUR CANDIDATE EARTH EXPLORER CORE MISSIONS

Atmospheric Dynamics Mission

***European Space Agency
Agence spatiale européenne***

ESA SP-1233 (4) – The Four Candidate Earth Explorer Core Missions –
ATMOSPHERIC DYNAMICS

Report prepared by:

Earth Sciences Division
Scientific Co-ordinator: Paul Ingmann

Earth Observation Preparatory Programme
Technical Co-ordinator: Joachim Fuchs

Cover:

Richard Francis & Carel Haakman

Published by:

ESA Publications Division
c/o ESTEC, Noordwijk, The Netherlands
Editor: Bruce Battrock

Copyright:

© 1999 European Space Agency
ISBN 92-9092-528-0

Price:

70 DFI

CONTENTS

1	INTRODUCTION	5
2	BACKGROUND AND SCIENTIFIC JUSTIFICATION	9
2.1	GLOBAL WIND PROFILE MEASUREMENTS FOR CLIMATE AND NWP	9
2.2	THE NEED FOR ATMOSPHERIC WIND FIELDS FOR ATMOSPHERIC ANALYSES	10
2.3	POTENTIAL IMPROVEMENT OF NWP BY ENHANCED WIND OBSERVATIONS	14
2.4	THE NEED FOR ATMOSPHERIC WIND FIELDS FOR CLIMATE STUDIES	22
2.5	FUTURE STUDIES AND PERSPECTIVES AIMING AT IMPROVING THE WIND FIELD KNOWLEDGE IN THE POST-2000 TIME FRAME.....	31
2.6	CONCLUSIONS ON NWP AND CLIMATE STUDIES	33
3	RESEARCH OBJECTIVES	35
3.1	MISSION OBJECTIVES	35
3.2	NUMERICAL WEATHER PREDICTION.....	36
3.3	CLIMATE	37
3.4	ADDITIONAL OBSERVATIONS.....	39
4	OBSERVATIONAL REQUIREMENTS	41
4.1	INTRODUCTION	41
4.2	METEOROLOGICAL ANALYSIS.....	42
4.3	COVERAGE REQUIREMENTS	46
4.4	QUALITY OF OBSERVATIONS.....	48
4.5	RELIABILITY AND DATA AVAILABILITY	52
4.6	CONCLUSION.....	53
5	MISSION ELEMENTS.....	57
5.1	INTRODUCTION	57
5.2	INSTRUMENTS AND DATA	57
5.3	ATMOSPHERIC ANALYSES AND NWP FORECASTS.....	61
6	SYSTEM CONCEPT	63
6.1	FROM MISSION TO SYSTEM REQUIREMENTS	63
6.2	MISSION DESIGN AND OPERATIONS.....	66
6.3	THE ALADIN INSTRUMENT	73
6.4	THE SATELLITE.....	95
6.5	THE LAUNCHER	113
6.6	THE GROUND SEGMENT	115
7	DATA PROCESSING AND VALIDATION	121
7.1	INTRODUCTION	121
7.2	SPECTRA AND DOPPLER FREQUENCIES.....	123
7.3	QUALITY CONTROL	124
7.4	IMPORTANCE OF CLOUDS	126
7.5	DISTRIBUTION AND ARCHIVING.....	127
7.6	GEOPHYSICAL PROCESSING CENTRE	127
7.7	CONCLUSIONS.....	128

8	MISSION PERFORMANCE	131
8.1	INTRODUCTION	131
8.2	PERFORMANCE IN CLEAR AIR	133
8.3	THE IMPACT OF CLOUDS	134
8.4	USEFULNESS FOR NWP	137
8.5	USEFULNESS FOR CLIMATE STUDIES	138
8.6	OTHER ELEMENTS PROVIDED BY THE ADM	140
8.7	CONCLUSIONS	141
9	PROGRAMMATICS	143
9.1	DEVELOPMENT APPROACH	143
9.2	HERITAGE, CRITICAL AREAS AND RISKS	145
9.3	RELATED MISSIONS, INTERNATIONAL CO-OPERATION POSSIBILITIES AND TIMELINESS	147
9.4	ENHANCEMENT OF CAPABILITIES AND APPLICATIONS POTENTIAL	148
	REFERENCES.....	149
	GLOSSARY.....	153
	ACKNOWLEDGEMENTS.....	157



‘Hurricane force winds raged across Britain on Christmas Eve and yesterday leaving five people dead, five French fishermen feared drowned in the Irish Sea, thousands of people without power and scores of roads blocked by fallen trees and masonry.

As the emergency services battled to cope, a fresh wave of storms with winds gusting up to 70 mph swept across London and much of southern England last night.’

(from ‘The Times’, 26 December 1997)

1 Introduction

The ‘ESA Living Planet Programme’ (ESA, 1998) describes the plans for the Agency's new strategy for Earth Observation in the post 2000 time frame. It marks a new era for European Earth Observation based on smaller more focused missions and a programme that is user driven, covering the whole spectrum of interests ranging from scientific research-driven Earth Explorer missions through to application-driven

Earth Watch missions. The user community is therefore now able to look forward to a programme of more frequent but very specific missions directed at the fundamental problems of Earth system sciences.

Out of the nine Earth Explorer core missions identified in ESA SP-1196 (1-9), four core missions were selected for Phase-A studies, which began in June 1998, namely: the Land-Surface Processes and Interactions Mission; the Earth Radiation Mission; the Gravity Field and Steady-State Ocean Circulation Mission; and the Atmospheric Dynamics Mission. The Phase-A studies were all completed in June 1999.

This 'Report for Mission Selection' for the Atmospheric Dynamics Core Mission (ADM) was prepared by a Core Mission Drafting Team consisting of four members of the ADM Advisory Group (ADMAG); E. Källén, J. Pailleux, A. Stoffelen and M. Vaughan. They were supported by the other members of the ADMAG, namely L. Isaksen, P. Flamant, and W. Wergen. The technical content of the report (notably Chapter 6) has been compiled by the Executive based on inputs provided by the industrial Phase-A contractor. Others who, in various ways, have contributed to the report are listed in the Acknowledgements.

The primary aim of the Earth Explorer Atmospheric Dynamics Mission is to provide improved analyses of the global three-dimensional wind field by demonstrating the capability to correct the major deficiency in wind-profiling of the current Global Observing System (GOS) and Global Climate Observing System (GCOS). The ADM will provide the wind-profile measurements to establish advancements in atmospheric modelling and analysis. There is an intimate link between progress in climate modelling and progress in numerical weather prediction (NWP) as our understanding of the atmosphere is largely based on the experience of operational weather centres. Long-term data bases are being created by NWP data assimilation systems to serve the climate research community. It is widely recognised therefore that the impact of a new global atmospheric observing system on our understanding of atmospheric dynamics should be evaluated primarily in the context of operational weather forecasting.

New insights into the atmosphere through the provision of wind profiles are expected for NWP, but also for climate research. The ADM is addressing one of the main areas discussed under Theme 2 of the 'ESA Living Planet Programme' (ESA, 1998). Although there are several ways of measuring wind from a satellite, only the active Doppler Wind Lidar (DWL) has the potential to provide the requisite data globally. It is the only candidate so far that can provide direct observations of wind profiles. In addition, a DWL will not only provide wind data, but also has the potential to provide ancillary information on cloud top heights, vertical distribution of cloud, aerosol properties, and wind variability as by-products.

This Report for Mission Selection for the ADM, together with those for the other three Earth Explorer Core Missions, is being circulated amongst the Earth Observation

research community in preparation for The Four Candidate Earth Explorer Core Missions Consultative Workshop in Granada (Spain) in October 1999.

Following this introduction, the report is divided into eight chapters:

- 1) Chapter 2 addresses the background and provides the scientific justification for the mission set in the context of issues of concern and the associated need to advance current scientific understanding. The chapter identifies the problem and gives the relevant background. It provides a review of the current status and the clear identification of the 'gaps' in knowledge. In so doing, it provides a clear identification of the potential 'delta' this mission would provide.
- 2) Drawing on these arguments, Chapter 3 discusses the importance of the scientific objectives. It identifies the need for such observations by comparing the data that will be provided by this mission with that available from existing and planned data sources, highlighting the unique contribution of the mission.
- 3) Chapter 4 focuses on mission requirements comparing 'current practice' with the novelty of the mission and derives, in the context of the scientific objectives, the mission specific observational requirements. It confirms that the ADM, with its well-balanced measurement capabilities, would be unique in obtaining a new and quantitative understanding of the Earth's wind field.
- 4) Chapter 5 provides an overview of the various mission elements such as space and ground segments and external sources laying the foundations for mission implementation.
- 5) Drawing on Chapter 5, Chapter 6 provides a complete summary description of the proposed technical concept (space and ground segments). The technical maturity of the concept is illustrated by the way it meets the observational requirements addressed in Chapter 4.
- 6) Chapter 7 outlines the envisaged data processing scheme. It includes a description of the algorithms proposed. The processing chain is described, clearly demonstrating the feasibility of transforming the raw data via calibration and validation into the requisite geophysical products.
- 7) Drawing on Chapters 5 to 7, a comparison of expected mission performance versus performance requirements (Chapter 4) is provided in Chapter 8. This draws on the main findings of the previous chapters, complemented by results of an end-to-end simulation tool, to demonstrate that the expected mission performance is indeed capable of meeting (a) the observational requirements (Chapter 4) and (b) the ADM scientific objectives as outlined in Chapter 2.
- 8) Programme implementation, including risks, development schedule and international collaboration, is discussed in Chapter 9. In particular, drawing on the previous chapters, Chapter 9 discusses the ADM in the context of other related missions. It is finally concluded that the proposed launch time in the 2004 time-frame would be very timely for the scientific community.

2 Background and Scientific Justification

2.1 Global Wind Profile Measurements for Climate and NWP

Reliable instantaneous analyses and longer term climatologies of winds are needed to improve our understanding of atmospheric dynamics and the global atmospheric transport and the cycling of energy, water, aerosols, chemicals and other airborne materials. However, improvement in analysing global climate, its variability, predictability and change requires measurements of winds throughout the atmosphere. In order to do so, it is a pre-requisite to improve NWP as progress in climate-related studies is intimately linked to progress in operational weather forecasting. The World Meteorological Organisation (WMO) states in their recent evaluation of user requirements and satellite capabilities that for global meteorological analyses measurement of wind profiles remains most challenging and most important (WMO, 1998).

After several decades of observations from space, direct measurements of the fully global, three-dimensional wind field remain elusive. Deficiencies, including coverage and frequency of observations, in the current observing system are impeding progress in both climate-related studies and operational weather forecasting. There is a clear requirement for a high-resolution observing system for atmospheric winds with full global coverage.

At present, our information on the three-dimensional wind field over the oceans, the tropics and the southern hemisphere is indirect. It is severely limited by having to rely on mainly space-borne observation of the mass field and geostrophic adjustment theory. Improvements in the available wind data are needed urgently if we are to exploit fully the potential of recent advances in climate prediction and NWP and continue to make significant progress in the field.

There is a synergy between advances in climate-related studies and those in NWP. Indeed, climate studies are increasingly using analyses of atmospheric (and other) fields from data assimilation systems designed originally to provide initial conditions for operational weather forecasting models. Understanding of the atmosphere and its evolution is based to a large extent on the analysed fields from continuous data assimilation carried out at operational weather centres, so that progress in climate analysis is closely linked to corresponding progress in NWP. In line with this, extended atmospheric reanalysis projects (ERA15, ERA40, NCEP) are being carried out to provide the climate and research community with consistent data sets. The analysis of the atmospheric flow is further of prime interest for studies on atmospheric composition and chemistry. In presenting the scientific justification for the requirement for better global measurements of atmospheric winds, given the importance of data assimilation, first their importance for NWP is considered, followed by a discussion of the corresponding requirement for climate studies and atmospheric research. Before concluding this chapter, the role of atmospheric

dynamics for atmospheric chemistry is discussed. The atmospheric requirements are put in perspective with other requirements of the Earth's system in ESA (1998) where the hierarchy of Earth system models is also described in general.

2.2 The Need for Atmospheric Wind Fields for Atmospheric Analyses

2.2.1 Background

Analyses of the atmospheric state are needed for a wide range of climate-related studies and for NWP. Such meteorological analyses provide a complete three-dimensional picture of the dynamical variables of an atmospheric model at a particular time.

In an operational data assimilation system, these analyses are produced continuously and in sequence. In NWP, medium-range forecasts, which predict the evolution of the global atmosphere typically from four to ten days ahead, are generally started twice a day, at 00 and 12 UTC. Often embedded in the global models are high-resolution, limited-area models for high-resolution analyses and for short-range predictions up to 2 to 3 days ahead, which are started from initial times usually only 6 or 3 hours apart. The most common prognostic model variables are: the horizontal wind components, temperature, humidity and surface pressure. In the future, more and more atmospheric models will require additional initial values, such as cloud water, cloud ice, cloud amount, turbulent kinetic energy and densities of various constituents, such as ozone and aerosol.

In order to obtain an appropriate description of the atmosphere, a composite operational observing system has been established under the auspices of the WMO. The World Weather Watch (WWW) of the WMO is a well-established system coordinating the operational provision of meteorological data. It consists of a number of different observing platforms which take observations either at pre-specified times (synoptic hours) or quasi-continuously. They can be grouped further into in-situ or remote-sensing measurements. They either provide information for one level only (surface or upper-air) or give profiles for a number of levels in the vertical.

2.2.2 Data Deficiencies

The different types of observations currently available and constituting the Global Observing System (GOS) are documented in full detail in ESA (1996). They can be classified in the following way:

- *Surface data* – they are the synoptic reports from land stations and ships, the (moored and drifting) buoys, and also the scatterometer winds from satellites

(such as ERS). They are all single level data, and cannot provide any information on atmospheric profiles.

- *Single-level upper-air data* – mainly aircraft reports and cloud motion winds derived from geostationary satellite imagery. More and more aircraft observations (wind and temperature) are being made during ascent and descent phases, thus tending to become ‘multi-level’. Their main deficiency is the poor data coverage: observations are provided only along the air routes and they never provide any profile-type information over the oceans. Satellite cloud (or water vapour) winds are derived from the motion of some targets like clouds, assuming that this target is advected by the atmospheric flow; an intrinsic assumption which is not always true. Compared with other single-level data, they have another deficiency: the significant uncertainty in knowledge of the level. Finally they are available only in a latitude belt around the equator: 50°S to 50°N.
- *Multi-level upper-air data* – mainly the radiosondes (Fig. 2.1) and the polar orbiting sounder data (Fig. 2.2). Satellite sounders provide global coverage with radiance data, which can only be used indirectly for the definition of the mass field (temperature and humidity). Radiosondes are the only current observing system providing vertical profiles of the wind field, but they are available mainly from the continents in the northern hemisphere. The radiosonde network has been gradually deteriorating in recent years. As such, three-dimensional wind measurements remain relatively scarce.

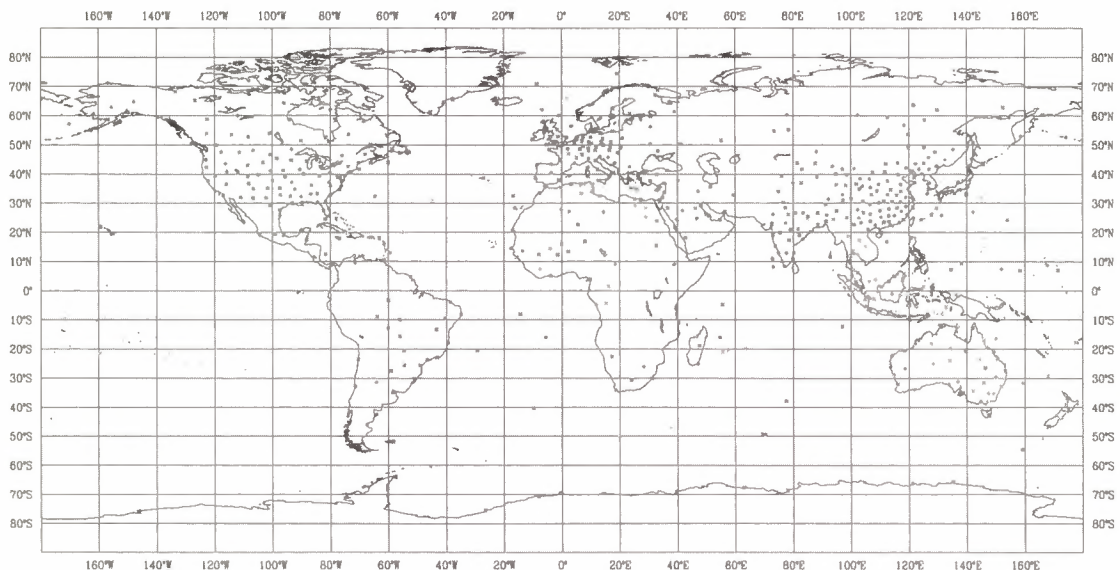


Figure 2.1. The radiosonde network – radiosonde/pilot ascents containing wind profile information that were available at DWD for the 6-hour time window centred around 12 UTC, 28 April 1999. This is a typical distribution and wind profile information is generally lacking over all ocean areas.

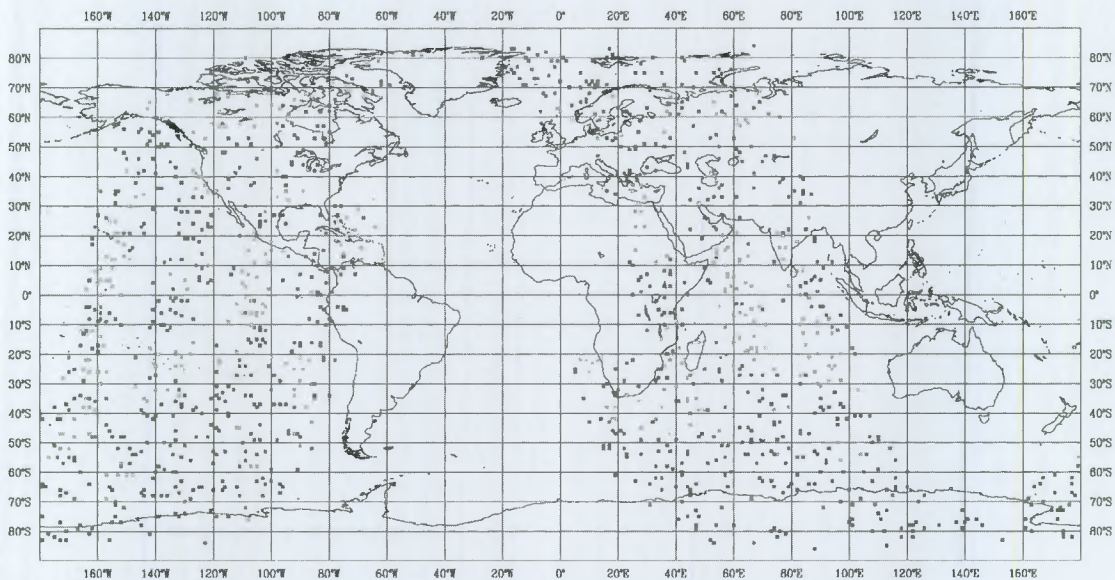


Figure 2.2. Satellite soundings – temperature and humidity soundings from the polar orbiting satellite NOAA-14 as available at DWD for the 6-hour time window centred around 12 UTC, 28 April 1999. Temperature and humidity profile information from satellites provides reasonably uniform coverage.

2.2.3 The Importance of Wind Profile Measurements

In order to analyse the importance of wind data, the notion of Rossby radius of deformation is very useful. It helps one to understand the wind profile observation deficiency (in particular in the context of NWP), the results of observation impact studies, and the potential impact of new wind measurements. It also helps one to understand the importance of three-dimensional wind data in general (beyond the NWP context) and, especially, the variation of this importance with horizontal scale, vertical scale, and latitude.

Under some simplifying assumptions, the Rossby radius of deformation R identifies the low frequency (or Rossby) modes of atmospheric motion. The Rossby radius can be expressed as

$$R = \frac{\sqrt{gh}}{2\Omega \sin \Phi} \quad (2.1)$$

where g is the acceleration due to gravity, h the equivalent depth of the atmosphere, Ω the angular velocity of the Earth, and Φ the latitude (see Fig. 2.3).

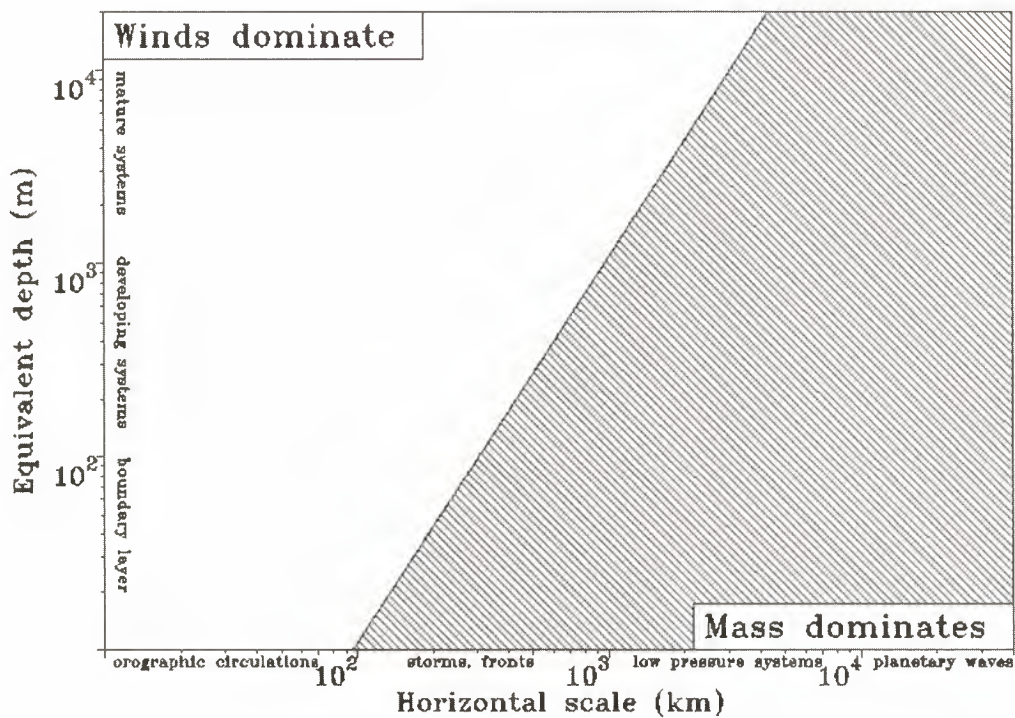


Figure 2.3. Rossby radius of deformation for a latitude of 45° as a function of horizontal scale and equivalent depth. Open area denotes the range within which the wind field dominates the atmospheric dynamics, and three-dimensional wind measurements are important.

For horizontal scales smaller than R , the wind is the essential information and the atmospheric mass field adjusts to it. For horizontal scales larger than R , the wind adjusts to the mass field. R also depends on the vertical scale of the atmospheric feature that is being considered (equivalent depth):

- At the equator, R goes to infinity, so in the tropics information on the wind field is essential as it governs tropical dynamics. In the extra-tropics, wind data are the primary source of information for small horizontal scale features (length scales $L \ll R$) and deep vertical structures.
- Mass field information is important for large horizontal scale features ($L \gg R$) and shallow vertical structures.

Between these two extremes, there is a wide range where both mass and wind data are required.

From this simple theoretical analysis (see ESA, 1996), it is expected that wind profile observations have a major impact on forecasting in the tropics and the prediction of small-scale structures in the extra-tropics (deriving small-scale winds from height field

observations does not reflect the true dynamics). Having wind profile observations in the tropics would help considerably in advancing understanding of tropical dynamics and, probably, the forecasting of severe events such as tropical cyclones.

In the extra-tropics, the availability of more wind profile data is expected to lead to capturing, much better and much earlier, of initial instabilities of the flow in the storm tracks, and subsequently to improve considerably forecasts of storm developments (especially the intense ones). Even for large-scale structures in the extra-tropics, when the wind field adjusts to the height data, wind data are still useful for at least two reasons. Firstly, because for large planetary scales the geostrophic relation between mass and wind is not valid. Secondly, when deriving the wind field from observed height, relatively small observation errors on the height can lead to significant errors in the derived wind. Therefore, it is important to measure the three-dimensional wind field directly.

2.3 Potential Improvement of NWP by Enhanced Wind Observations

2.3.1 Implication of Data Deficiencies for NWP

A typical NWP model contains many more variables in its initial state than the accumulation of all the pieces of data from the observations accumulated over a 6-hour period (typical for most of the operational data assimilation systems; see ESA, 1996 for a detailed quantitative assessment). This means that NWP is a seriously under-determined initial-value problem. With increasing computer power and increased resolution, it is likely to become more and more under-determined, in spite of new satellite instruments bringing higher and higher data volumes (ATOVS sounder replacing TOVS in 1999 with more channels; plans for a new generation of sounders giving more details on the vertical distribution of temperature and humidity).

Modern data assimilation systems are quite efficient in making optimal use of the current operational observations. They help in reducing the under-determination problem by bringing in additional statistical and dynamical information (see Meteorological Society of Japan (1997) for an overview of the data assimilation algorithms and problems, and Rabier et al. (1998a) for the description of a modern operational data assimilation system, based on a four-dimensional variational assimilation scheme, 4D-Var). Such a scheme is likely to be used in many NWP centres in a few years and is currently the natural candidate to assimilate wind data.

However, despite the sophistication of modern data assimilation schemes, large uncertainties are left in some wide areas on the globe, for the wind field itself, for other fields that are important for NWP, and for diagnosed integrated quantities which are important to understand the climate. Some of these uncertainties are documented in ESA (1996).

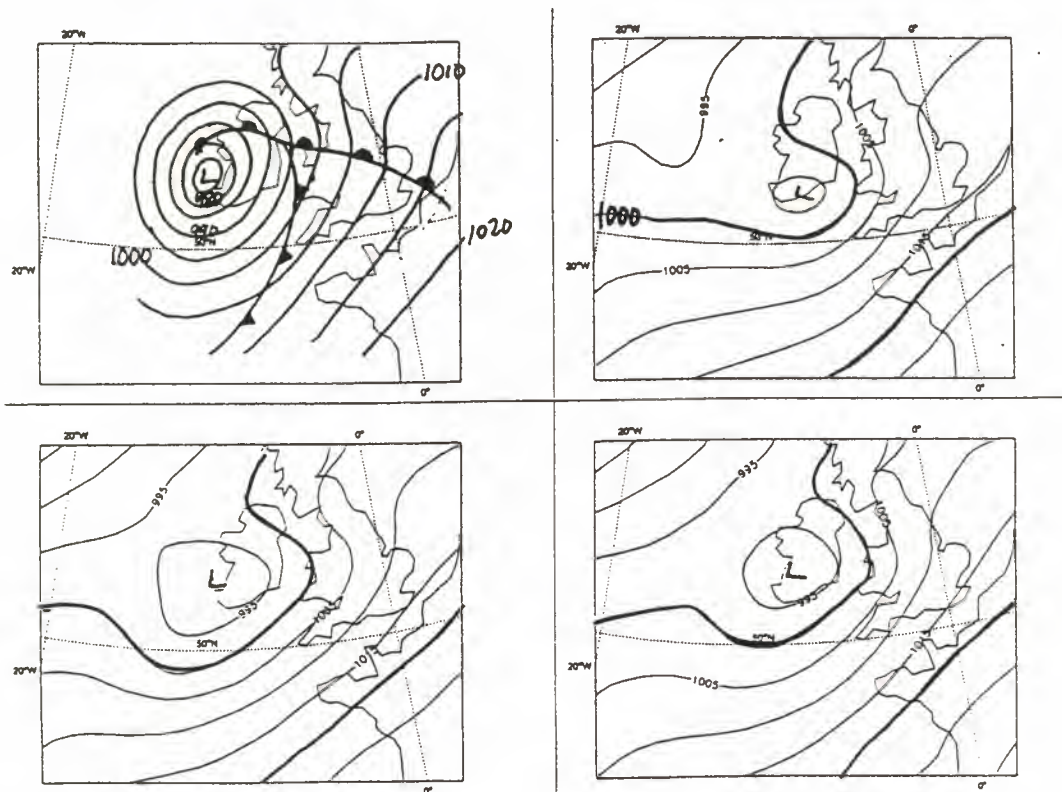


Figure 2.4. Analysis and forecasts of the ‘Christmas Eve Storm’ – Mean Sea Level Pressure (MSLP) maps illustrating the ‘Christmas Eve Storm’ which hit the British Isles on 24 December 1997, 12 UTC, after a rapid development from the middle of the Atlantic Ocean (Courtesy A. Persson, ECMWF).

- Top left: manual analysis for 24 December 1997, 12 UTC;
- Top right: ECMWF 12-hour forecast from 24 December 1997, 00 UTC (valid 12 UTC);
- Bottom: equivalent 12-hour forecasts from the UKMO (left) and the DWD (right) models.

Even at very short range, NWP models can be hit by severe failures which, although it cannot be always proven, are suspected to be due to a lack of meteorological observations in some areas which are critical for the initial state of these models. One example is the storm of 24 December 1997 (now called ‘Christmas Eve Storm’, see Chapter 1), which deepened very quickly in the middle of the Atlantic Ocean on the 23rd and 24th of December 1997, then hit Ireland and the Irish Sea in the afternoon of the 24th, and finally the North of England and Scotland. The short-term forecasts of the storm from all operational models were poor, even at very short range as illustrated in Figure 2.4. Figure 2.5 shows the 36 hour forecast produced by the French operational model (ARPEGE) valid also for 24 December, 12 UTC: it missed the Irish storm and developed another one which was about 1000 km to the southwest (this can be interpreted as an enormous phase error). It has to be noted that even at very

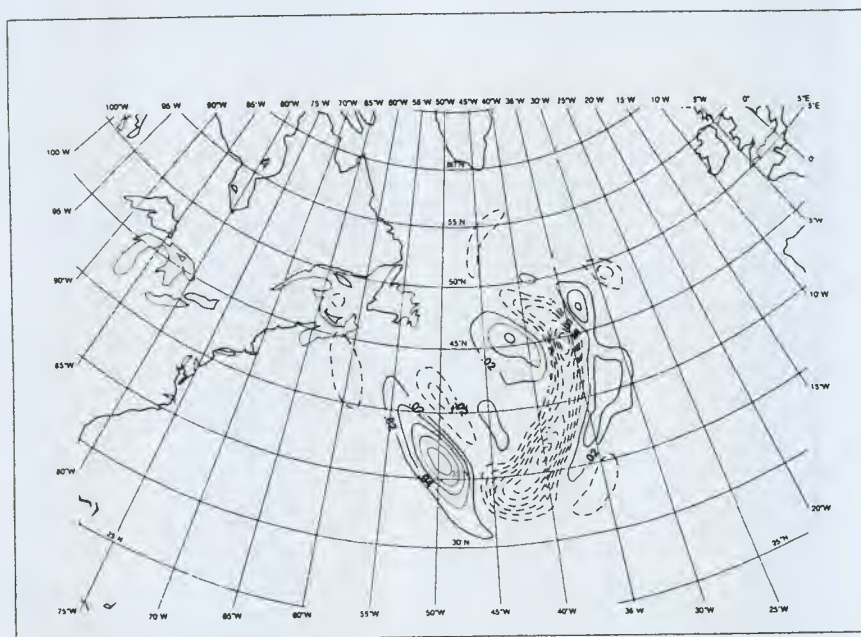
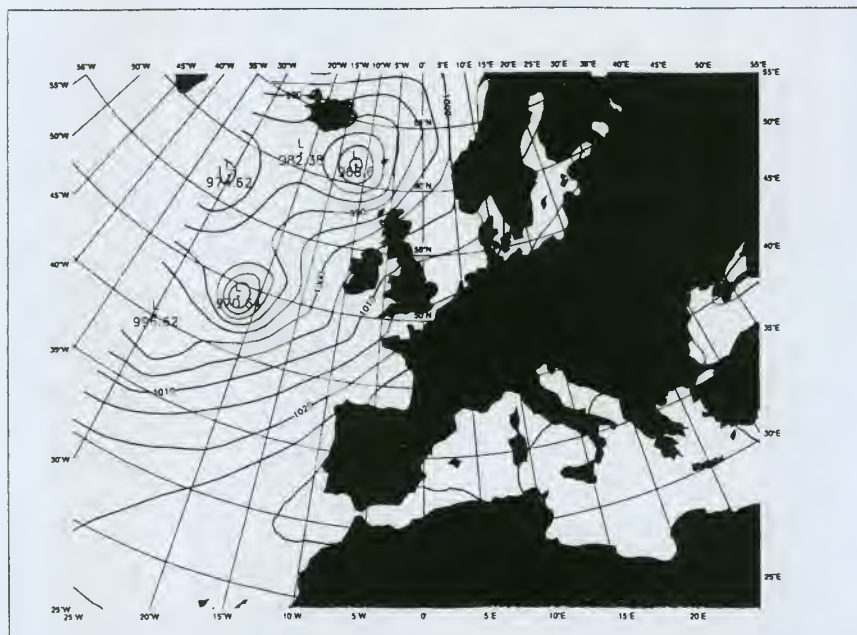


Figure 2.5. Forecast using the Modified Operational Model of Météo-France – 36-hour MSLP forecast valid 24 December 1997, 12 UTC (top). The sensitivity of the storm forecast with respect to a modification of the initial conditions (on 23 December 1997, 00 UTC) has been computed using a modified forecast model (Courtesy G. Hello, Météo-France).

short range (12-hour), the operational models produce extremely poor forecasts of the storm (the pressure error near the centre of the low exceeds 20 hPa). In most of the operational assimilation systems, the (computer-based) objective MSLP analysis underestimates the depth of the low, because the available observations were so different from the very poor first guess that they were rejected in the analysis. This explains why a manual analysis (rather than an objective one) has to be shown in this figure.

The examination of the different operational analyses on the 22nd and 23rd, together with the satellite imagery, indicates that these analyses were often unable to catch accurately the different weather systems (cyclogenesis, developing waves, and their precursors), presumably because of rapid cross-Atlantic circulation, rapid baroclinic developments and insufficient data coverage.

A modified version of the ARPEGE model was then used to compute three-dimensional sensitivity fields, which indicate where and to what extent the initial conditions should have been modified on 23 December, 00 UTC, in order to predict correctly the storm at 36-hour range for 24 December, 12 UTC. The outcome of this example of sensitivity study is that a small change in the middle of the Atlantic (see temperature modification in Fig. 2.5 – bottom), for the three-dimensional thermodynamical structure of the analysis would have converted this 36-hour forecast failure into a good storm forecast; see Hello et al. (1999). A simple calculation shows that this small change corresponds to 1 or 2 ms⁻¹ on the wind shear taken between 700 and 850 hPa (for example) in some areas of the middle Atlantic. It is then likely that a good three-dimensional coverage of observations in this area would have improved the forecast considerably. More generally one can reasonably think that a good three-dimensional coverage of observations over the North Atlantic would have improved considerably the forecasts over the North Atlantic and Europe during this few days' period before Christmas 1997, including the dangerous meteorological event of the 'Christmas Eve Storm'.

The requisite wind profiles would be available from the ADM meeting the requirement for high accuracy wind observations.

2.3.2 OSE and OSSE: Principles, Limitations and Some General Results

In order to assess the impact of wind profile data on NWP in a way which is more quantitative than the previous theoretical developments in Section 2.2, Observing System Experiments (OSE) and Observing System Simulation Experiments (OSSE) have been run in NWP for at least twenty years. OSE are impact studies carried out with existing observations: two parallel data assimilations are carried out, with and without the observing system to be evaluated; resulting analyses and subsequent forecasts are then compared. OSSE are similar to OSE except the observations to be tested are simulated rather than real: simulated observations are produced from an

NWP model integration assumed to be the ‘known truth’ and usually called the ‘nature run’. For a quantitative assessment of a non-existing observing system like the global wind profiles, which may be produced by a space Doppler lidar in the next decade, OSSE are required.

WMO (1997) gives an overview of the impact of existing operational observing systems on the forecast, through a synthesis of OSE carried out until April 1997. It also presents (paper by Atlas in WMO, 1997) the details of the OSSE methodology and its limitations, which have to be kept in mind when evaluating the results. It underlines ‘the need for providing observations from a realistic nature run, for simulating properly the observation errors, for calibrating properly all the components of the OSSE, and for using an assimilating model different enough from the model producing the nature run’. Finally, from old OSSE results, it indicates a significant potential for further improvement from a space-based wind profiler, also with respect to the TOVS observing system. The OSE run by Graham et al. (ibid) indicates that, on average, for predicting cyclogenesis over the North Atlantic and Europe, wind profile observations are somewhat more important than temperature profile observations.

Table 2.1 (extracted from WMO, 1997) shows a summary of the impact of different observation types over the northern-hemisphere extratropics. The values given for each observation type represent results from impact studies carried out during the period 1994-97. The results are expressed in terms of maximum gain in large-scale forecast skill at short and medium range. This table is only meant as a rough guide. The magnitudes of the impact depend, for example, upon the model and assimilation scheme used and the observed variables. Therefore, generalisation of impact magnitudes must be treated with caution. However, it is clear that the northern-hemisphere radiosonde network stands out as being especially important (presumably because it is the only system providing accurate profiles of wind and temperature on a significant portion of the hemisphere).

	Neutral to Few Hours	Up to 1/4 day	0.5 day	1.0 days	1.5 days
TOVS	→				
Cloud motion winds	→				
Sondes	→				
Aircraft	→		→	(*)	
Scatterometer	→				

Note: (*) impact only locally

Table 2.1. Impact of different types of observation on forecast skill (from WMO, 1997). Vertical soundings that include wind observations have large impact.

2.3.3 Results of Recent Studies on the Impact of Wind Profiles

A very good estimate of the potential impact of a future space-based Doppler wind lidar system can be obtained by running an OSE evaluating the impact of real wind profile observations available on a data-dense area like North America. This was done by Cress (1999) using the Deutscher Wetterdienst global data assimilation and forecasting system. Figure 2.6 shows the drastic degradation of the forecasts over the North Atlantic and Europe produced by the withdrawal of radiosonde and aircraft wind profiles over North America (USA plus Canada). The start date of the forecast is 30 January 1998, 12 UTC and the differences are for the initial state (a) and after 3.5 days (b), 5.5 days (c) and 7.5 days (d) forecast time. The detailed evaluation of the scores show that the forecast is degraded by about 24 hours.

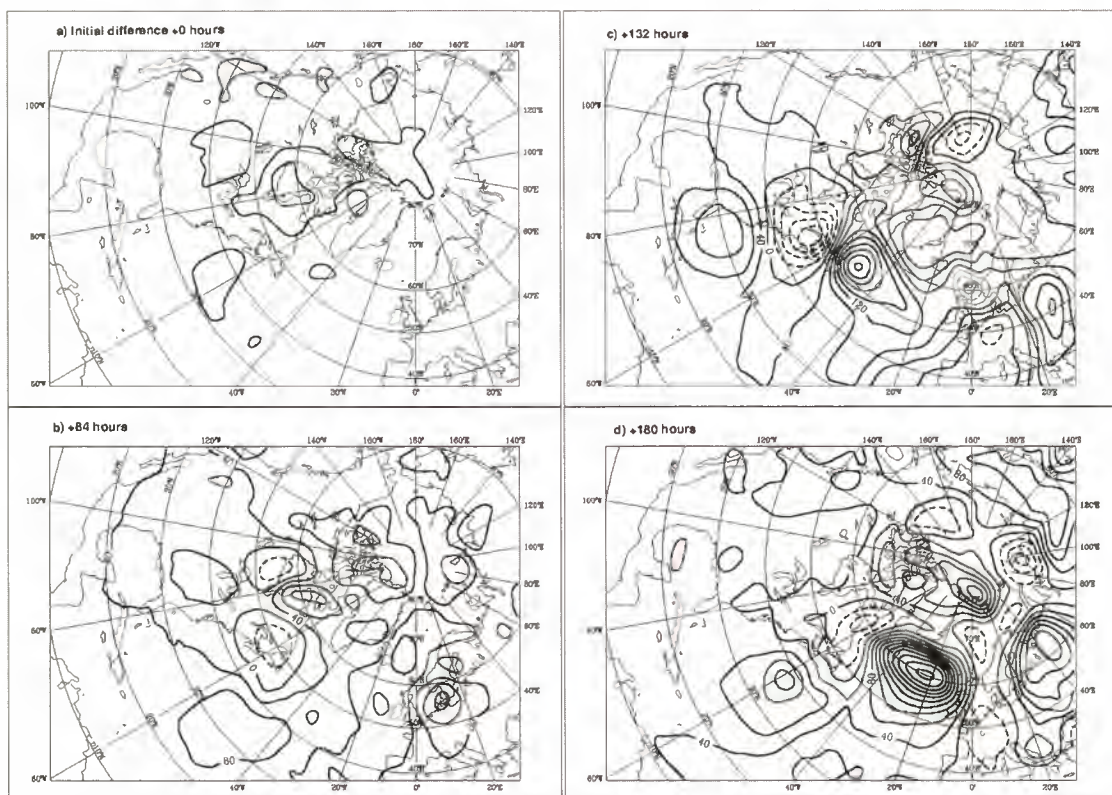


Figure 2.6. Illustration of degradation of forecasts without wind profiles – differences in the 500 hPa geopotential height field between a forecast using all available observations and experiments not using radiosonde, pilot and aircraft wind data over the United States and Canada. Contour interval is 20 m for a) and 40 m for b) to d) (from Cress, 1999).

In a recent OSSE performed in Germany as a continuation of this OSE, it was shown that a system providing only a small number of wind profiles in place of the

conventional wind observations over North America would recover more than half of this forecast degradation. Figure 2.7 (from the same study) illustrates that even at forecast range 0 (model initial state), systematically removing the North-American wind profiles produces wind uncertainties over almost the entire tropical area, indicating that the tropical flow is rather uncertain. This experiment provides a rough estimate of the potential impact of wind profile data available in a data sparse area of the size equivalent to North America. Forecasts started from the degraded analysis reduced the operational medium-range forecast skill by 20 hours.

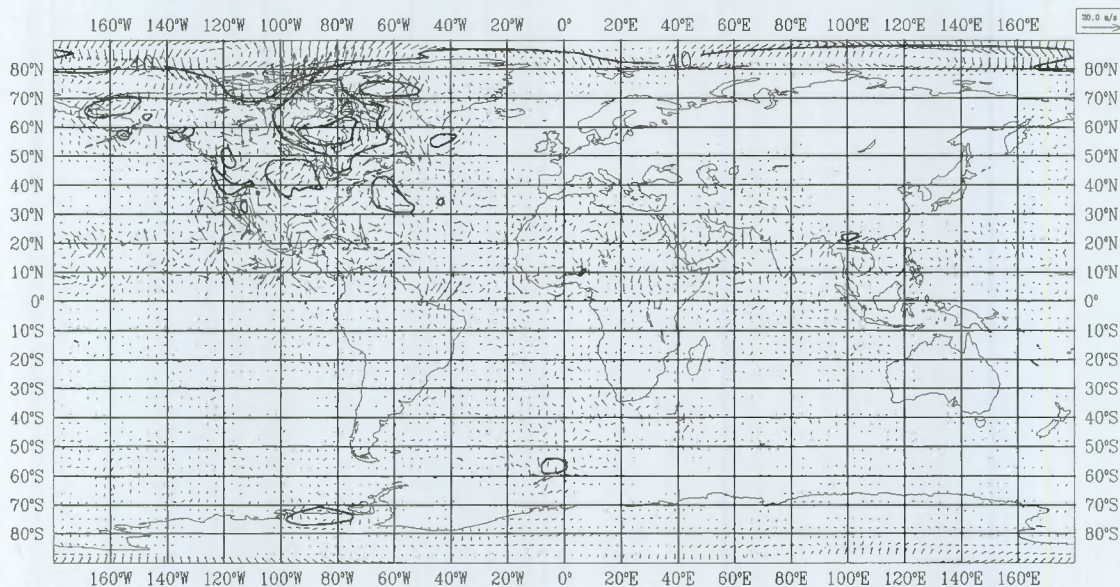


Figure 2.7. Degradation of the global wind field – analysis of differences in the geopotential height and wind field at 500 hPa between an 11 day long assimilation not using wind profile observation from radiosondes, pilots and aircraft over the United States and Canada and the control assimilation using all observations. The difference is valid for 30 January 1998, the contour interval for the height field is 20 m (from Cress, 1999).

Another interesting OSE has been carried out by Isaksen (Ingmann et al., 1999) with the 1997 ECMWF global data assimilation and forecasting system. It evaluates the impact of all the radiosonde wind profiles above the planetary boundary layer (PBL) versus the impact of the radiosonde mass profiles (geopotential height) and also that of all the available radiosonde information. The results expressed in terms of average skill scores are displayed in Figure 2.8. The impact is found to be much larger than the impact of any single-level data observing system, and equivalent to a big portion of the total radiosonde network impact, which includes temperature and humidity information.

An ECMWF model nature run was used to produce an OSSE data base simulating a scenario in which wind data (assumed from a DWL) were available (Stoffelen and Marseille, 1998). In the same reference, one can read about the analysis of the data base: ‘Vertical wind-shear is only weakly correlated to cloud coverage, implying that shear is well observed from space; we conclude that such data may bring an important improvement to the forecast of cyclogenesis, since it would provide wind profiles in otherwise data-sparse regions’.

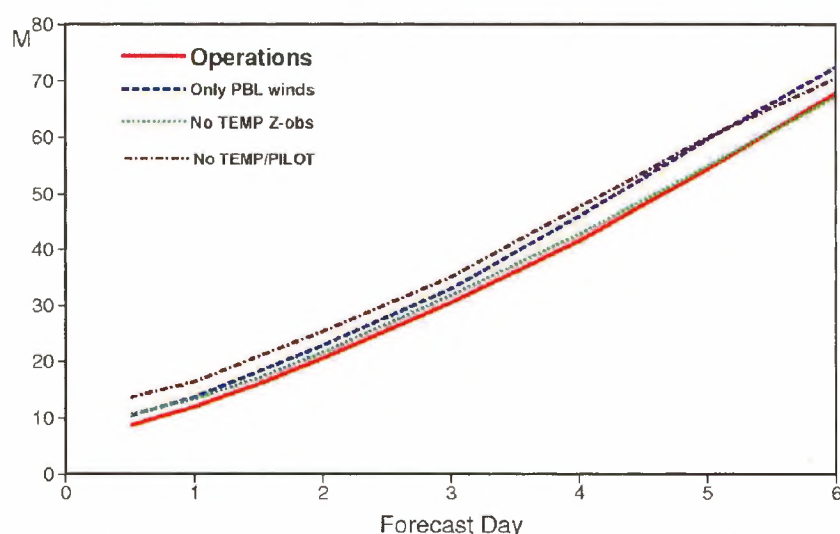


Figure 2.8. Results of assimilation studies – carried out with ECMWF’s three-dimensional variational system for the Northern Hemisphere for a) full set of observations (red line), b) no use of TEMP/PILOT (brown line), c) no use of TEMP/PILOT winds above 775 hPa (blue line), d) no use of TEMP/PILOT temperature profiles but only winds (green line).

This data base has been used by Cardinali et al. (1998) to carry out an OSSE with a version of the Météo-France global model at low resolution and 4-DVar assimilation scheme. It was shown that near a trough situated over the Pacific Ocean, to the west of the Canadian coast, the availability of wind profiles helped considerably the wind analysis (confirmation of the finding of Stoffelen and Marseille, 1998). In Cardinali et al. (1998), three different scenarios have been intercompared:

- ONLYLOS: only DWL data have been assimilated
- CONTROL: corresponding roughly to current observing systems; note however that TOVS data were not used in CONTROL
- LIDAR: DWL data have been added to the observations of CONTROL.

Table 2.2 shows the performance of the three different scenarios in terms of analysis errors (mean and standard deviations of the differences to the nature run), for three different areas and three different levels. It is clear that the LIDAR scenario is much

improved compared to CONTROL, especially in the Southern Hemisphere and in the tropics.

Area	Level (hPa)	ONLYLOS		CONTROL		LIDAR	
		Mean	St. Dev.	Mean	St. Dev.	Mean	St. Dev.
Northern H.	850	3.56	2.15	2.63	1.82	2.39	1.54
	500	4.77	2.95	3.20	2.22	2.88	1.87
	250	6.03	3.64	3.28	2.20	3.06	2.01
Tropics	850	3.38	2.51	3.04	2.13	2.60	1.74
	500	4.48	2.69	3.96	2.36	3.20	1.95
	250	6.18	3.99	5.29	3.39	4.20	2.62
Southern H.	850	3.76	2.34	3.89	3.58	2.74	1.70
	500	4.51	2.70	5.73	3.60	3.48	2.06
	250	6.98	4.59	7.62	5.08	4.76	3.16

Table 2.2. Mean and standard deviations of the analysis errors (expressed in ms^{-1} as the module of the vector 'Analysis - Truth') for three OSSE scenarios at three different levels and in three different areas over the globe (from Cardinali et al., 1998). A DWL well complements the existing GOS in improving atmospheric analyses.

The results of OSEs and OSSEs carried out indicate that improved wind profile observations as will be provided by the ADM would have a large impact over different regions of the globe.

2.4 The Need for Atmospheric Wind Fields for Climate Studies

2.4.1 Background

Climate-change issues have received substantial attention in recent years due to the increasing awareness that human activities may substantially modify the future climate of the Earth. The globally averaged temperature has increased by about 0.6 degrees Celsius over the past hundred years and 1998 was the warmest year recorded on instrumental temperature record covering the last 150 years. These facts and other pieces of evidence suggest that an increased greenhouse effect due to human activities is starting to influence the global climate system. A very important question is thus to assess how a further future increase in greenhouse gases may affect this system. The most effective tools available to answer such questions are global and regional climate models, which to a very large extent resemble the corresponding NWP models. All the benefits of wind data discussed in the previous section relating to NWP models are also relevant to circulation models used for climate studies as both model types are based on the same physical and numerical principles.

An illustration of the uncertainties involved in climate-change scenarios can be seen in Figure 2.9. Twelve different state-of-the-art global, coupled atmosphere-ocean climate models have been forced with identical, prescribed changes in atmospheric composition. The resulting globally averaged temperature and precipitation changes show an appreciable scatter. To reduce this uncertainty range, careful model evaluations using comprehensive observed climate data sets are necessary. In particular, tropical wind data is needed to improve the quality of the basic data sets. Large interannual variations are a characteristic feature of tropical circulations; an example of the wind field variability in connection with El Niño events is shown in Figure 2.10. Monthly averaged wind fields in March 1982 and March 1983 are quite different; the 1982 wind field is unaffected by El Niño, while in 1983 a strong El Niño event occurred. Furthermore, it is known that different assimilation systems may give large differences for the same time period, indicating that the data coverage in the tropics is not sufficient to give a well-defined climate wind field. This makes the verification of climate models even more difficult.

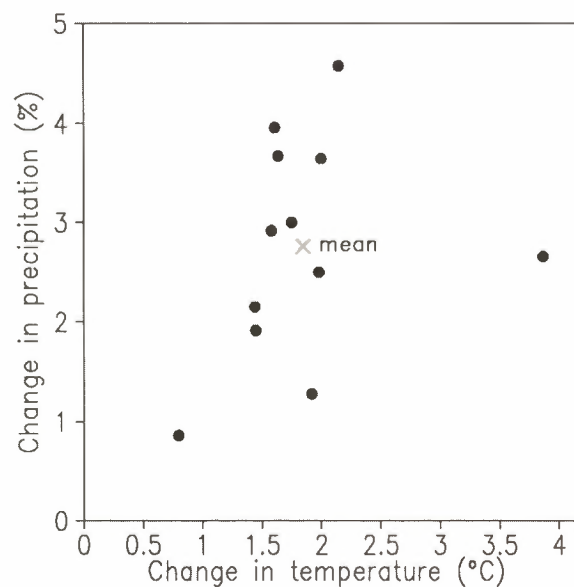


Figure 2.9. Comparison of twelve climate models – globally averaged climate change of temperature and precipitation for twelve different coupled atmosphere-ocean models. The spread illustrates the current uncertainty in climate change prediction. The cross indicates an average over all twelve models (from Räisänen, 1998).

A simple definition of climate is ‘the average weather’. A description of the climate over a specified period (which, typically, may be from a few years to a few centuries) involves the averages of appropriate weather characteristics over that period, together with the statistical variation of these characteristics. As a result of natural processes, the climate fluctuates on many time scales and this intrinsic feature is often referred to

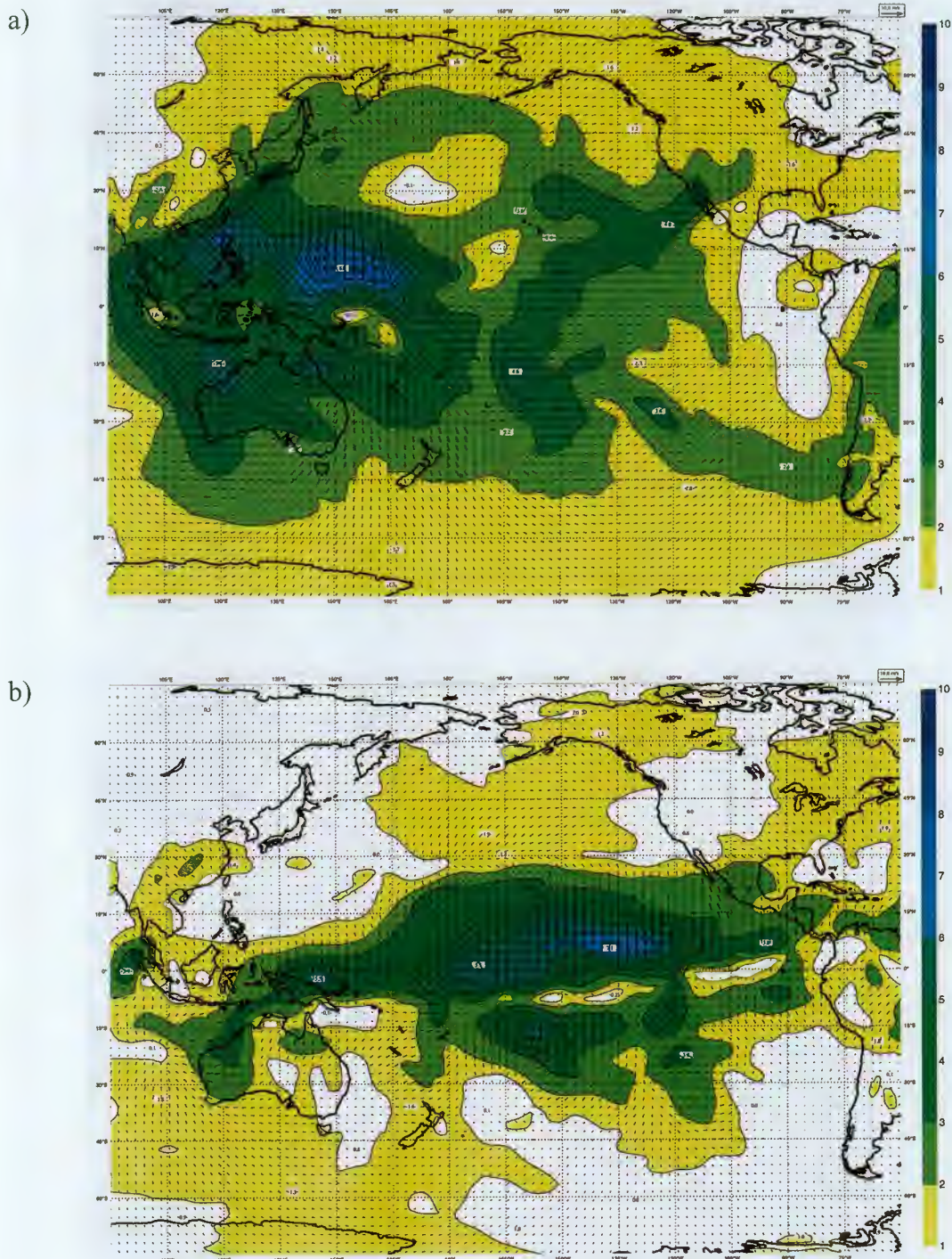


Figure 2.10. Divergent wind field at 150 hPa – monthly mean divergent winds over the Pacific region for the months of March 1982 (a) and March 1983 (b). In (a) there is a divergent outflow over the Indonesian region which is associated with normal tropical heating. In (b) the outflow has moved to the Central Pacific and this shift is associated with the El Niño event extending over 1982 and 1983.

as natural climate variability. In this report, the term ‘climate change’ refers to any change in climate over time, whether this is due to natural variability or human activity or, indeed, is a consequence of both these causes.

Although the climate varies over a vast range of time scales, from inter-annual to many thousands of years, two ranges are currently receiving particular attention. These are, firstly, the seasonal-to-interannual time-scale range and, secondly, the decadal-to-centennial time-scale range. These, particularly the latter, provide the focus for this section of the report. Following brief comments on the general data requirements for current studies involving these two time-scale ranges, this section discusses the particular needs for wind data for climate studies, including atmospheric composition, with separate comments on tropospheric and stratospheric winds.

In the context of climate studies, one of the highest-priority concerns for better global wind measurements has been expressed by the Scientific Steering Group of the Global Energy and Water Cycle Experiment (GEWEX), a major component of the World Climate Research Programme (WCRP).

2.4.2 Seasonal-to-Interannual Variability and Predictability

Recent research has achieved significant progress in making credible predictions for a few seasons ahead for certain regions of the globe. Success to date has been most evident for some tropical areas and has resulted from research conducted principally under the auspices of the WCRP, to understand the interactions of the tropical ocean and global atmosphere (TOGA) and the related large-scale ENSO (El Niño/Southern Oscillation) phenomenon.

Standard meteorological data sets are required to initialise and validate seasonal-to-interannual climate predictions. In this context, atmospheric wind is a key meteorological variable, particularly in the tropics where reliable wind observations are crucial as their inclusion in the NWP assimilation process strongly affects the large-scale features of the analysed tropical wind field. For example, westerly wind bursts (WWB) or events (WWE) play an important role in the onset of El Niño by providing a strong and irreversible forcing on the upper ocean. However, the cause and occurrence of these WWB in relation to the ambient tropical dynamics is poorly known.

Whilst the evidence for seasonal predictability is strongest in the tropics, there is now also growing evidence of some predictability in the extra-tropics. Global data, including atmospheric winds, are therefore required for a range of uses in connection with the investigation of seasonal variability and predictability, and the development and application of seasonal-to-interannual prediction techniques.

The ADM will provide the wind profiles needed to initialise models and validate seasonal-to-interannual predictions.

2.4.3 Decadal-to-Centennial Climate Variability and Predictability, Including Modelling and Detection of Anthropogenic Climate Change

The prospect that the global climate may be modified by human influence has led to the establishment of international programmes to monitor and increase the understanding of climate and to detect, attribute and predict climate change. Comprehensive observations of the climate system are recognised as being an essential component of these programmes and so the Global Climate Observing System (GCOS) has been established to ensure that the observational needs for climate are met in a co-ordinated and systematic manner.

In the current debate about climate change, it is evident that adequate information is not available to answer fully the critical scientific questions. While many observational programmes are currently under way, systematic global observations of key variables, including atmospheric winds, are urgently needed to:

- monitor the climate and its variability at global, regional and more local scales, thereby enabling quantification of natural climatic fluctuations and extreme events on a range of temporal and spatial scales and the detection of climate change
- establish 'fingerprints' of climate change, which will allow not only detection of change but also some attribution to its causes
- conduct diagnostic studies to document and understand better the behaviour of the climate system and its component parts, including studies of the mechanisms of natural climate variability
- model climate and predict climate change.

Model-related climate studies require global observations for a number of reasons. Atmospheric wind data are required principally for the validation of the models, i.e. to assess the performance of models being used for climate simulation and prediction. Model behaviour is compared with that of the 'observed' climate, often leading to further development and improvement of the models. This applies not only to multi-decadal simulation and prediction, but also to the seasonal-to-interannual studies discussed above.

The acquisition of systematic and comprehensive space-based global observations with adequate coverage in space and time is essential to meet the above aims. However, in addition to the requirements for continuous, systematic data collection, special data are also needed in support of detailed research studies of a wide variety of

complex dynamical, physical and other processes that govern the state and evolution of the climate system. Such specialised data sets are likely to need to be highly resolved in time and space and may therefore need to be gathered for a limited period only. In particular, further progress in understanding and predicting global climate change is critically dependent upon improvements in the ability to model energetic processes, as detailed in the scientific plan for GEWEX. The high priority attached to wind data in support of GEWEX is discussed below.

The ADM will provide the systematic and comprehensive data needed to enable predictions of climate change.

2.4.4 The Importance of Wind Data for Climate Studies

Climate research is highly dependent upon reliable global analyses of standard atmospheric variables, including winds throughout the atmosphere. These constitute the basic data needed to infer more complicated quantities, such as the properties of atmospheric transport and the surface fluxes of momentum, energy and mass, which are not measured directly or routinely. Global coverage with optimal vertical resolution and representative horizontal spacing are the crucial requirements for many climate activities and so, as in the case of NWP (Section 2.2), space-based observations are particularly important in this context. Earlier expert studies have already stressed the great importance of accurate vertical profiles of wind and temperature which largely determine the quality of many of the other important meteorological fields. To provide such profiles in a consistent way over several decades for atmospheric scientists, re-analysis projects are carried out (ERA15, NCEP, ERA40).

Atmospheric data, including winds, are required to better understand the dynamics of the climate system and its natural variability. In particular, as implied above, atmospheric data are needed to monitor the current state of the climate, to detect change and to validate the models that are used for seasonal forecasting, simulating climate and providing projections of climate change due to human activities. Related research, such as studies of the serious depletions of stratospheric ozone over the Arctic and Antarctic, would also be much better served by the availability of global wind data.

The main requirement is for long-term, consistent and representative global data sets, but there is also a call for shorter-period data sets to aid understanding through process and diagnostic studies. Better information is needed on the atmospheric circulation to try to attribute climate change to particular causes. A comprehensive view of observed climate change must be pursued by analysing all climate variables and accounting for relationships among them wherever possible. The fundamental atmospheric variables needed are principally those measured routinely for weather forecasting, including

upper-air wind velocity. Current accuracy and coverage are inadequate for many such studies and improvements are needed.

Changes in the atmospheric circulation are potentially very important because it forms the main link between regional changes in wind, temperatures and precipitation in the atmosphere and other climatic variables such as ocean currents and sea-surface temperatures through changes in surface fluxes of heat, moisture and momentum. Internal consistency among analysed changes in the variables can add substantial confidence to results and provides the physical setting for understanding the changes taking place. A strong case can be made that local climate change can only be understood if the changes in the atmospheric circulation are fully factored in.

Note that an ADM has already been recognised as one of the seven 'missions' defined as necessary to meet the requirements of the GCOS from space programmes and the provision of wind profiles is one of the principal observations listed for such a mission (WMO, 1995). Indeed, GCOS is giving close attention to achieving more comprehensive and complete analyses of the full three-dimensional structures of both the atmosphere and the oceans.

The ADM will provide the data needed for performing refined studies of global circulation.

2.4.5 Wind Profiles

Troposphere

The current deficiency in the coverage of in-situ measurements of atmospheric winds throughout the troposphere is worse than with the corresponding data for temperature and humidity. This makes in-situ data sets largely inadequate for climate purposes through a combination of sparse coverage and poor quality. Coverage is particularly poor over the oceans and it is here that satellite data potentially have much to offer. In particular, wind observations in the tropics are crucial as their inclusion or exclusion in Numerical Weather Prediction data assimilation determines the analysis of large-scale features of the tropical wind field.

As pointed out earlier (Section 2.2) existing sensors only allow winds in the tropics and extra-tropics to be inferred (from cloud motion vectors) at one or two vertical levels and only when tractable features are imaged. Application of improved tracking algorithms to the old data (as being done now for Meteosat) will reduce the time-varying bias problem. For all satellite measurements, it is vital that a period of overlapping, independent (in-situ) observations exists for validation and calibration purposes.

Although assimilated wind fields are highly desirable for climate purposes, it is vital that there are also high-quality, single-source data sets available to validate specific model-generated atmospheric processes. To this end, it is important to promote and support missions that seek to demonstrate new and potentially valuable technologies.

Stratosphere

Although the more pressing immediate need is for tropospheric winds, there is also a strong climate requirement for stratospheric winds. In addition to its important role in the climate-change debate, the stratosphere is being studied increasingly in its own right. In particular, it is necessary to establish if the stratosphere will continue to be perturbed by changing atmospheric composition and chemistry resulting in severe stratospheric ozone depletion, particularly in the polar regions, and, if so, how long will this continue for and with what consequences.

The accurate determination of stratospheric winds is likely to become an increasingly important issue in addressing such problems as models increase their vertical resolution and domain, and begin to resolve more realistically climate perturbations, such as ‘sudden warming’ events. As in the case of tropospheric winds, the assimilated wind product is vital for climate purposes. Increased observational accuracy and spatial resolution are needed. Improvement in vertical resolution is required for the monitoring of ‘sudden warming’ events, which have vertical scales of typically several kilometres, and for studying the processes involved.

Wind-profile observations of the ADM are needed to provide tropospheric and stratospheric winds with higher accuracy and better vertical resolution than currently available in climate research.

2.4.6 The Role of Winds in Defining Atmospheric Composition

Research associated with atmospheric composition and chemistry receives much attention. Issues related to the distribution of atmospheric gasses, including ozone and aerosol are important as they are associated with heterogeneous chemical processes and increased greenhouse warming in the atmosphere. Large amounts of potentially hazardous atmospheric constituents are being released in the tropics, mainly due to forest burning. However, the atmospheric flow in the tropics is rather uncertain and so the implications are not clear.

In other areas of the World, the atmospheric dispersion of atmospheric constituents is equally important, for instance, due to increasing air traffic. Chemical transport models are being used to advect chemically active constituents through the atmosphere. Usually, these models are driven by analysed wind fields from NWP centres. More recently, attempts have been made to produce fully consistent chemical

and dynamical analyses of the troposphere and stratosphere (Stoffelen and Eskes, 1999).

Section 2.5 discusses the potential advantages of using atmospheric tracer ('passive advection') information for NWP, but conversely the consistent dynamical-chemical analyses are also of prime benefit for research in atmospheric chemistry. A first step is to introduce ozone as a variable in a global circulation model and to use the analysed atmospheric flow to define the ozone distribution. Since ozone acts as a passive tracer in much of the atmosphere, its distribution is largely determined by the dynamics of the atmosphere. In particular, high-resolution dynamical processes are relevant in the interaction of tropospheric and stratospheric air masses.

Figure 2.11 shows an ozone distribution, simulated using three weeks of analysed atmospheric dynamics ('active advection'), an initial climatological ozone distribution

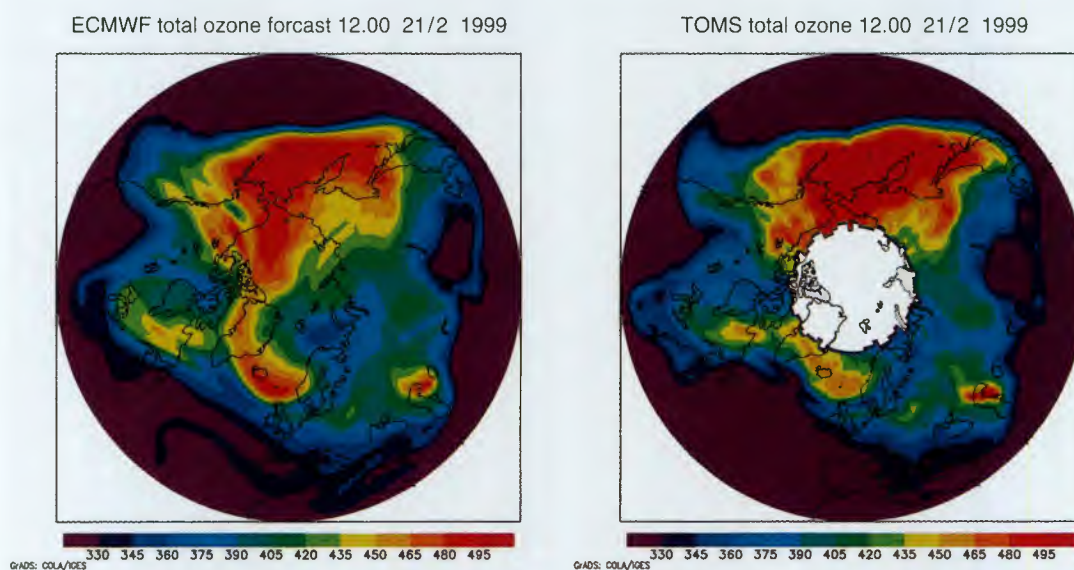


Figure 2.11. Total ozone distribution – vertically integrated (total) ozone distribution on 21 February 1999 as forecast by ECMWF on 12 GMT (left) and as retrieved from TOMS measurements during the whole day (right). The ozone distribution is dynamically forced (Courtesy E. Holm, ECMWF).

and a simple parameterised chemistry scheme. The ECMWF three-dimensional ozone field was obtained by forcing the analysed dynamics into the forecast in the first three weeks of February. The forecast ozone distribution captures many of the detailed spatial features observed by TOMS, although over the three-week forecast period starting 00 GMT 1 February 1999 no ozone observation has been used, i.e. three-dimensional structure is mainly inferred from the three-week atmospheric dynamics. Similar comparisons have been done for satellite measurements of water vapour and

modelled water vapour distributions (e.g. Kelly et al., 1996) with similarly striking agreement. It is clear that the distribution of any tracer, passive or active, is affected by the detailed atmospheric flow.

Improved wind analyses, which will be possible with the ADM, are beneficial for research on atmospheric chemistry and composition, and for the validation of satellite measurements of atmospheric constituents.

2.5 Future Studies and Perspectives Aiming at Improving the Wind Field Knowledge in the Post-2000 Time Frame

In Section 2.2 it was shown that in the current operational global observing system there are more temperature and humidity data than wind data, reflecting the characteristics of existing satellite sounders like TOVS or ATOVS. This imbalance (in favour of the mass field) is expected to increase during the next decade unless a space-borne wind observing system becomes available.

There are plans for implementing better sounders both in Europe and the USA. An interferometer (IASI) is expected to be launched on the European satellite Metop; equivalent plans exist in the USA. The new instruments will provide higher horizontal resolution and much higher vertical resolution temperature and humidity profiles. Exploitation of the space-borne Global Navigation Satellite System (GNSS) by radio-occultation may also provide very useful information on temperature and humidity profiles, especially in the stratosphere and the upper troposphere. Special microwave sensors may give more information on the atmospheric water (vapour but also liquid and ice), on the cloud structures and radiative properties of the clouds and on the land surface.

Through modern data-assimilation schemes, these new instruments are also expected to provide indirectly some information on the wind field. However, the requirement for direct wind-profile measurements in the tropics and in the mid-latitudes will in all probability become more critical once these data are available. Meteorologists will then try to improve the availability of wind measurements by acquiring more aircraft observations and using more passive tracers in the atmosphere. As explained below, these observation systems will not provide wind-profiles of the required accuracy and coverage.

2.5.1 Perspectives for More Aircraft Observations

More and more aircraft are being equipped with automatic systems for measuring wind and temperature, including during the ascent and descent phases. Consequently, the number of aircraft data available for operational NWP is increasing very quickly. This tendency is expected to be sustained for several years, and the operational

assimilation systems will have available more and more airport wind/temperature profiles.

However, compared to the requirement for three-dimensional global wind data coverage, aircraft data will always suffer from a basic weakness, namely data will be concentrated along the aircraft routes, which cover only a small portion of the globe, and aircraft profiles can only be obtained at the airports. Furthermore, most of the airports are in regions well covered by radiosondes. The likely evolution of the global observing system is then more a replacement of some existing radiosonde stations by aircraft data in ascent and descent phases, in order to save money on the cost of the radiosonde network, rather than a genuine improvement of the three-dimensional wind-field observation by new aircraft data.

2.5.2 Perspectives for Improving the Wind Field from Passive Tracers

The next generation of geostationary satellites will have better instruments and higher horizontal resolution. In that way they will improve both the quantity and the quality of their observed winds. So the operational cloud-track winds will keep improving. This is also true for water-vapour winds. Moreover, with continuous data-assimilation techniques such as 4D-Var, the frequent observation of the water-vapour fields (made by any instrument on a geostationary or polar-orbiting satellite) can provide information on the assimilated wind field without any explicit computation of a wind observation: the motion of passive structures in the flow is used by a 4D-Var algorithm to extract information on the wind field advecting these structures. When dealing with geostationary satellites, these techniques are limited in their performance at the higher latitudes.

This is true also for a 4D-Var assimilating frequent observations of ozone (rather than water vapour). Ozone is interesting as such in atmospheric modelling: it is more and more likely that during the next decade it will become a new prognostic variable of several operational NWP models. Frequent assimilation of ozone data obtained from some satellite instruments will contribute to improve the knowledge of the wind field. Some preliminary studies illustrating the potential of total ozone data from TOVS are available in Peuch et al. (1999).

In principle, the measurement of any constituent of the atmosphere, behaving like a passive tracer over a few-hour time period, can be used to extract some information on the atmospheric wind field. This type of technique will, however, never fulfil the NWP requirements for a global three-dimensional wind field, because they can produce wind information only at a very limited number of levels in the vertical: true wind profiles will never be obtained by tracking passive tracers in the atmosphere. Wind profile observations that will be provided by the ADM are unique in this respect.

The capability of the ADM to provide wind profiles globally will be unique.

2.6 Conclusions on NWP and Climate Studies

Reliable measurements of the tropospheric, three-dimensional wind field are of the utmost importance for NWP, seasonal-to-interannual forecasting and for studying atmospheric dynamics, energetics and the water, chemical and aerosol cycles associated with the state of the global climate and its future evolution.

In the context of atmospheric data, it has been argued that progress in climate analysis depends to a large extent on progress in NWP; the two cannot be separated. Indeed, operational and extended-range weather prediction offers an ideal opportunity for the detailed verification and improvement of model physics, at least for the so-called ‘fast’ atmospheric processes. Furthermore, climate research depends on the products of operational, meteorological analyses for much of the basic climatological information, including many second-order quantities that cannot be determined directly from observations on the global scale (e.g. heat and water fluxes). For this reason, both weather forecasting and climate research place highest priority on improving the basic meteorological fields. These are required not only for initialising operational weather forecasts and for estimating global climatological quantities, but also for the formulation of physical processes in weather-prediction and climate models, which are essential for both successful extended-range forecasts and meaningful assessments of climate change. Filling the gaps in existing wind observations, especially in the tropics and over the oceans, is regarded by the WMO as the first priority to achieve these objectives.

Modern data-assimilation systems with their ability to incorporate all available observations for the free atmosphere and the surface are now the most reliable sources of analysed data for a number of applications. Indeed, in all likelihood, comprehensive analyses of global atmospheric fields, based on four-dimensional assimilation of meteorological and marine data, will constitute the main source of information on the Earth's budgets for energy, momentum and water. For this reason, further improvements in the analysis of the global atmospheric circulation and the computation of budgets and fluxes are essential for both weather forecasting and to meet the objectives of major international climate-research projects such as GEWEX.

The OSEs and OSSEs carried out so far (including the recent ones documented in 2.3) show a large positive impact of existing wind-profile observations, as well as a large potential impact of a future spaceborne wind-profiling systems.

3 Research Objectives

3.1 Mission Objectives

The primary aim of the Earth Explorer Atmospheric Dynamics Mission is to provide improved analyses of the global three-dimensional wind field by demonstrating the capability to correct the major deficiency in wind-profiling of the current GOS and GCOS. The ADM will provide the wind-profile measurements to establish advancements in atmospheric modelling and analysis. As explained in Section 2.1 progress in climate modelling is intimately linked to progress in NWP. For example, as our understanding of the atmosphere is largely based on the experience of operational weather centres, long-term data bases are being created by NWP data assimilation systems to serve the climate research community. It is widely recognised therefore that the impact of a new global atmospheric observing system on our understanding of atmospheric dynamics should be evaluated primarily in the context of operational weather forecasting.

Besides increased skill in NWP, the mission will also provide data needed to address some of the key concerns of the WCRP, i.e. quantification of climate variability, validation and improvement of climate models and process studies relevant to climate change.

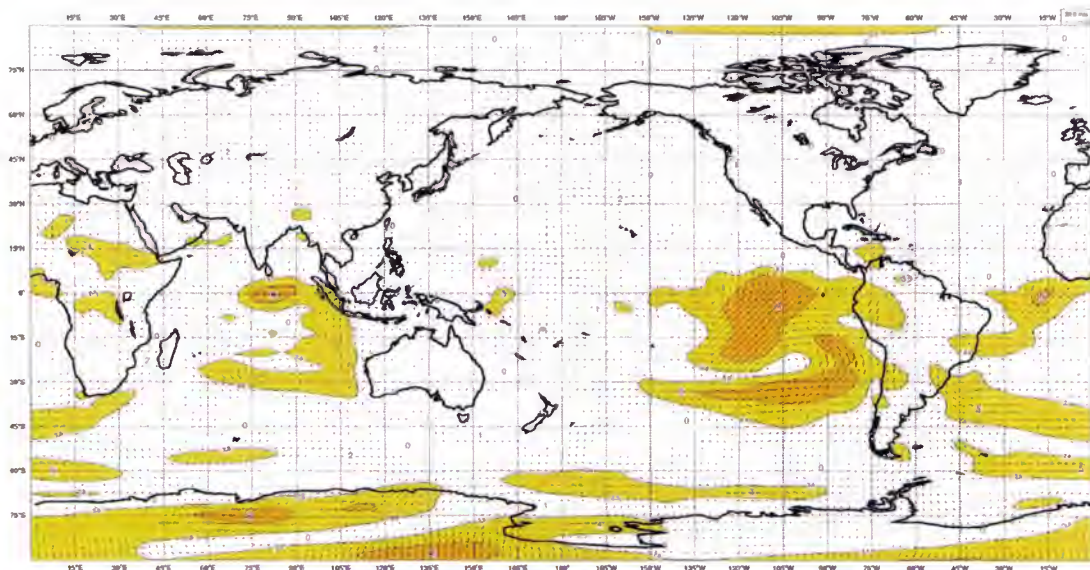


Figure 3.1. ECMWF-NCEP wind differences – vector wind difference of the 250 mb wind analysis of ECMWF and NCEP re-analyses averaged over a three-month period (June, July, August 1987). 2.5 m/s and 5 m/s isotachs are shown. Large differences of up to 7 m/s are found in the tropics, especially when considering that it an average over a three-month period (Courtesy P. Kållberg, ECMWF).

Figure 3.1 shows an example of the differences in analysis between the ECMWF and NCEP models. The differences shown here illustrate the uncertainties in atmospheric flow. In this case, the uncertainty is very large in the tropics and in the Southern Hemisphere, while differences in the Northern Hemisphere are smaller. These differences are expected to be reduced with the ADM.

3.2 Numerical Weather Prediction

From the discussion in Chapter 2 it is clear that the provision of global wind profiles is expected to provide the following benefits of direct value to NWP (and climate):

- a) A major improvement in the understanding and modelling of tropical dynamics through the provision of observations of the flow.

One important research tool to achieve this objective will be global parallel data assimilations performed on extended periods with and without wind profile observations. These analysis sets will be examined not only in terms of instantaneous flow, but also in terms of fields that are averaged over long periods. The essential components of the energy and water budgets and of the tropical circulation will be intercompared in the runs with and without wind-profile observations.

McNally and Vesperini (1995) have shown the strong interactions that occur between wind, temperature and humidity in the tropical dynamics. This type of study, repeated when the ADM data are available, will provide further insights into the importance of wind, not only for NWP, but also for most of the aspects of the tropical circulation. The description of the Hadley circulation, mean precipitation, humidity, and the distribution of other constituents are expected to be much improved. All these aspects have important implications for the observational strategy planned for GEWEX and other WCRP programmes (see ESA, 1998).

- b) A significant increase in the usefulness of tropical forecasts through a more precise definition of the initial state and through better modelling.

The evaluation of parallel forecasts in the tropics performed with and without wind-profile observations will give an objective estimate of this benefit. Benefits are expected for the large-scale components of the flow as well as for smaller scale weather features, e.g. better position and intensity estimates of tropical cyclones in NWP forecasts.

- c) Improvements in short-range forecasts, especially for intense wind events through proper definition of the wind field for the small scales.

In the Southern Hemisphere extra-tropics, a dramatic improvement is expected in the short-range forecasting of synoptic events. The magnitude of the expected improvement is comparable to the current quality difference between the two hemispheres (see WMO, 1997 for an evaluation of the quality of Northern Hemisphere forecasts with respect to those for the Southern Hemisphere). In the Northern Hemisphere, there are still cases of dramatic forecast failures, at day 1 or 2, on synoptic events such as strong mid-latitude storms (as shown in Section 2.3). The percentage of failures is expected to be much reduced with the availability of ADM observations. Over the whole globe, small-scale details of intense wind events are expected to be much improved for short-range forecasts because of the earlier detection of their development.

- d) An increase in the usefulness of medium-range forecasts for the extra-tropical region through a better definition of the planetary-scale waves.

Due to the conventional data coverage, this improvement in forecast skill is expected to be larger in the Southern than in the Northern Hemisphere. However, spaceborne wind profiles will also bring a more uniform spatial coverage of observations in the Northern Hemisphere.

- e) A much needed quality-control standard for the retrievals of temperature from sounders on polar orbiters, which will lead indirectly to improvements in forecasting skill, particularly in the Southern Hemisphere, where remote-sensing data are the primary source of information.

Before the ADM can provide a new source of wind data, a new generation of vertical temperature and humidity sounders is likely to become operational. By this time, data assimilation will be capable of extracting the information from both the sounders and the wind-profile observations. It is clear that a new observation type, providing direct wind information, will help to validate observations from all other sources and, thus, directly improve their potential benefits.

In summary, a primary objective of this mission will be to contribute to improvements in NWP, in the areas detailed above, by the provision of three-dimensional wind information.

3.3 Climate

The following benefits for climate studies would come from the ADM:

- a) contributing directly to the study of the Earth's global energy budget (by measuring three-dimensional wind fields globally)
- b) providing data for the study of the global atmospheric circulation and related features such as precipitation systems, the El Niño and the Southern

Oscillation phenomena, the distribution of atmospheric constituents like ozone or aerosol, and stratosphere/troposphere exchange.

Process research is needed to improve understanding of the climate system and the capability to model climate and detect, attribute and predict climate change on decadal and centennial time scales. This is addressed by the WCRP whose overall objectives are to observe, understand, model and ultimately predict climatic variations and climate change. In particular, through CLIVAR and GEWEX the WCRP places a high priority on achieving accurate computations (and therefore a better understanding) of energy and water fluxes on the global scale, which determine the current state and the future evolution of the climate. In addition to progress in understanding and predicting global (climate) change, further progress in weather forecasting beyond a few days, and seasonal-to-interannual forecasting are also critically dependent upon improvements in our ability to model energetic processes.

The need for accurate global measurements of tropospheric winds for numerical weather forecasting and climate studies has been highlighted as a serious issue by the GEWEX Scientific Steering Group. Indeed, it has identified inadequate tropospheric wind measurements as one of the three global data areas of most concern for GEWEX studies (the other two being, cloud, aerosol and radiation measurements, and soil moisture measurements) and therefore warranting the highest scientific priority and more attention in the planning of future observation programmes.

The CLIVAR research programme aims at further understanding of the physical processes in the climate system which are responsible for climate variability on time scales ranging from seasons to centuries. The collection and analysis of observations, as well as development of global, coupled ocean-atmosphere predictive models, are the main activities within CLIVAR. Key data for understanding climate variability relate to the processes (very dependent on wind) that govern the coupling between the oceans and the atmosphere on a global scale. Within CLIVAR the ENSO system, as well as monsoon systems and WWB in the tropics, have been identified as principal research areas. In addition decadal-to-centennial variability and anthropogenic influences on the global climate are major programme topics.

The WCRP in general, and GEWEX and CLIVAR in particular, require knowledge of basic meteorological variables to estimate energy and water transformation in the atmosphere and fluxes at the air-sea interface. Tropospheric winds remain a weak point. This deficiency poses a considerable limitation for scientific diagnostics of large-scale diabatic processes from the divergent component of the wind field. The problem is most serious in the tropics where the wind field is a critical dynamical variable. Tropical winds in particular are currently very poorly determined because of the almost complete lack of direct observations. In the CLIVAR context requirements for surface fluxes are specified. To meet these requirements, wind and humidity structure in the lower troposphere need improvement.

Many remote-sensing data on atmospheric composition are and will become available. The transport of constituents through the atmosphere often determines to a large extent their spatial distribution. A new three-dimensional wind-sensing system will improve the representation of transports in the models of the atmosphere and, consequently, the spatial distribution of atmospheric constituents. This will aid in the validation and calibration of variables in atmospheric chemistry.

3.4 Additional Observations

In addition to its primary role as a wind-measuring system, the ADM can also provide sorely needed information on cloud top heights, vertical distribution of cloud, aerosol properties, tropospheric height, and height of the atmospheric boundary layer. However, as the ADM shall not be driven by any such requirements, they are regarded as an additional benefit.

4 Observational Requirements

4.1 Introduction

Based on what has been outlined in Chapter 2, existing and planned systems will not meet the requirements for better wind profiles. In order to meet the numerical weather prediction, climate and atmospheric research objectives put forward in Chapter 3, an observing system is needed that provides three-dimensional winds over the globe. This means that it is essential to put significant effort into the development of a space-based system.

The WMO recognises the prime need for wind-profile data (WMO, 1998) and has defined a set of optimum wind-profile measurement requirements (WMO, 1996). User requirements for synoptic use are as or more stringent than those for climatological use (see Section 2). Quoting from WMO (1996): ‘Various statements of requirements have been made, and both needs and capability change with time. The statements given here were the most authoritative at the time of writing, and may be taken as useful guides to development, but are not fully definite’. The WMO assigns great importance to wind-profile measurements. The realisation of their requirements would represent a major step forward in improving the quality of atmospheric flow analyses.

Current satellite capabilities for wind profiles consist of image-derived cloud motion winds (CMWs). However, it should be noted that in the absence of any appreciable wind-profiling capability, the current satellite winds mainly improve wind analysis in the tropics (e.g. Kelly, 1997, or Kållberg and Uppala, 1999), and thus do not at all meet the objectives as set out in Chapter 3 and explained in Chapter 2. In order to better guide developers of observation systems, the WMO has used the current satellite capability (i.e. CMW) to set a threshold below which no impact is expected from additional wind measurements. Table 4.1 specifies the principal parameters for wind-profile observations that have been extracted from the above-mentioned WMO requirements and capabilities documents.

The goal of the ADM is to provide the data to substantially improve the analysis of the atmospheric flow over the whole globe by the provision of global space-borne wind-profile observations. For this purpose, it is not necessary to entirely fulfil the optimum requirements as proposed by the WMO. Rather, a useful demonstration would be to show the beneficial impact of wind-profile observations on atmospheric analyses with a performance better than current satellite wind-sensing capabilities. With respect to this threshold, as given in Table 4.1, the vertical resolution and accuracy requirements are of particular importance in order to meet the objectives of the ADM. Obviously, in selecting a candidate demonstration mission, a requirement is the perspective of the growth potential to provide improved performance in a follow-on operational mission.

		Ideal Requirements			Threshold Requirements		
		PBL	Tropo- sph.	Strato- sph.	Troposphere Lower Higher		Strato- sph.
Vertical Domain	[km]	0-2	2-16	16-30	0-5	5-16	16-20
Vertical Resolution	[km]	0.1	0.5	2.0	5	10	10
Horizontal Domain		global			global		
Number of Profiles	[hour ⁻¹]	30,000			100		
Profile Separation	[km]	50			> 500		
Temporal Sampling	[hour]	3			12		
Accuracy (Component)	[ms ⁻¹]	1.5	1.5	2	5	5	5
Horizontal Integration	[km]	50			50		
Error Correlation		0			-		
Reliability	[%]	High			High		
Timeliness	[hour]	1			4		

Table 4.1. Ideal and threshold requirements (indicating minimal impact) for providing global wind-profile measurements as derived from WMO (1996, 1998). Much room is provided for improving the global wind-sensing capability.

This chapter discusses the useful performance specifications for a global spaceborne wind-profiling demonstration mission, meeting the objectives as set out in Chapter 3.

In order to derive useful performance specifications, it is important to assess what scales are being analysed through the current GOS and atmospheric data-assimilation systems through a discussion of the meteorological analysis problem. Based on what is being analysed, the characteristics of complementary wind information in order to meet the ADM objectives are discussed.

4.2 Meteorological Analysis

Section 2.2 describes the general problem of meteorological analysis in the context of NWP and climate studies. Here, the data-assimilation methodology is addressed,

namely how the information contained in the GOS is projected into a spatially and temporally consistent atmospheric state.

Figure 4.1 illustrates the process of meteorological data assimilation. The vertical axis represents the atmospheric state. The atmospheric state is usually discretised on a three-dimensional grid. Global models typically have an effective grid distance (sampling) of 50 km in the horizontal and about 500-1000 m in the vertical. This is also compatible with many regional NWP models. A sample of the atmosphere has thus substantial spatial dimensions and only sample-mean quantities are analysed and represented in a meteorological model. The meteorological model first guess (typically a 6-hour forecast) is not perfect and data-assimilation schemes estimate its error size and error structure.

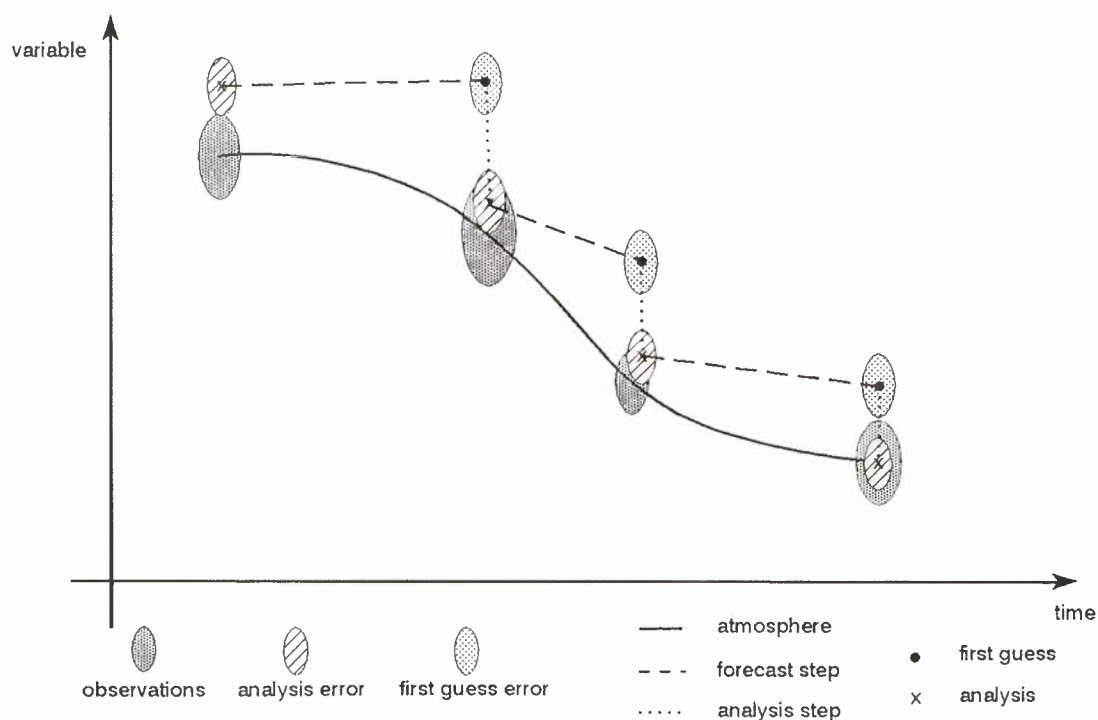


Figure 4.1. Meteorological data assimilation.

Meteorological models describe the evolution of the atmospheric state. Its chaotic behaviour causes small-scale uncertainties to grow rapidly in amplitude and size, i.e. they form unstable small-scale atmospheric perturbations. Moreover, meteorological models may under- or overestimate weather developments. It is clear that observations are needed to determine the precise atmospheric circulation. The observations indicate the state of the atmosphere, but may contain detection or processing (interpretation)

uncertainties and they might be in a different spatial and temporal representation than the meteorological model variables (vertical axis in Fig. 4.1).

The first guess contains information on past observations, which are, after incorporation into the analysis, projected forward in time by the meteorological model. Figure 4.1 illustrates a sequential process, where an instantaneous spatial (three-dimensional) analysis is performed at regular time intervals. Many centres are now developing data-assimilation procedures that take into account the dynamics during the assimilation period of the meteorological model and are therefore four-dimensional in nature. Otherwise these four-dimensional schemes are conceptually similar to the three-dimensional schemes.

The analysis step of the data-assimilation cycle combines the knowledge on the atmospheric state from observations and first guess. It maximises the probability of the atmospheric state being close to reality, given the current observations and the first guess by varying the atmospheric state until its probability is maximal (Lorenz, 1986). So, if at a particular location the observation and the first guess disagree, then the model state is modified, such that a more likely state results. The amplitude of the modification depends on the estimated error covariance of the observation relative to the estimated error covariance of the model. The lower the estimated observation error, the more impact the observation will have. In order to predict the first-guess error, the expected analysis error is computed and projected forward in time to match the forecast-lead-time of the first guess. The errors of the observations and the first guess are by approximation independent.

4.2.1 Horizontal and Vertical Scales

From statistical studies (e.g. Hollingsworth and Lönnberg, 1987) it is well known that errors in the first guess are spatially correlated. The analysis thus includes a spatial filter consistent with these error correlation scales (Rabier et al., 1998b). Moreover, errors in the mass (pressure, temperature) and wind fields are approximately in geostrophic balance, which suggests that a multivariate analysis is necessary. This means that mass observations impact the wind field and vice versa (through the geostrophic balance). An example of the multivariate spatial first-guess error structure is given in Figure 4.2. The vertical depth is small and roughly 2 km in most places, but depending on height. In the horizontal, meteorological model wind errors are lateral in nature and small-scale in the transverse direction, typically 200 km (half-width half-maximum), but depending on latitude.

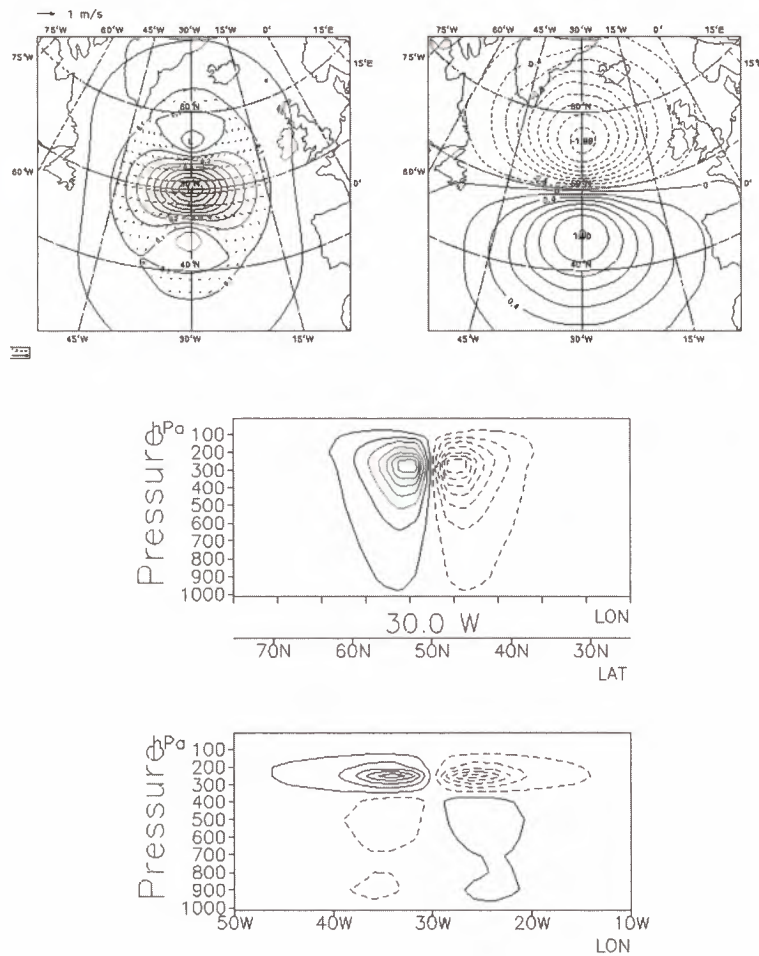


Figure 4.2. Multivariate spatial structure used for filtering in meteorological data assimilation (Courtesy E. Andersson, ECMWF).

4.2.2 Wind Components and Line-of-Sight Winds

In the multivariate analysis, the wind vector is decomposed into two independent horizontal wind components, although there is no principle problem for assimilating a true three-dimensional wind vector into atmospheric models. The average vertical-wind component is small over a typical meteorological model grid box (Courtier et al., 1992). The two components may be taken relative to an instrument line-of-sight (LOS) direction. So, the horizontal LOS wind component (HLOS) can be simulated from the model state. The provision of only one wind component is thus of no limitation to the data assimilation process, just as it is no problem to assimilate a temperature measurement without a wind measurement. A measurement of any one variable leads to a balanced impact on all analysis variables.

Lorenz et al. (1992) have verified the hypothesis that LOS winds are sufficient in an OSE where either no, one, or two components of a CMW vector were assimilated, and

they found half the impact when only one wind component, rather than both, was used. Moreover, in an additional experiment, where 50% of all CMW vectors were randomly removed, 50% of the impact of all CMW was also found. Thus, the expected analysis impact of two-wind-component measurements is the same for two collocated orthogonal components and for two spatially well-separated measurements of one single component. This means that matching of multiple azimuth 'looks' in one geographical area is not very useful.

At very small scales (e.g. the footprint of a DWL) and in extreme cases (e.g. thunderstorms) the vertical component of the wind may be quite substantial and the assumption to neglect vertical motion is strictly not valid in such situations. However, current NWP models cannot represent these small scales and as such the vertical motion is regarded as an unwanted component of the measurement and treated as part of the so-called representativeness error. The representativeness error is further discussed below.

4.3 Coverage Requirements

4.3.1 Vertical Domain

While observations of wind profiles are most wanted in the upper troposphere, i.e. between 5 and 16 km (upper limit depending on latitude) wind profiles will be useful over the full range between 0 and 16 km. In addition, as more forecast models are being extended into the stratosphere, wind profiles in the lower stratosphere (between 16 and 20 km) will be useful as well.

4.3.2 Vertical Resolution

In the vertical, meteorological model levels are at roughly 500-1000 m separation and typical error correlation lengths around 2000 m. Range integration over 1000 m is thus appropriate. The required resolution in the stratosphere is lower, i.e. 2000 m. In the planetary boundary layer the required useful resolution is higher because of the particular vertical structure of the flow. On the other hand, observations close to surface are relatively abundant in the current GOS (e.g. scatterometer, SSM/I winds and CMW) so new wind observations are expected to have less impact than those in the higher troposphere.

4.3.3 Horizontal Domain

Wind-profile observations are required globally. Due to the shortcomings of the current observing system (see Section 2.2), they are particularly needed over the oceans, in the tropics, and in the Southern Hemisphere.

4.3.4 Horizontal Resolution

What horizontal scales are resolved in current meteorological analyses depends on the current GOS and on the data-assimilation methodology. Although both meteorological models and analysis methodologies are evolving, it is noted that the spatial extent of the horizontal error correlation structures (such as in Fig. 4.2) is to some extent determined by the density of the GOS. If a much denser observation network was available, then smaller scales would be resolved. However, it is difficult to achieve this with a single supplementary observation type, so it is not expected that the spatial extent of these functions will change dramatically in the coming decade, without the availability of a global wind-profiling network (see also Section 2.4).

Small-scale weather is determined by coherent structures such as that provided by the structure functions (see Fig. 4.2). Currently, the transverse wind correlation distance is roughly 200 km (half-width half-maximum). This means that one observation mainly provides information on the error of the model state in a spatial context of about 200 km. Consequently, observation information on the model atmospheric state is independent as long as observations are at least separated by 200 km. Reflecting the above needs, a horizontal sampling of 200 km is required for the ADM.

There is no requirement on a particular sampling scheme since the assimilation process is capable of handling varying spatial representation.

4.3.5 Space and Time Scales

A requirement on temporal coverage may be derived by considering the typical time scale of evolution associated with structures of a spatial dimension equal to the structure functions. This time scale is a day, and a sensible requirement is full global sampling every 12 hours.

If each wind profile represents a box of 200 km by 200 km on the Earth's surface, then the total Earth surface contains about 13 000 boxes. Therefore, 26 000 independent wind-component-profile observations every 12 hours would define the three-dimensional global wind vector field completely, resulting in about 2000 observations per hour. It is clear that the threshold coverage, which beneficially impacts the analyses and can be used to demonstrate the potential of a spaceborne wind-profiling mission, can be significantly smaller. This is reflected in Table 4.1 (and the results in Section 2.3), which indicates the potential for improving meteorological analyses by wind profiling. It is useful for future operational missions to have capabilities beyond that of the ADM.

An improved analysis of the atmospheric flow will lead to an improved NWP skill. Experiments (OSE) with conventional radiosonde wind profiles at ECMWF (Kelly, 1997, and Ingmann et al., 1999) and NCEP (Atlas, 1998) have shown that the density of this network is sufficient to be a key component of the GOS for providing NWP improvement (see Section 2.3). However, its coverage is limited to land areas and furthermore most concentrated over Europe and the USA; the total number of wind component profiles is 1200 per 12 hours (600 vector profiles) or 100 per hour. Based on these findings emerging from the OSEs, it is argued that the extension of the wind-profile coverage to the oceans at a similar density to the current (land-based) radiosonde network would provide an analysis with much more uniform quality. This would improve atmospheric flow analyses and be of great benefit to NWP and climate studies. Therefore, 100 HLOS profiles are required for the ADM.

4.4 Quality of Observations

The quality of observations can be expressed in terms of their accuracy, error correlation and reliability.

4.4.1 Definitions

For wind observation in low-backscatter regime, the number of events (photoelectrons) per measurement interval, detected at receiver level, can be close to the number of 'noise' events. Speed estimation performed on such noisy signal leads to bad estimates of speed for some realisations of the process where noise mimics the signal. Making many realisations of the process with a given retrieval algorithm, a probability density function (PDF) of the speed estimation (V_w) can be computed. It looks like a cluster of localised good estimates (bell shape) around the true mean speed (V_{true}) sitting on a pedestal of uniformly distributed bad estimates (shaded zone) extending over the wind search window ($2 \cdot V_{search}$), as shown in Figure 4.3.

An approximate model of the estimation PDF is as follows:

$$PDF(V_w) = (1 - F) \frac{1}{V_{search}} + \frac{F}{(2\pi)^{\frac{1}{2}} \sigma_w} \exp \frac{-(V_w - V_{true})^2}{2\sigma_w^2} \quad (4.1)$$

The accuracy (σ_w) is the random part of the wind-speed estimation error. It is defined as the standard deviation of the estimates (σ_w) (good estimates) falling under the bell shape. The reliability (F) is the complement to unity of the percentage of estimates (bad estimates) contained in the pedestal of uniform distribution.

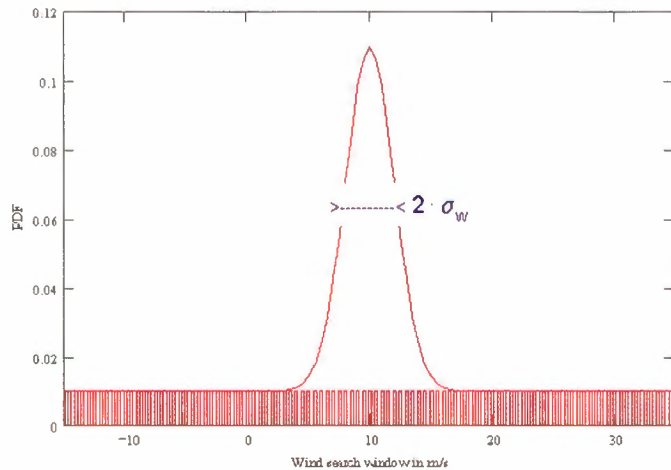


Figure 4.3. The estimates PDF model looks like a cluster of localised good estimates (bell shape) around the true mean speed sitting on a pedestal of uniformly distributed bad estimates (shaded zone) extending over the wind search window.

4.4.2 Accuracy

Wind variability depends on height, and as such the accuracy requirement is height-dependent. Wind variability spectra will be discussed in the context of the representativeness error in the next paragraph.

Given the experience gained from meteorological analysis for NWP, it is clear that radiosonde wind observations are a key element of the GOS. Their wind component accuracy varies from 2 ms^{-1} close to the surface to 3 ms^{-1} around the tropopause level, which is close to the accuracy of the first guess. As a demonstration, Figure 4.4 shows a vertical profile root-mean-square (RMS) first guess minus observation differences, including both the first-guess and observation-error variances.

Over data-sparse areas the $2\text{-}3 \text{ ms}^{-1}$ accuracy requirement is expected to be sufficient to provide a beneficial impact on meteorological analyses. This requirement is significantly higher than the threshold requirement quoted in Table 4.1, as experience in meteorological data assimilation shows that observations with an accuracy poorer than the first guess often fail to have a beneficial impact on NWP. In fact, data substantially poorer often have a detrimental impact.

Provision of quantities over volumes that are representative of the meteorological model's grid box is needed. A typical horizontal grid box size is 50 km. However, often a true mean quantity can not be derived, so a spatial representativeness error remains. Lorenc et al. (1992) investigated this representativeness error for HLOS in detail by considering typical wind-component-variability energy-density spectra. The representativeness error turns out to be height-dependent (Table 4.2), but the dependency of this error on mean wind speed appears not demonstrable for jet-level

winds (at 10 km height). This error should be added to the detection and processing errors (error variances) of a wind-profile measurement before attempting to validate it against the accuracy requirement. A line-averaged wind has a smaller representativeness error than a point measurement by a factor of $\sqrt{2}$. For the ADM, a horizontal integration of 50 km within a 200 km box (see Section 4.3) is required.

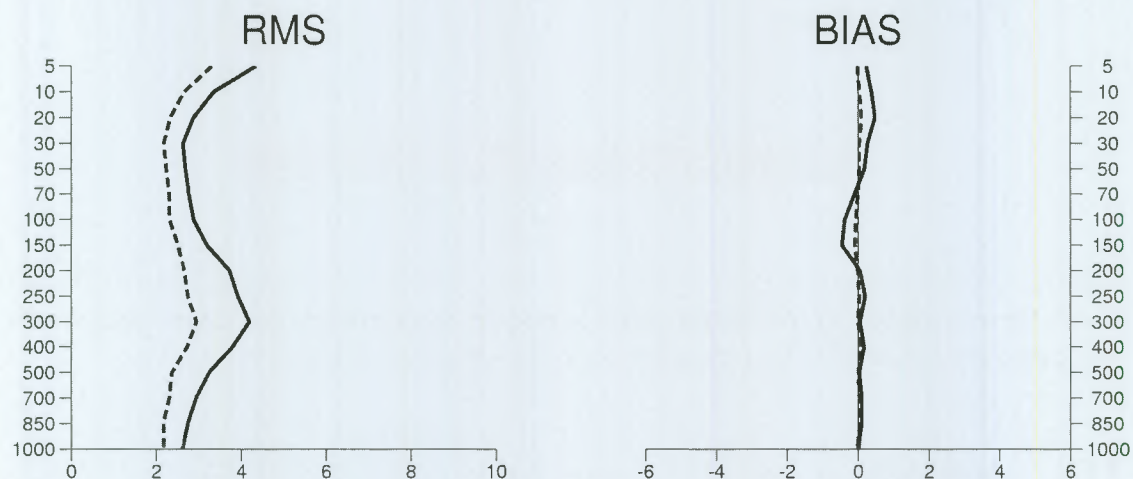


Figure 4.4. Vertical profile RMS first guess minus observation differences – differences (left) and biases (right) in ms^{-1} for Northern Hemisphere latitudes between 20 and 90 degrees. The vertical axis is in hPa (left). Dashed lines indicate the differences of the radiosondes with the analysis. The graphs provide an indication of the first guess and radiosonde wind errors (Courtesy L. Isaksen, ECMWF).

Pressure [hPa]	Point Error [ms^{-1}]	Line Error [ms^{-1}]
1000	2.1	1.5
750	2.0	1.4
500	2.4	1.7
250	3.3	2.3
150	2.4	1.7
50	2.1	1.5

Table 4.2. Spatial representativeness error for a point measurement and for a line-averaged component wind for a 50 km horizontal scale.

Observation accuracy and first-guess-field accuracy are used to determine the weight of an observation over the first guess. Improper prior specification of the observation error will therefore lead to a wrong assessment of the value of the observation, and consequently to an inferior analysis. As DWL winds have variable accuracy, it is important to develop algorithms that are able to define their accuracy prior to assimilation.

From these consideration an accuracy of 2-3 ms⁻¹ over the height range from 2 to 16 km is required from the ADM.

4.4.3 Error Correlation

Bias has a context-sensitive interpretation and as such this term may cause confusion. Spatial or temporal error correlation is more specific if one furthermore specifies the spatial or temporal scales involved. Below, several relevant spatial scales are discussed. Error correlation requirements on the smallest or shortest scales are usually the most difficult to meet.

Spatially correlated error is potentially very damaging in data assimilation, in particular when the error structure is a priori not well known. For example, the spatial error structure in satellite temperature and humidity profiles (TOVS) has been a problem in meteorological data assimilation for more than a decade. In particular, when the precise spatial observation error correlation characteristics are poorly known, then the analysis may have high-pass-filter characteristics and the resulting analysis can be noisy.

Any systematic error in the analysis will have the multivariate and spatial structure prescribed by the structure functions, i.e. the error is meteorologically balanced and will influence the evolution of the model state in an effective way. Air-mass-dependent errors are the most damaging, since these potentially change the way in which air masses interact.

One piece of information required from wind profiles is the vertical wind-shear. The first-guess vertical error-correlation scale is small and so, given the filter properties of the analysis, it is clear that any vertical correlation structure of error in the wind-profile measurements may be potentially very damaging, since the wind-shear information may be lost. If the aim is to be able to measure a wind shear of 2 ms⁻¹ between two adjacent levels, then a correlated error of a few tenths of a ms⁻¹ may already significantly blur the detection of such shear instability. (Note that a data assimilation system can handle wind-shear measurements directly. However, in this case it is even more important to have independent measurements in a vertical wind profile.)

Correlation of error between profiles, although possibly less damaging than vertical error correlation, does require attention. Experience with other satellite sensors has shown that systematic errors or errors that depend only on specific instrument characteristics or orbit phase (Sun angle) can be taken out by calibration against a meteorological model (e.g. Stoffelen, 1998). Obviously, in this case the meteorological model is calibrated by using conventional observations. For calibration

of an observing system against a meteorological model, it is an absolute requirement that the observing system is stable.

In summary, a useful and practical specification for systematic offsets is that the correlation between the error variances of any two wind measurements is less than 0.01.

4.5 Reliability and Data Availability

4.5.1 Reliability

Routine data-assimilation systems include a quality-control procedure to prevent measurements that are grossly in error affecting the atmospheric analysis. When a gross error occurs, the observation does not relate to the (model) atmospheric state and can therefore potentially damage the objective analysis, leading to an incorrect picture of the state of the atmosphere. For conventional systems, gross errors are usually due to transmission or instrument failure, or to unrepresentative measurements. A classic example of the latter is the release of a radiosonde through a thunderstorm. Forecasts are known to be sensitive to gross-error elimination procedures in critical atmospheric conditions (ESA, 1996).

Many operational centres are using or developing variational analysis systems. The variational analysis system is quite flexible in dealing with observations with complex error characteristics. However, for the measurements to be useful, these observation characteristics have to be known in detail a priori. Experience with conventional observation systems and associated quality control (QC) decisions in operational meteorological analysis indicate that the rate of gross errors presented to the analysis (after QC) should be only a few percent. As such, all signal characteristics have to be used in the processing to optimally specify the observation operator and cost function in order to help reject measurements containing no information on the true atmospheric state. All this is necessary to prevent random wind estimates, by coincidence close to the true wind, from influencing the analysis. Based on this experience, it is required that the observations need to have a reliability of 95 %.

4.5.2 Data Availability

In a meteorological data-assimilation system those meteorological observations provided in a timely fashion by the GOS are compared to the first-guess atmospheric state. As such, the error characteristics of the first guess are well monitored and the first guess is a well-defined reference atmospheric state. In turn, this reference atmospheric state is used to routinely monitor and control the observations. If observations are not available in due time, then this routine monitoring and control is not performed, and special measures have to be taken to collocate the observations

with the meteorological model and other observations in order to characterise the error properties of such observations. It is clear that the routine monitoring, collocation, and control of observations in the main real-time data stream is to be preferred above an off-line processing.

After the error characteristics of a new observing system have been determined, experimentation with the assimilation of the data will commence. If the observations are delivered in real time, then the operational data assimilation and forecast suite can be used as a reference or for a control experiment. If it is demonstrated that the new observing system adds to the improvement of the weather forecast of the control experiment, then the real-time assimilation of the data would start for NWP.

Timely data delivery is then required since analyses start at pre-specified times and a data cut-off time is applied. For NWP, acceptable data-delivery times for short- and medium-range forecasting vary generally between 30 minutes and more than 6 hours, depending on the analysis time window and analysis cut-off delay. A data-delivery requirement of 3 hours is usually specified for spaceborne data (as practicable for global and regional NWP) and is common for polar-orbiting spaceborne operational meteorological instrumentation.

The length of the observational data set needed to achieve the objectives of the ADM is at least 3 years.

4.6 Conclusion

The observation requirements discussed in this chapter consider the presence of the current GOS and the complementarity with it. Alike many other meteorological observations, the spaceborne LOS wind-component profiles by themselves seem at first glance to be of limited value, but in the context of atmospheric data-assimilation systems they would in fact be an essential component of the GOS. Besides better weather forecasts, improved meteorological analyses are very useful for studying circulation and transport phenomena relevant to climate and atmospheric composition studies. Moreover, the meteorological analysis fields already provide consistent atmospheric data sets of wind, humidity, temperature and, in the coming years, ozone and probably aerosol distributions. The monitoring of the quality of meteorological analyses is best done in real time by collocation with and rigorous comparison to a wide range of real-time meteorological observations, complemented by off-line validation studies.

For a mission intended to demonstrate the feasibility of a full-scale spaceborne wind observing system to improve global atmospheric analyses, the requirements on data quality and vertical resolution are the most stringent and most important to achieve. Under this assumption, the horizontal density of observations is of the lowest priority amongst the requirements discussed in this chapter. The derivation of the coverage

specification is supported by weather-forecast-impact experiments, which included the inputs of the conventional wind-profile network that is thin and irregular but of key importance. Moreover, the coverage specification reflects the WMO threshold requirements (see Table 4.1).

Table 4.3 provides an overview on the requirements discussed previously.

		Observational Requirements		
		PBL	Troposph.	Stratosph.
Vertical Domain	[km]	0-2	2-16	16-20
Vertical Resolution	[km]	0.5	1.0	2.0
Horizontal Domain		global		
Number of Profiles	[hour ⁻¹]	100		
Profile Separation	[km]	> 200		
Temporal Sampling	[hour]	12		
Accuracy (Component)	[ms ⁻¹]	2	2-3	3
Horizontal Integration	[km]	50		
Error Correlation		0.01		
Reliability	[%]	95		
Timeliness	[hour]	3		
Length of Observational Data Set	[yr]	3		

Table 4.3. *Observational requirements of the Atmospheric Dynamics Mission.*

As explained above, the meteorological impact in the tropics is the most certain, and, from a climate point of view, also the most useful. Moreover, to improve atmospheric analysis beyond the tropics and in particular NWP in Europe, the above requirements have been chosen to demonstrate the advantageous impact of DWL winds at high latitudes.

The implementation of the ADM will be a major step forward in providing greater insight into atmospheric processes by providing wind profiles over the whole globe for the first time. This makes this mission unique and a true explorer mission.

5 Mission Elements

5.1 Introduction

The innovative element of the Earth Explorer ADM is the provision of wind-component profiles by a DWL onboard a polar-orbiting satellite. The wind profiles will be provided by an instrument based on the direct detection technique. After pre-processing, the DWL data will appear as profiles of LOS winds, i.e. a profile of one wind component per observation point. These DWL data will be an extra input data set to atmospheric analysis systems, added to the other observation types currently available (see Chapter 2). The analyses provided by different data-assimilation systems in different NWP centres will be used for climate studies, for forecasting the weather, and form the natural basis for most of the other studies. Figure 5.1 illustrates these links.

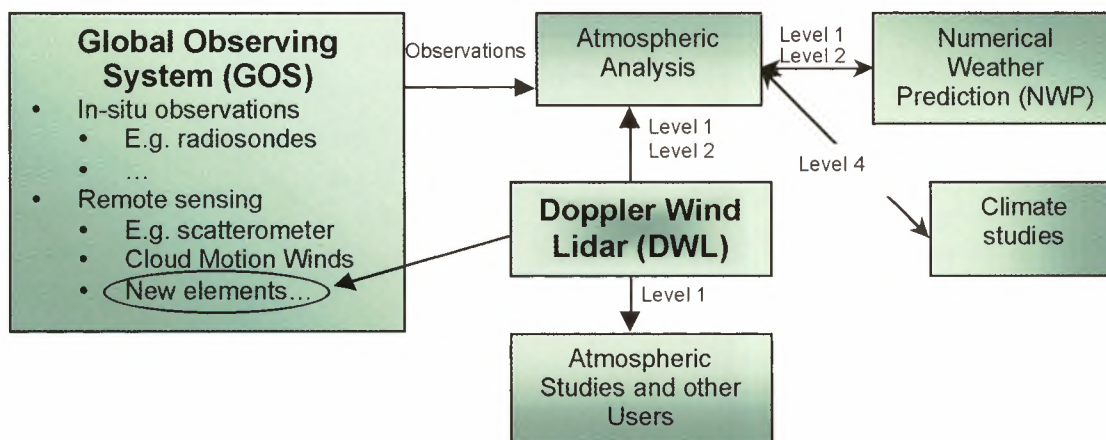


Figure 5.1. End-to-end elements of the Atmospheric Dynamics Mission.

The direct use of LOS winds for geophysical studies will be exceptional, although LOS winds are likely to be used directly for validation and retrieval process development purposes. However, the backscatter data from the instrument provides information instrumental for some aspects of atmospheric research and will be used as such.

5.2 Instruments and Data

5.2.1 Doppler Wind Lidar Instrument Principle

The DWL is an active instrument which fires laser pulses towards the atmosphere and measures the Doppler shift of the collected return signal, backscattered at different

levels in the atmosphere. The frequency shift results from the relative movement of the scatter elements along the line of sight of the instrument. This movement relates to the mean wind in the observed volume. The measurement volume is determined by the maximum ground integration length of 50 km, the required height resolution and the width of the laser footprint. The measurements are continuously repeated at distances of about 200 km.

Light is scattered either by interaction with aerosol or cloud particles (Mie scattering) or by interaction with air molecules (Rayleigh scattering). The two scattering mechanisms exhibit different spectral properties and different wavelength dependencies such that instruments evaluating only one signal type or both in separate processing chains can be constructed.

For Mie backscattering, the spectrum of the received Doppler shifted light equals the transmitted spectrum slightly broadened by the wind variability within the measurement volume. In case of molecular scattering, the Brownian motion of air molecules significantly broadens the received spectrum to a width equivalent to wind speed such that the spectral width resembles Doppler shifts equivalent to several 100 ms^{-1} . The mean Doppler shift resulting from average air motion represents therefore in this case a much smaller fraction of the spectral width than in the case of aerosol scattering. Thus for molecular scattering, a much higher signal is needed for the same velocity measurement performance, but as noted above the received signal level from molecules has different dependencies compared with aerosol scattering.

The return signal strength from aerosols scattering depends on their concentration, which varies largely over different locations, altitudes, and time. Aerosols are most concentrated in the lower 4 km of the troposphere and diminish above the troposphere. A system relying only on aerosol backscattering can therefore not provide measurements at higher altitudes. On the other hand, ground return signals useful for ground-speed calibration and signals from clouds exhibit the same spectral properties as the aerosol signal and can hence be best processed by such a receiver system.

Contrary to the Mie signal, the molecular backscattering signal under clear atmospheric conditions is only weakly dependent on the aerosol content (attenuation) and exhibits only small variation with altitude. This allows more consistent measurements up to altitudes above 20 km. However, Rayleigh receivers suffer from accuracy limitations at low altitudes ($< 2 \text{ km}$) due to the aerosol absorption.

This complementary behaviour of Mie and Rayleigh return signals suggests a combination of two dedicated receivers in a single instrument in order to allow accurate measurements over the entire altitude range.

There are two measurement techniques to measure these effects, namely the coherent heterodyne systems and the direct detection, interferometric systems. There are in fact very profound differences of principle in their respective operation. Coherent

heterodyne systems operate by beating the scattered and Doppler shifted radiation with an optical laser oscillator at the surface of a detector. The resultant electrical beat-frequency signal is thus analysed post-detection to produce the Doppler frequency. On the other hand, in the direct detection methods the optical signal field is analysed and dispersed in an interferometric filter prior to detection. Both systems require interferometric precision in the optical manipulation of the signal beam. However, due to the very different physics of these schemes, the performances are very different in principle. For heterodyne systems the key parameter is shown to be the photon degeneracy – that is the number of photo-detections per optical mode (i.e. in a single coherence area and coherence time). In low-backscatter conditions, this requires that the available laser power to be distributed into pulses of the largest possible energy. However, for direct-detection interferometric systems, the accuracy depends only on the total scattered signal and is not dependent on the energy of individual pulses, only on the total laser energy.

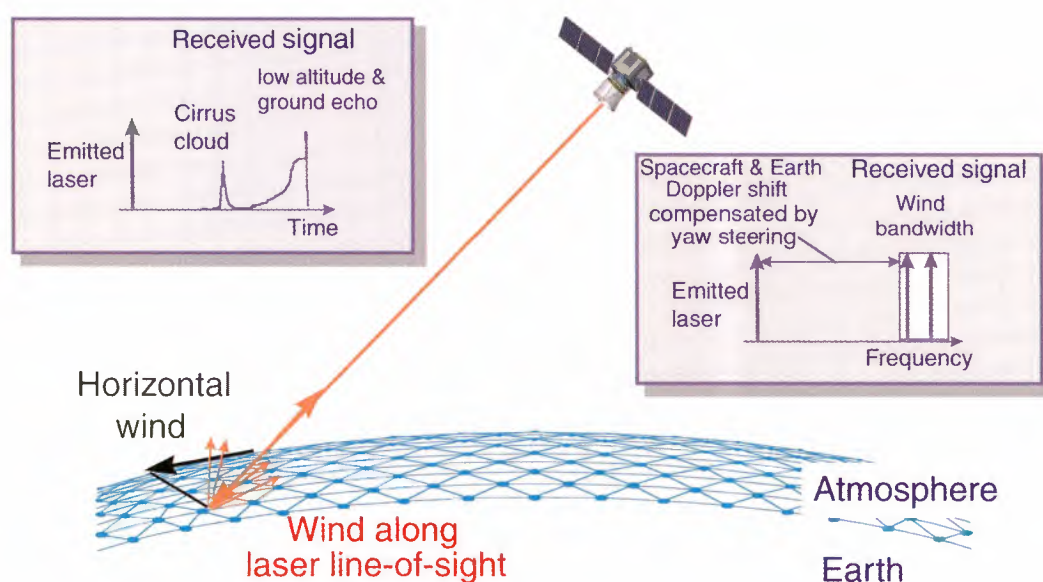


Figure 5.2. *Doppler Wind Lidar principle: The lidar emits a laser pulse towards the atmosphere, then collects, samples, and retrieves the frequency of the backscattered signal. The received signal frequency is Doppler-shifted from the emitted laser due to the spacecraft, Earth, and wind velocity. The lidar measures the wind projection along the laser line-of-sight, using a slant angle versus nadir.*

There is a considerable heritage of ground and airborne laser Doppler systems for wind measurement. Validation and calibration studies have been carried out with coherent detection of aerosol scattering at 2 and 10 μm and show performance very close to the expected quantum limit. Investigations include measurements throughout the troposphere, studies of valley drainage, boundary-layer phenomena and movement of pollution, studies of aircraft wake vortices, airborne measurements of clear-air

turbulence, wind shear and backscatter strength around the Atlantic and Pacific Oceans. Direct-detection systems have been developed more recently; very promising performance has been demonstrated with both the multi-channel (MC) and double-edged (DE) variants of the basic technique. These include scattering from both aerosol and molecular sources. All of these systems and their variants have the potential for application to spaceborne operation, and detailed investigations have been undertaken to model their use.

5.2.2 Core Space Elements

The core space element of the ADM is ALADIN (Atmospheric Laser Doppler Instrument), a direct detection lidar incorporating a fringe-imaging receiver (analysing aerosol and cloud backscatter) and a double-edge receiver (analysing molecular backscatter). The instrument will be accommodated on a satellite, flying in a Sun-synchronous, polar orbit, at an altitude of 400 km and with a local equator crossing at 06:00 and 18:00 hrs. This orbit allows a (near-)global coverage.

The processing of the backscatter signals will produce LOS wind profiles above thick clouds or down to the surface in clear air along the satellite track, every 200 km. Wind information in thin cloud or at the tops of thick cloud is also attainable. From the data processing, information on other elements like clouds and aerosols can also be extracted. The data will be disseminated to the main NWP centres in near-real-time.

5.2.3 Ground Segment

In order to fulfil the near-real-time requirement, the proposed ground segment is based on two receiving locations for the scientific data, situated in the Northern Hemisphere (Kiruna and the Barrows meteorological station). The downlink is based on the HRPT (high-resolution picture transmission) standard, as it is being defined and implemented for the METOP mission, allowing the use of equipment familiar to the meteorological community. For satellite command and control, the Kiruna Salmijaervi station will be used.

The data will then be relayed via standard communication links to the mission operations centre. This centre takes responsibility for the spacecraft operations, as well as the data processing up to Level 1. After the data is processed and calibrated, it will be sent to a dedicated scientific data centre, which will be responsible for the quality control, as well as the dissemination of the data to the meteorological centres and other end users.

5.3 Atmospheric Analyses and NWP Forecasts

Although any observation type can be used on its own for particular studies, it is clear that the most powerful usage is achieved through data-assimilation systems in which the different data and observations are combined (synergetic use of observations and an atmospheric model) in order to provide the best estimate of the atmospheric parameters which are relevant for forecasting and other process studies. In this synergy, the DWL measurements will complement other data in order to fill major gaps in wind-profile observations, which currently are mainly provided by radiosonde stations. No other observing system is planned to fill this gap except the ADM. The DWL data will provide an important new input element to data-assimilation systems which are run in several NWP centres.

Data from other sources will be needed for the analysis of the DWL observations. The different observation types are described in Chapter 2, together with their respective performances and limitations. They are in particular

- the in-situ meteorological data (surface and upper-air ground-based data) and
- the current remote-sensing data.

The link between the lidar processing and a data assimilation system will be interactive, as it is for example already now with satellite sounder data whose retrieval is supported by the knowledge of a background field (generally a short-range numerical forecast, using schemes called RT-TOVS in the case of TOVS or ATOVS). A prior knowledge of the atmospheric state from a background may help the signal processing. It is, however, expected that the information fed back from the NWP models to the DWL data production will remain small, and that the lidar wind errors will not be dependent on any NWP model error.

6 System Concept

6.1 From Mission to System Requirements

The mission requirements, as defined in Chapter 4, have been translated into system observational requirements in order to highlight the design drivers for the engineering work.

Measurement Accuracy Requirement

The mission requires the measurement of horizontal wind velocity components from the lower part of the troposphere to the lower part of the stratosphere (up to 20 km altitude). The observation of a single component of the horizontal wind velocity is required to ease the instrument design since it has been shown to be adequate for the ADM (see Chapter 4). Furthermore, there is no particular requirement on the direction of the wind component to be measured.

The required instrumental accuracy for any horizontal wind component, hereafter called HLOS, has been translated from the mission accuracy requirement of $2\text{-}3\text{ ms}^{-1}$. The background representativeness error for a line-averaged wind component measurement of 50 km (see Table 4.2) has been quadratically subtracted from the mission accuracy requirement, yielding an instrumental accuracy requirement of $1\text{-}2\text{ ms}^{-1}$ for the HLOS wind component. It has to be noted that this representativeness error includes the contribution from the vertical wind component.

Stringent requirements on both wind accuracy and large vertical domain (up to 20 km) lead to consider an instrument concept relying on molecular backscatter at high altitude, where background aerosols become rare (Vaughan et al., 1999), and on aerosol backscatter at lower altitude.

Instrument Pointing

The LOS of the instrument has to be oriented such that the HLOS measurement accuracy is optimised. A flat optimum of HLOS measurement accuracy exists for LOS angles pointing between 35° to 50° off nadir. It results from an improvement of the horizontally projected LOS wind accuracy, balanced by the increasing range with increasing nadir angle. For the selected 35° LOS nadir angle, the viewing geometry requires an instrumental LOS wind accuracy a factor 0.6 more accurate than the specified HLOS wind accuracy, i.e. $0.6\text{-}1.2\text{ ms}^{-1}$. The lower value ($0.6\text{ m}\cdot\text{s}^{-1}$) has been applied for the altitude range from 0 to 2 km, whereas the higher value is considered as a driving requirement up to the stratosphere (2 to 16 km).

Any wind-speed-component observation to be delivered to the end-users is to be referenced to an Earth surface frame located at the vertical of the probed volume. It implies, at system level, an accurate knowledge of the relative velocities of the spacecraft and the local Earth frame and of the instrument LOS pointing. The spurious Doppler shifts induced along the instrument LOS by both spacecraft and Earth rotation velocities are typically much larger than the LOS wind speed and need to be compensated to ease the instrument design. The instrument LOS pointing is set perpendicular to the spacecraft velocity, minimising the spacecraft-velocity-induced Doppler shift. A 'yaw steering' mode is implemented at spacecraft level to compensate the HLOS Earth rotation velocity. Determination of the residual spurious Doppler shift is performed by evaluation of ground echo signals where available. To maintain a sufficient knowledge of the true ground speed in periods where the ground is obscured by clouds, exact pointing measurements in combination with position knowledge is used to interpolate between calibrations.

Spatial and Temporal Coverage

The requirement of global coverage in combination with a temporal sampling of 12h requires a high-inclination orbit. Due to the measurement accuracy's dependency on range, the orbit should be as low as possible, but must not impose unacceptable constraints on the orbit (i.e. fuel needed to maintain the orbit and the requirement to ensure the contact times). No particular requirement with respect to the local time of the wind measurements has been specified; however, measurements around sunrise/sunset may benefit from fewer obstructions by clouds, at least over land. The coverage requirement does not have an impact on the altitude. Thus, a Sun-synchronous orbit at about 400 km altitude has been chosen as an appropriate compromise to meet the spatial/temporal coverage requirements. Furthermore, the selection of a local time at the ascending node around 6h or 18h (dawn-dusk) simplifies the layout of the solar-panel mechanics.

The integration length of 50 km and the measurement separation of 200 km imply an instrument duty cycle of 25%.

Data Delivery Timeliness

The requirements specify a data delay not exceeding three hours. With a time for an orbital revolution of about 1.5 h, it is necessary to download measurement data once per orbit. This requires at least two ground stations for data reception at high latitudes (e.g. Kiruna/ESA and Barrows/NOAA). Public data networks can disseminate the data due to its small volume.

The task of the data-processing centre of the ground segment consists of deriving high-quality wind-component data from the raw data. This includes application of

instrument-specific calibration procedures and instrument-specific quality control to achieve the 95% data reliability requirement.

The main system requirements derived from the mission requirements are summarised in Table 6.1.

System Requirements		Value	Origin
Mission	Operational Lifetime	3 years (consumables 4 years)	Explicit mission requirement
Instrument	Principle	LIDAR with a two-channel receiver for molecular and aerosol backscattered signals	High-quality observation requirement up to 20 km altitude
	Viewing geometry	400 km altitude; 35° off-nadir looking;	System-level trade-off
	Geometrical resolution	0.5 km vertical resolution in the PBL; 1 km vertical resolution below 16 km altitude; 2 km vertical resolution above 16 km; max. altitude 20...30 km; along-track integration 50 km	Observation requirement
	LOS wind-speed error after calibrations	0.6 m/s from 0 to 2 km < 1.2 m/s rms for 2 to 16 km	From observation requirement accounting for system geometry
	Correlated error across altitude cells and between subsequent measured vectors	< 0.06 m/s LOS or equivalently 0.1 m/s in HLOS	From observation requirement accounting for system geometry and apportioning of largest error allowance to the instrument.
	Velocity, Location and Pointing	Sensor LOS restitution between calibrations	< 0.1 m/s
Alignment stability		< 0.15 m/s	
Yaw steering		Apparent LOS ground speed < 10 m/s	To make ground Doppler variation insignificant for the definition of the dynamic range of the instrument.
Height assignment		± 250 m	Correct assignment to atmospheric layer
Data Handling, Communication	Downlink of on-board accumulated measurement and ancillary data	Once per orbit	System level allocation for timeliness requirement
Ground Processing	Time for generation of Level 1 data product, including all corrections depending on restituted orbit and pointing data	90 minutes, including time of all data transfers	

Table 6.1. Main system requirements.

6.2 Mission Design and Operations

6.2.1 Measurement Geometry

The baseline measurement geometry is shown in Figure 6.1. All measurements are taken from measurement volume cells along the LOS. The Doppler shift is determined with respect to the spacecraft movement and has to be processed to a horizontal wind speed component (HLOS) referenced to the ground.

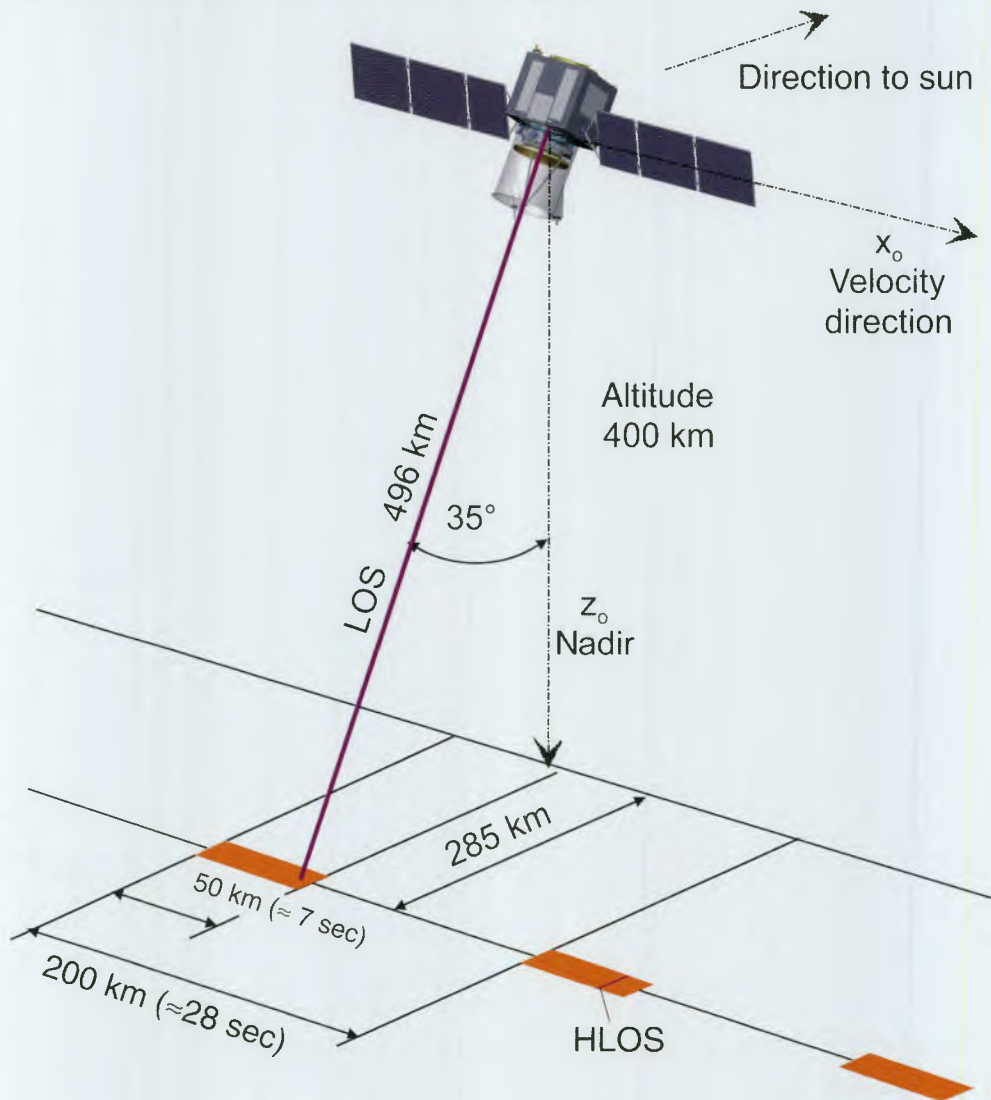


Figure 6.1. Baseline ADM measurement geometry

The actual measurement volume, as shown in Figure 6.1, is characterised by

- its vertical extension determined by measurement timing

-
- the integration length in the flight direction determined by the number of pulses contributing to a single Doppler evaluation, and
 - a negligible extension in the direction orthogonal to both other directions.

The measurement volume of the return signal from a single shot is defined by the lateral extension of the transmitted beam (a few metres in diameter) and the time gating of the receiver, which is adopted to the desired vertical resolution (several 100 m to 2 km). Furthermore, it is assured that the spatial pulse length is much shorter than the desired vertical resolution. Due to the fact that the signal from a single shot is too weak for the evaluation, several shots along a ground track of up to 50 km have to be accumulated.

6.2.2 Orbit Selection

Orbit Parameters

As justified in 6.2.2, a Sun-synchronous dawn-dusk orbit has been selected. It provides quasi-global coverage (the 7° polar gap is acceptable) and corresponds to a lower cloud coverage. Moreover, it facilitates some aspects of the satellite design.

The LOS of the instrument will be 35° off nadir to ensure the best instrument performance, and 90° across the flight direction to avoid a contribution from the satellite velocity to the Doppler-frequency shift. As the instrument should not point toward the Sun, the LOS of the instrument will point to the anti-Sun direction. The selected dawn-dusk orbit will have a LTAN of 18:00 in order to provide a slightly better coverage over the North Pole. The resulting orbit geometry and the instrument orientation is depicted in Figure 6.1.

There have been no specific requirements driving the choice of the orbit altitude. The resulting freedom has been used to optimise the mission performance while reducing the satellite and ground-segment complexity. Detailed performance simulations have been done, taking into account the main instrument parameters (telescope diameter, laser power and PRF) and the main system parameters (fuel demand and frequency of orbit maintenance manoeuvres), as well as the number of ground stations required. Orbits between 350 km and 450 km altitude are best suited in order to optimise the overall system (Fig. 6.2).

A baseline altitude of 400 km has been selected. Its parameters are summarised in Table 6.2. This orbit represents a compromise between instrument performance, data down-link capability and orbit maintenance requirements, because it offers at least one data down-link per orbit assuming only two ground stations, and reduces the fuel demand to about 65 kg for the required mission lifetime.

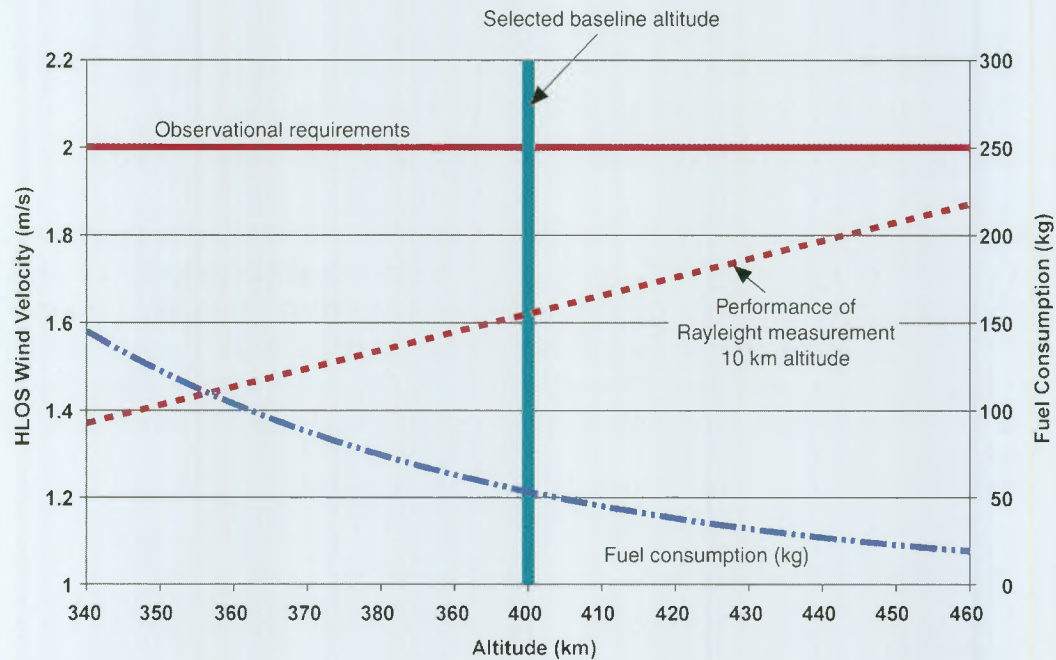


Figure 6.2. Orbit altitude versus instrument performance and fuel consumption.

	Mean Orbit Parameters
Orbit Type	Sun-synchronous frozen orbit at 18:00 LTAN
Altitude at Ascending Node	400 km
Mean Altitude	408 km
Reference Epoch	21.3.2004, 12:00:00
Semi-Major Axis	6769.14 km
Eccentricity	0.001165
Inclination	96.99°
RAAN	90°
Argument of Perigee	90°
True Anomaly	-90°

Table 6.2. Parameters of selected baseline orbit.

The selected orbit corresponds to a frozen orbit, offering constant instrument range gate timing parameters for each specific latitude. In this case the radial velocity of the spacecraft, i.e. the radius rate, is only a function of the latitude, which simplifies the

yaw steering control law. Figure 6.3 shows the altitude and altitude rate of the satellite due to the reference Earth ellipsoid (WGS '84) and the orbit eccentricity.

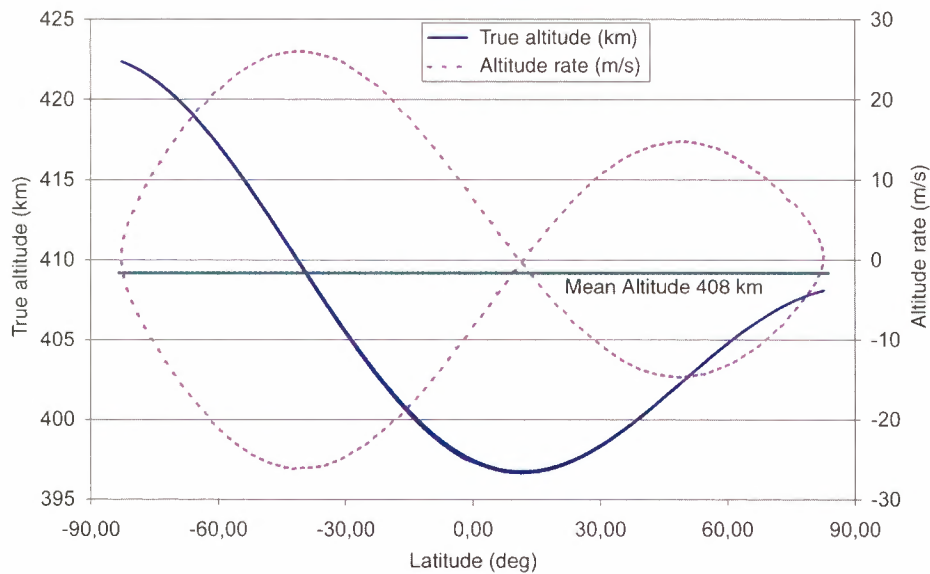


Figure 6.3. Altitude and altitude rate of selected 400 km orbit.

Orbit Maintenance

The estimated altitude decay rates are depicted in Figure 6.4, for an effective cross-sectional area of the satellite of 3 m^2 , corresponding to the selected baseline satellite configuration described in Section 6.4. For the 400 km orbit, the altitude decay after

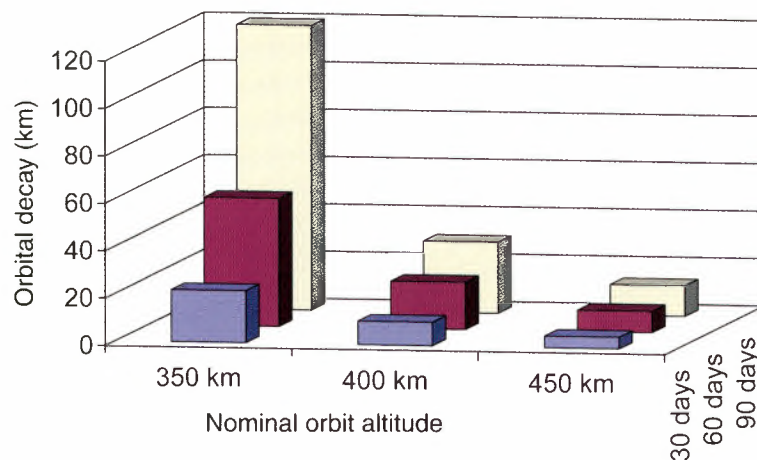


Figure 6.4. Orbital decay and fuel consumption.

30, 60 and 90 days is rather moderate and periods of up to 90 days are feasible without any orbit manoeuvre. Over the required mission lifetime of 3 years plus 1 year for consumables, the fuel consumption for maintaining the baseline altitude of 400 km will be about of 54 kg of hydrazine.

Ground Station Visibility

The ADM data shall be delivered to the user within 3 hours after data acquisition. It is necessary to have ground station contacts every orbit. A two-station combination has been selected. These are the existing ESA ground station in Kiruna and a second one in Barrow, a meteorological station located in the northern part of Alaska. The resulting ground-station visibility, assuming a minimum elevation angle of 5°, is depicted in Figure 6.39. The Barrow station already offers meteorological services and provides sufficient infrastructure for ground-station maintenance. The TC/TM ground receiving station will be co-located with the data receiving station in Kiruna.

6.2.3 Measurement Profile

Due to the required profile separation, the instrument will be operated with a duty cycle of 25 %. It will be fired during 6.93 seconds (equivalent to 50 km ground track) followed by a gap in observations of 20.79 seconds (equivalent to 150 km). As detailed later, the horizontal accumulation length can be varied from 500 m (Mie or Rayleigh channel) to 50 km without affecting performance for the integration over the full 50 km. The vertical sampling profile includes some altitude margin in order to ensure that the ground echo is acquired when the ground is visible, in order to provide calibration data.

All vertical integration intervals are pre-programmable with a vertical resolution, selectable between 100 m and 2 km up to an altitude of 40 km. The baseline measurement profile is depicted in Figure 6.5.

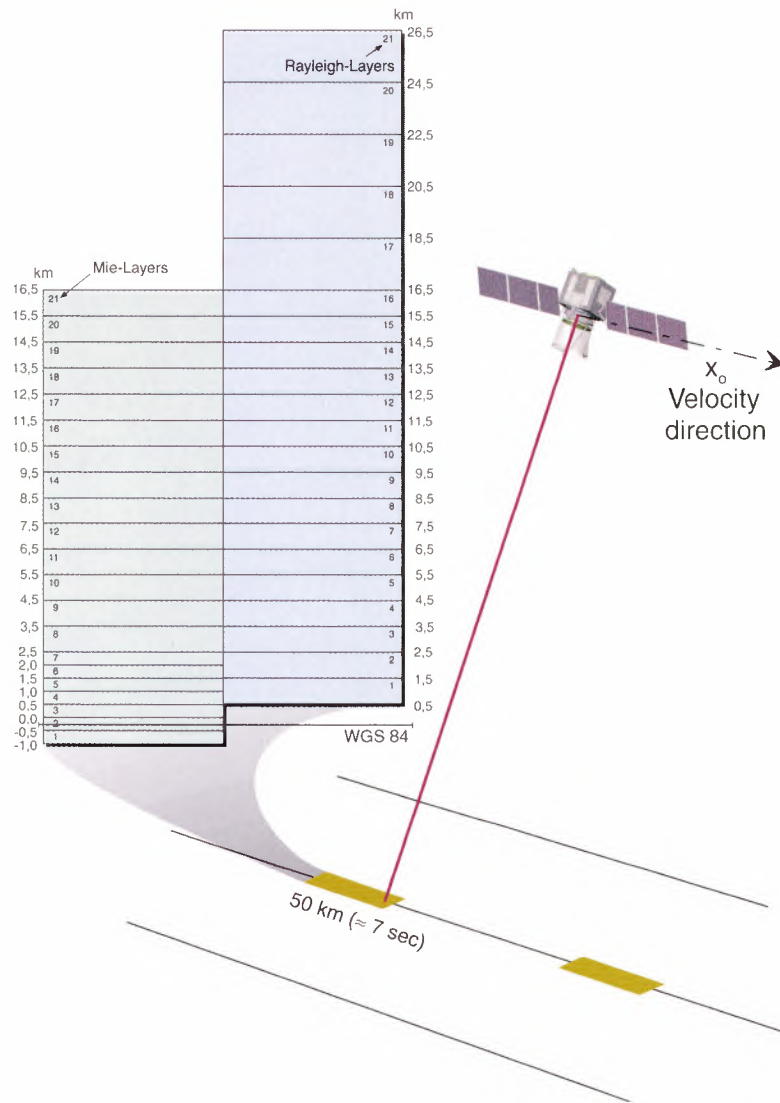


Figure 6.5. The baseline measurement profile, depicting the mapping of atmospheric heights to layers measured by the detector. The vertical as well as the horizontal values can be programmed, thus providing good flexibility.

6.2.4 Solar-Array Arrangement

Figure 6.6 depicts the relative orientation of the orbit plane with respect to the ecliptic plane for the summer and the winter solstice, while Figure 6.7 shows the eclipse times for the first year of the mission (2004). The angle between the orbit plane and the ecliptic is 60° during the summer solstice and 74° during the winter solstice. The maximum eclipse time during the summer solstice is about 27% of the orbit period. The solar array will be tilted about 10° relative to the orbital plane to optimise the energy generation during the phase with eclipse. This angle corresponds to a mean loss of efficiency of approx. 12% during non-eclipse times.

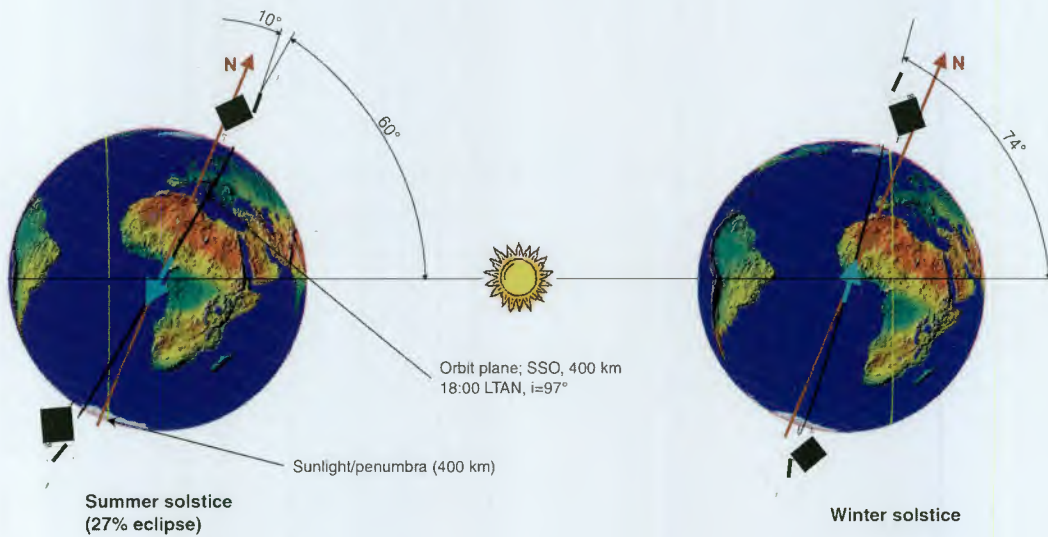


Figure 6.6. Orbit orientation during summer and winter solstice.

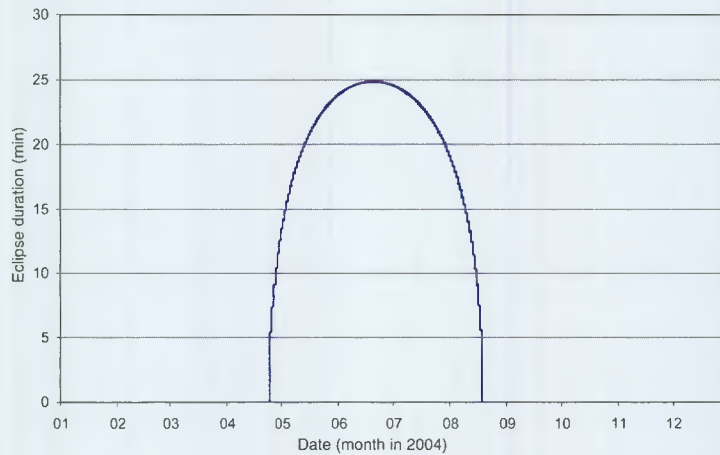


Figure 6.7. Eclipse duration for the 400 km orbit.

6.2.5 Mission Operation and Phases

The ADM is divided into distinct phases, namely the pre-launch and the launch and early orbit phase (LEOP), followed by the commissioning phase for the satellite as well as the instrument. This is followed by the normal operations phase of the mission. The launch phase and LEOP are described with the launcher in Section 6.5.

Commissioning Phase

After a successful LEOP, the satellite is in a safe hold mode. In this state, it can stay unattended for several days without any operation. From that moment on, the commissioning phase will begin. The main components of the satellite will be validated and the attitude will be changed into geocentric pointing. In a next step the yaw steering will be activated and a first thermal and electrical checkout of the instrument components will be performed. Then the instrument can be switched-on and first functional and performance tests can be established. After a thorough validation of all functions, normal operations can be started.

Normal Operation

During normal operation, the spacecraft will be operated in the yaw steering mode and the instrument will perform measurements over the complete orbit. The spacecraft will be capable of operating autonomously for at least 72 hours. As part of the instrument calibration, the receiver will be calibrated once per orbit for a period of 5 minutes. This calibration period can be performed over areas of less scientific interest, e.g. the poles. Orbit manoeuvres will be performed once per month.

6.3 The ALADIN Instrument

6.3.1 Instrument Concept Selection

Numerous instrument options have been investigated during the Phase-A (see Fig. 6.8), ranging from coherent lidars at 9-10 μm , 2 μm and 1.5 μm to direct detection lidars at 1.5 μm , 1 μm , 0.53 μm and 0.35 μm . Detailed performance analyses and technology reviews have been performed for all these concepts. All coherent concepts use aerosol (Mie) scattering and have similar performance behaviour, providing high accuracy at low altitude and reduced reliability above a given altitude threshold, depending on the aerosol conditions and the emitted laser energy.

Coherent Concepts

The coherent concept at 1.5 μm was rejected because of the low transmitter maturity and efficiency. The coherent concept at 9-10 μm was investigated in more detail, but has finally been put aside, mainly because of the difficulty of developing a space-qualified CO₂ laser, coupled with low industrial interest. The 2 μm system was further studied as it represented the best compromise in terms of performance and technical maturity among the coherent concepts.

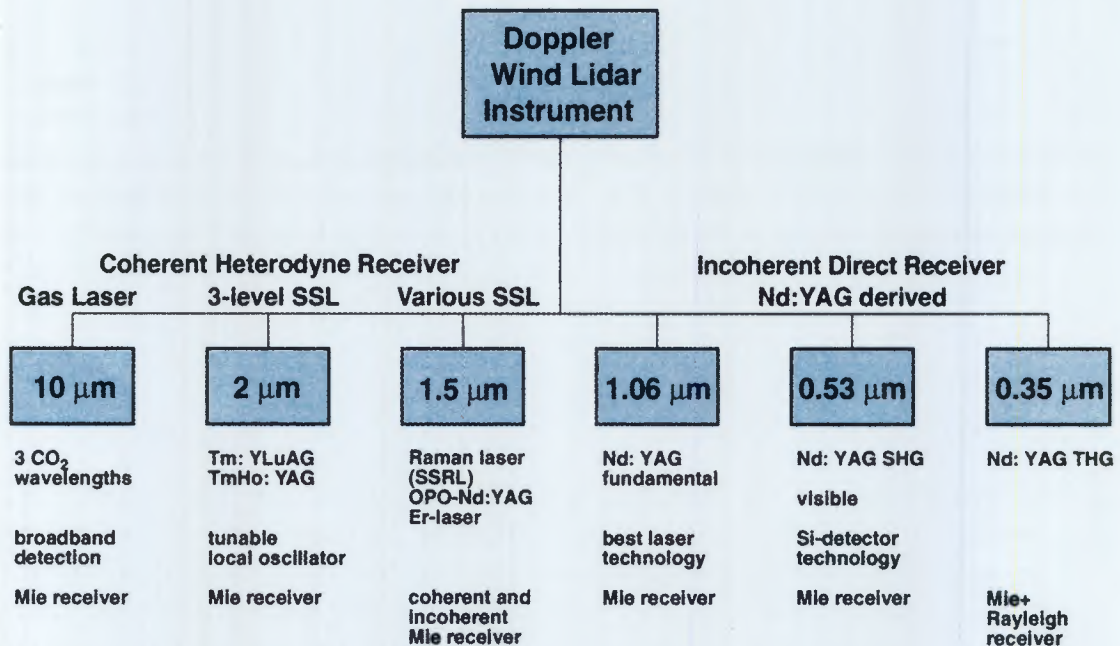


Figure 6.8. Instrument concepts studied in the trade-off activities during the Phase-A.

Incoherent Concepts

The direct detection at 1.5 μm was disregarded due to the poor maturity status of laser development. The 1 μm and 0.53 μm concepts were rejected because of low performance due to power limitations (for eye-safety reasons). The direct detection ultraviolet (UV) concept at 355 nm has been investigated in aerosol (Mie) and molecular (Rayleigh) measurement modes and a combination of both was selected as the best compromise in terms of performance, especially for its robustness vis-à-vis the aerosol-content variations.

Two concepts (2 μm coherent and 0.35 μm incoherent) have been further investigated in detail and compared with regard to performance, technical maturity, programmatics, and growth potential for a future operational mission. The coherent lidar at 2 μm features high accuracy at low altitude, but is limited to medium altitudes. This restriction comes mainly from the limited potential for a significant increase in laser pulse energy for such a system. The opto-mechanical and thermal concept was also considered rather complex (due to the laser crystal cooling and alignment requirements), and the programmatic risk was considered relatively high because only a single and non-European procurement source for the transmitter could be identified. Finally, the growth potential of the concept for a future operational mission is limited, since the aerosol concentration is quite low at higher altitudes.

Thus, the direct-detection UV concept has been selected as the baseline for ADM as it provides good performances up to high altitudes, and has high potential for an operational mission. A combined aerosol (Mie channel) and molecular (Rayleigh channel) receiver has been defined, in order to benefit from their complementarity. This concept can provide compliant wind measurements up to high altitudes (20 km and above) for an operational mission, basically independent of the aerosol content. The technical and programmatic risks were evaluated as low, as transmitter and receiver units with similar or better performances have already been developed and as multiple and European supplier sources are identified for each critical element. Finally, the growth potential for the future operational mission is sufficiently high that a mission fully compliant with the ideal WMO requirements can be proposed, based on the ADM instrument concept.

6.3.2 Technical Details of the selected Baseline

Operating Principle

The spaceborne lidar will emit a narrow linewidth laser pulse (a few tens of MHz) at an ultraviolet wavelength (355 nm). The laserbeam will be sent towards the atmosphere in a slant angle at 35° (Fig. 6.1). The laser light will then be scattered by aerosol particles (Mie lidar) and molecules (Rayleigh lidar) and a small part backscattered towards the lidar. The received signal frequency is Doppler-shifted relative to the emitted laser due to spacecraft movement, the Earth's rotation, and the wind velocity along the line-of-sight. In the proposed ADM concept, the spacecraft and Earth's rotation Doppler shifts are minimised by the use of a proper satellite attitude-control scheme (yaw steering mode). The instrument thus directly measures Doppler wind shifts, which can be expressed as follows:

$$V = \frac{\lambda}{2} \cdot \Delta f \quad (6.1)$$

where V (m/s) is the wind velocity along the line-of-sight, λ is the wavelength, and Δf is the frequency Doppler shift.

Winds are measured in clear air (i.e. above or in the absence of thick clouds), and within and through thin clouds (e.g. cirrus). The laser pulse is emitted at a relatively high repetition rate (100 Hz) such that subsequent laser shots can be averaged in order to reduce detection noise. Due to the satellite's movement, these laser shots form a line on the ground. The integration length is limited to 50 km in order to be compatible with the mission requirements.

The received light is collected by a telescope and is directed onto a receiver subsystem. The receiver samples the signal in the time domain in order to determine its arrival time and hence the distance to the atmospheric layer. For each layer the

spectral distribution of the return signal is analysed through a high-resolution spectrometer. Direct detection is used to measure the spectrum, requiring low-noise (quasi photon-counting) detectors which are available for the selected ultraviolet wavelength.

The return signal spectrum in Figure 6.9, is the sum of a wide-bandwidth Rayleigh signal due to molecular scattering (equivalent to 600 m/s FWHM) and a narrow-bandwidth Mie signal due to aerosol scattering, whose bandwidth is set by the laser spectrum (10 m/s FWHM typically).

Various techniques are available to measure the Rayleigh and Mie spectrum central frequency and they fall into two categories: fringe-imaging and edge techniques. An extensive trade-off has been performed between these two options during Phase-A, both in terms of performance and technical implementation.

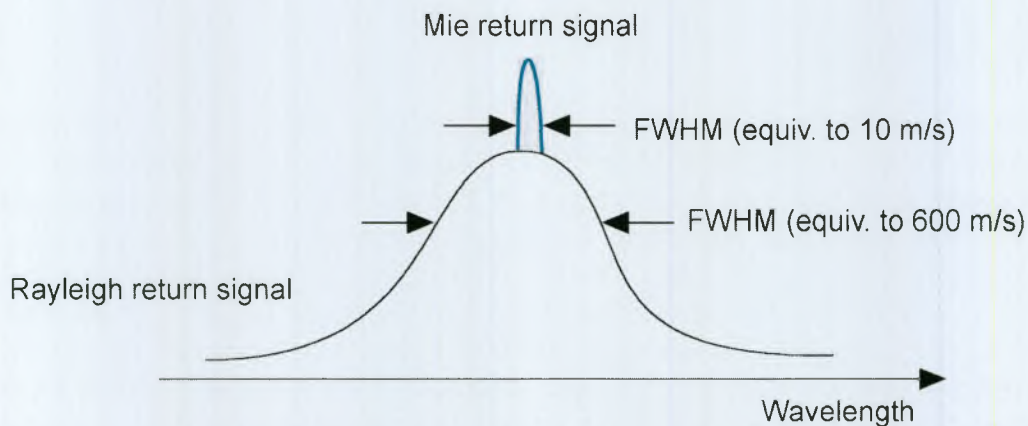


Figure 6.9. Spectral properties of the scattered return signal: The narrow bandwidth aerosol (Mie) signal is superimposed with the broadband molecular (Rayleigh) signal.

The fringe imaging technique (see Fig. 6.10) will be used for the Mie receiver. This concept was preferred over the edge technique as the latter is too sensitive to the Rayleigh background in the ultraviolet. It is intended to sample the received spectrum with a resolution compatible with the spectrum width. A centroid computation then provides the location of the spectrum centre. The fringe width obtained is set by the laser spectrum and the spectrometer resolution. After multi-channel sampling, the fringe spreads over a few spectral intervals. The total number of intervals is defined by the useful range (wind dynamic range + margin) of the receiver. The fringe is superimposed on the Rayleigh and atmosphere radiance spectra, which provide additional noise. This noise is kept negligible by making use of blocking spectral filters.

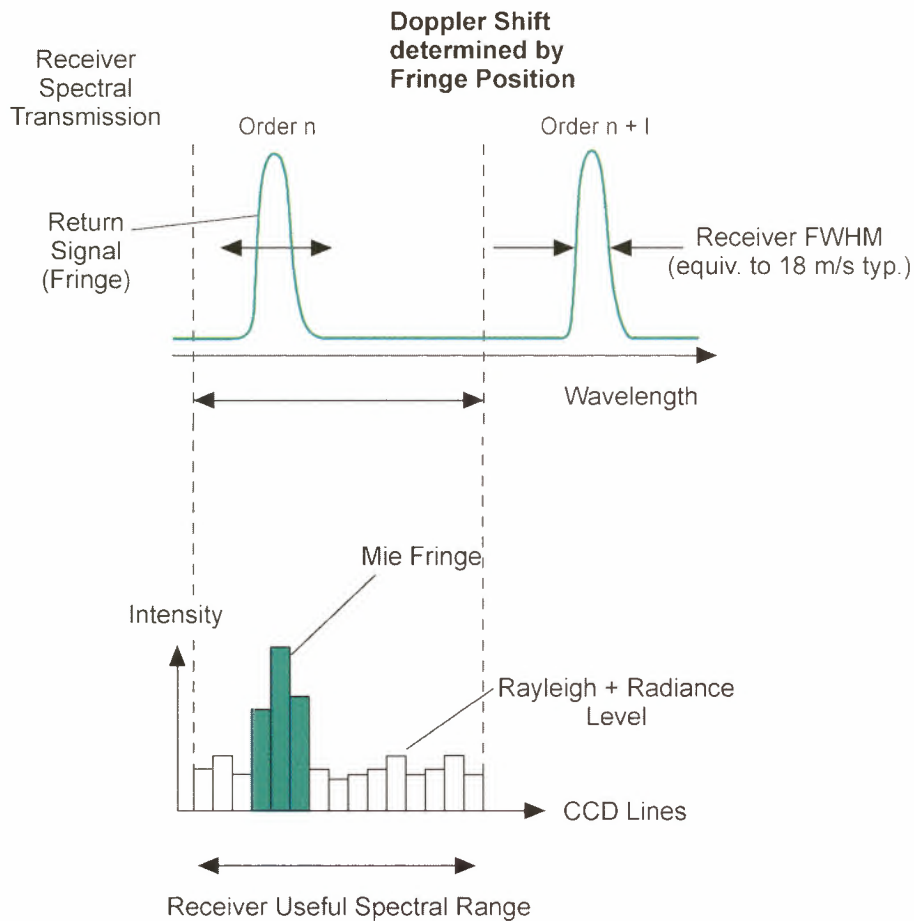


Figure 6.10. Mie receiver principle: multi-channel spectrometer with fringe imaging
 Top: Spectrometer illumination; Bottom: Measured spectrum.

The edge technique (Fig. 6.11) is used for the Rayleigh receiver. This concept was preferred over the fringe imaging technique which features similar performance but whose implementation imposes tighter alignment and detector requirements. Two filters are placed symmetrically from the centre wavelength position in order to perform a differential measurement. The filter outputs (A and B) are used directly as the estimator for the frequency shift.

The receiver concept proposed for ADM is capable of using both measurement principles simultaneously. A spectral filter extracts the central part of the spectrum and directs it towards the Mie receiver, whereas the wings of the spectrum are routed to the Rayleigh receiver.

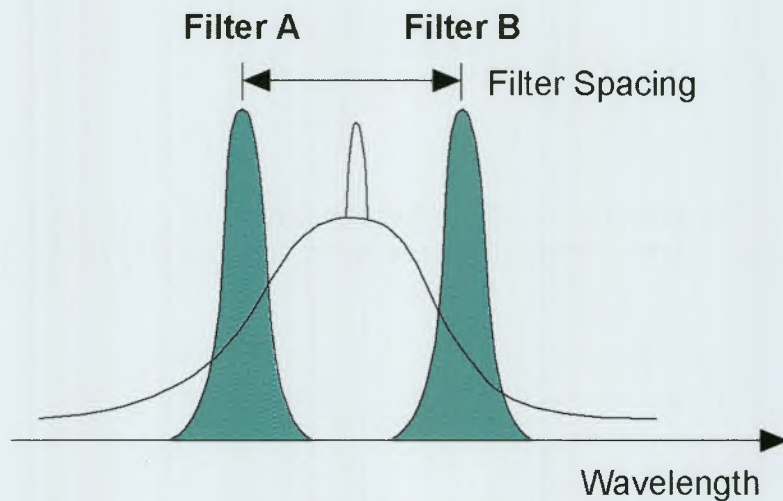


Figure 6.11. Rayleigh receiver principle: Edge measurement with two filters.

Instrument Overall Architecture

The baseline lidar instrument is based on a 130 mJ (150 mJ design goal) / 100 Hz diode-pumped frequency tripled Nd:YAG laser, and a 1.1 m diameter telescope. The power laser head is composed of a medium power oscillator, an amplifier, and a tripler. A small reference and seed laser head is used as frequency reference and is injected into the resonator through fibre optics. Two of each of the laser heads will be implemented for redundancy. The power laser head is conductively cooled via heat pipes, which are attached to the main heat sources, namely the laser slabs and the pump diodes. The heat pipes transport the heat flux to dedicated radiators on the anti-Sun side of the spacecraft. The laser head is derived from past developments in Europe.

In order to provide optimum performance over the whole altitude range, a combined Mie and Rayleigh receiver will be implemented. The Mie receiver is composed of a Fizeau spectrometer, associated to a thinned back-illuminated UV Si-CCD detector working in an accumulation mode which allows photon counting. This spectrometer has been validated in the frame of the ESA Technology Research Programme. The Rayleigh receiver is a double Fabry-Perot etalon, which analyses the wings of the Rayleigh spectrum with one CCD and two read-outs. This technique has been validated on ground by several laboratories, though with photomultiplier detectors (Garnier and Chanin, 1992; Chanin et al., 1994; Rees et al., 1996; Flesia and Korb, 1999). The CCD provides significantly higher quantum efficiency, and hence a performance gain.

A Cassegrain afocal telescope is used for both emission and reception. An isothermal and lightweight design based on an advanced material like SiC or C/SiC is proposed

for the telescope mirrors and structure, yielding the required optical quality and stability without a focusing or alignment mechanism.

The direct-detection receiver principle allows one to obtain an overall opto-mechanical design with large margins for the optical quality and pointing-stability performance. The proposed method for the emission / reception switch is a polarisation beam splitter associated to quarter-waveplate, which has been validated in the clear atmosphere by ground-based lidars.

The instrument core, which consists of the opto-mechanical part, the receiver and the detectors (Fig. 6.12 and Fig. 6.13), will be mounted on the top face of the spacecraft via three bipods. The instrument electronics (detection, transmitter) are mounted on the internal side of this top face. These electronics are connected to a radiator located on the anti-Sun side. The instrument core will be protected by a thermal baffle mounted on the satellite panel.

The star trackers (one operating, one cold redundant) are used for attitude estimation, which is used for control as well as the Doppler retrieval when no ground echo is available. They will be mounted on the instrument structure in order to limit misalignment errors.

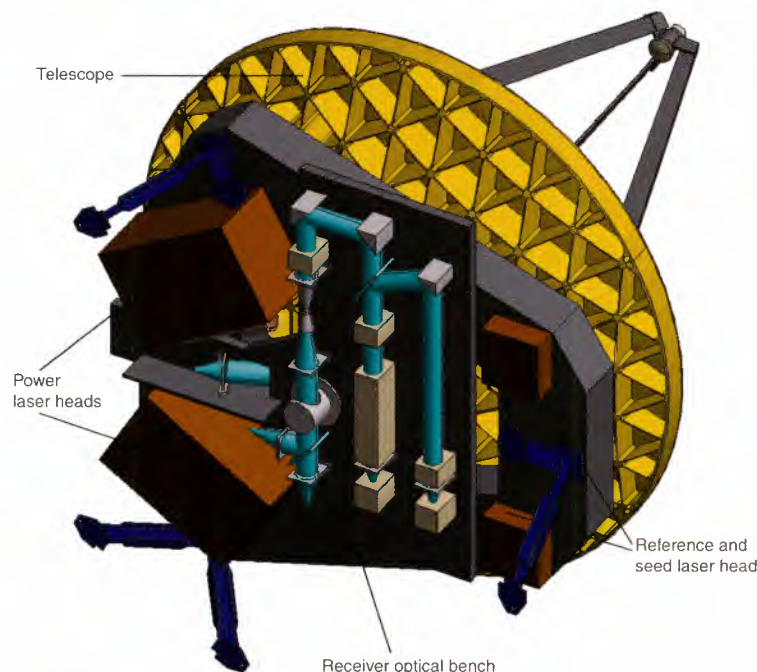


Figure 6.12 Layout of the instrument core, consisting of the opto-mechanical part, the receivers and the transmitters.

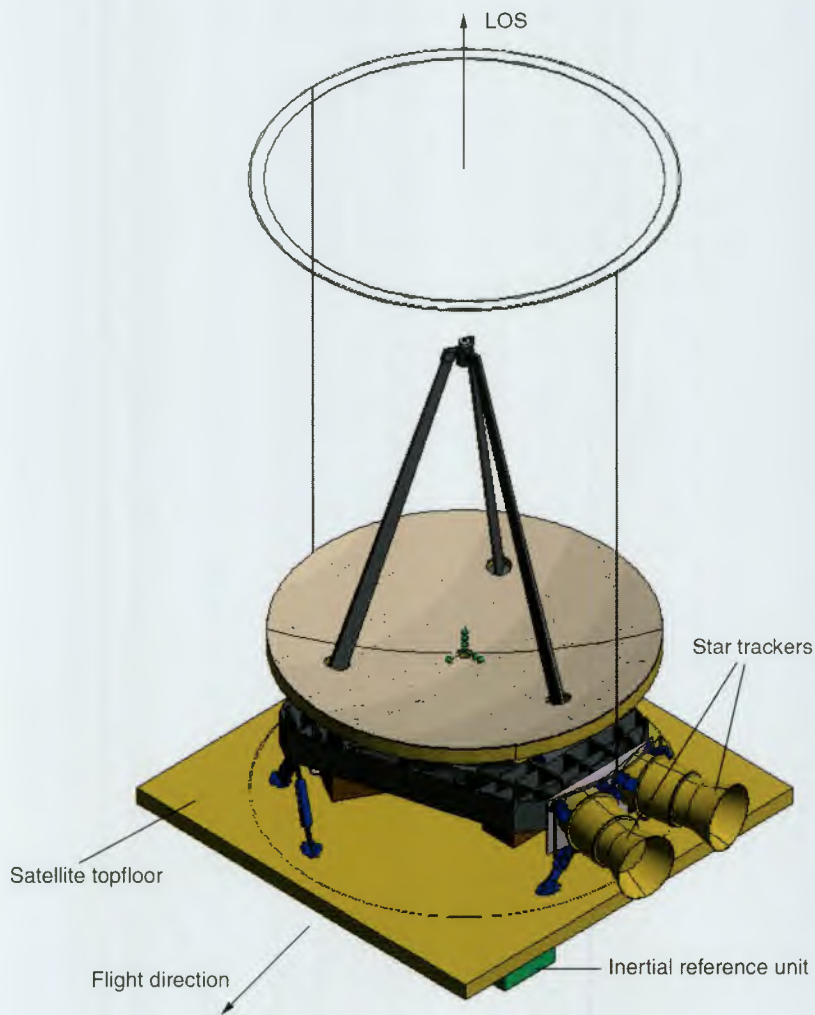


Figure 6.13. Instrument mounted on satellite top face (baffle only outlined).

Instrument Functions and Subsystem Breakdown

The ALADIN instrument is structured around three major functions and associated subsystems: transmitter, receiver and opto-mechanical subsystem (Fig. 6.14). The transmitter comprises a small reference laser head and the main power laser head. The transmitter electronics provide power supplies for the pump diodes, the active Q-switch, synchronisation functions, and thermal control. The laser pump units are cooled via dedicated heat pipes. The laser frequency is continuously calibrated by the receiver, thus cancelling internal frequency-drift errors.

The receiver subsystem comprises the blocking filters and etalons, used to reject the atmospheric radiance background and to separate the two channels, the Fizeau etalon for the Mie channel, the double Fabry-Perot for the Rayleigh channel and the CCD

detector front-end units and detection electronics. The latter comprises the specific power supplies as well as a programmable sequencer allowing one to change the measurement acquisition sequence (i.e. vertical and horizontal sampling length) during flight.

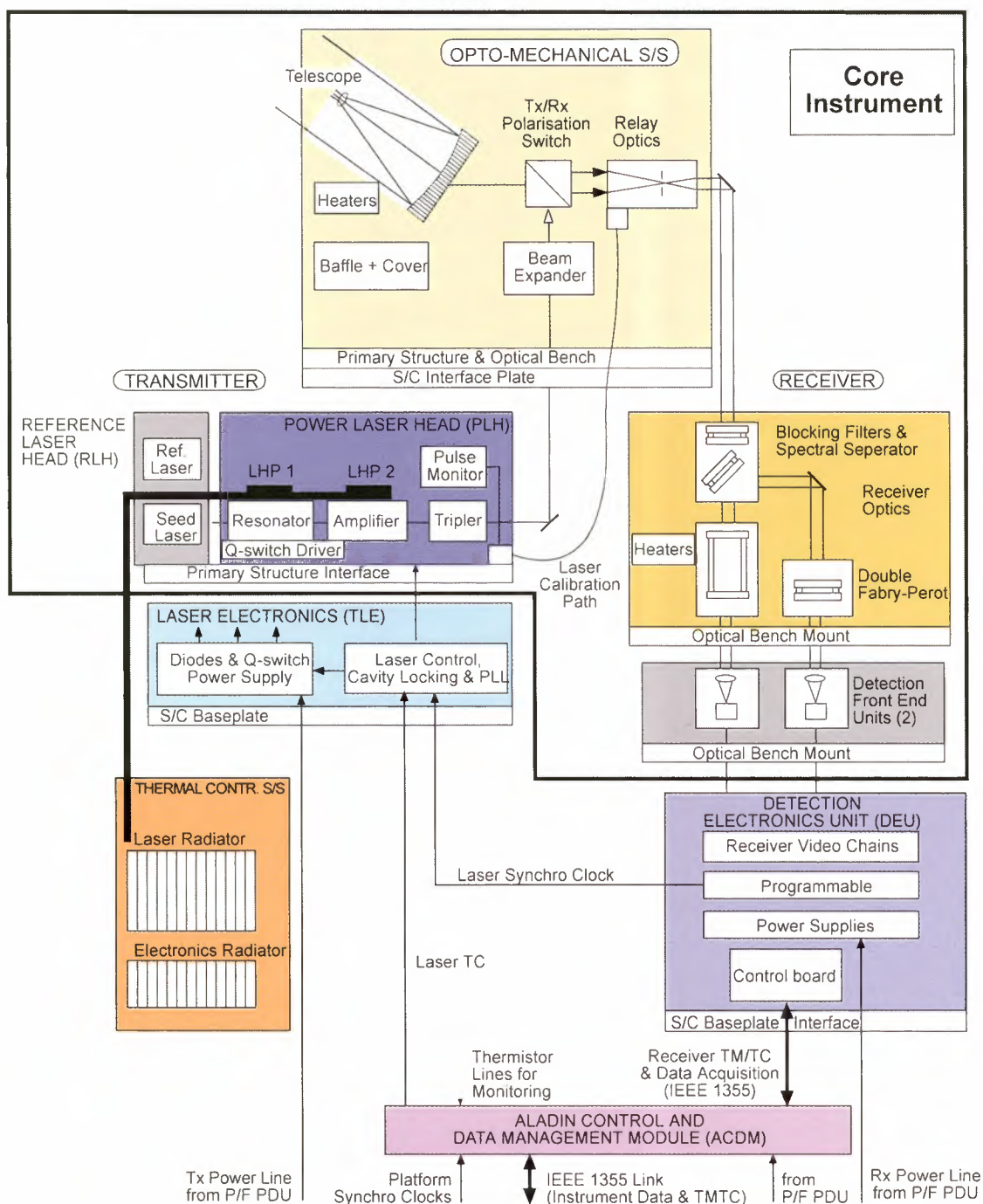


Figure 6.14. ALADIN instrument functional block diagram.

The opto-mechanical subsystem includes the telescope as well as ancillary optics for the laser (beam expander) and for the received path (relay optics) in order to match these beams to the telescope. The polarisation switches between the telescope are also part of this package and implemented on the optical bench. The main characteristics of the instrument are summarised in Table 6.3.

Parameters	Value
Platform	
Altitude	400 km
Orbit	Sun-synchronous 6 h – 18 h
Nadir slant angle	35°
Transmitter	
Wavelength	355 nm
Pulse energy	130 mJ (150 mJ goal)
Repetition rate	100 Hz
Line width	30 MHz
Duty cycle	25%
Receiver	
Fizeau line width (Mie)	30 MHz
Double Fabry-Perot (Rayleigh)	
Line width	2 GHz
Spacing	5 GHz
Optical efficiency (Mie/Rayleigh)	3.1% / 4.6%
Detector quantum efficiency (Mie/Rayleigh)	75%
Signal Processing	
Altitude range (Mie + Rayleigh)	-1 to +26.5 km (extendable)
Vertical resolution	1 km (adjustable)
On-chip horizontal accumulation length	3.5 km (adjustable)
Processing integration length	50 km
Opto-mechanical Subsystem	
Telescope diameter	1.1 m
Optical efficiency	0.8

Table 6.3. Major instrument characteristics.

The overall instrument-control and data-management functions are included in a specific software module, which is implemented as a module of the central data-handling subsystem in order to optimise the interface budgets and development cost. This module controls the transmitter and receiver electronics and interfaces with the satellite data bus.

The transmitter laser heads, electronics and thermal-control system and the receiver and control electronics are appropriately redundant.

Transmitter

The selected configuration is a diode-pumped Nd:YAG laser with a medium-power oscillator and single amplifier. The oscillator is actively Q-switched by a Pockels cell. To achieve a single frequency mode, the injection seeding technique is used with a low-power continuous-wave (CW) single-frequency laser. The medium oscillator output energy is about 100 mJ and is amplified by a single amplifier yielding 350 mJ at 1064 nm. The second and third harmonic generation crystals are placed external to the cavity, behind the amplifier. After frequency tripling, the laser produces about 130 mJ in the ultraviolet (355 nm). The key parameters are summarised in Table 6.4.

Parameter	Value
Type	Diode-pumped Nd:YAG Active Q-switch
Emission wavelength	355 nm
Pulse energy	130-150 mJ
Pulse repetition rate	100 Hz
Pulse width	15 ns
Spatial mode	unique, TEM ₀₀
Longitudinal mode	unique
Spectral width (FWHM)	< 30 MHz
Beam quality	$M^2 < 2$
Electro-optical efficiency	2.5%

Table 6.4. Major laser characteristics.

The laser electrical efficiency is about 2.5% and the power consumption in emitting mode is 450 W. The laser is operating at about 25% duty cycle, as required for the measurement, resulting in an average power consumption of 110 W. At minimum, twelve laser diodes with 1 kW peak power, 150 μ s duration are used for each pump unit (oscillator, amplifier). The typical lifetime of these diodes is about $5 \cdot 10^9$ shots, whereas the ADM requires at most 10^9 shots.

The oscillator design is based on an existing diode-pumped Nd:YAG, injection-seeded, conductively-cooled, 100 mJ laser (Fig. 6.15). The amplifier pump unit design is based on a 300 mJ diode-pumped Nd:YAG, conductively-cooled laser. Both lasers are packaged in small volumes. For an operational mission, the design can be scaled up to yield 300 mJ in the ultraviolet, by adding two identical amplifiers.



100 mJ @ 1.06 μm Laser, Single Frequency
Laser Oscillator



300 mJ @ 1.06 μm Laser Amplifier

Figure 6.15. Diode-pumped conductively-cooled Nd:YAG pulse lasers.



Seeder Design Reference



Q-Switch Design Reference

Figure 6.16. Monolithic ring laser.

Figure 6.17. ATLID pockels cell.



Diode Power Supply (DSS)



Q-Switch Driver (MMS)

Figure 6.18. ATLID laser electronics.

The ATLID Q-switch breadboard design, (Fig. 6.17), has been successfully submitted to performance and vibration tests. It will be re-used in the oscillator.

The reference laser head is composed of two small non-planar Nd:YAG ring lasers frequency-locked by means of a phase-lock loop (PLL). One laser head is accurately temperature stabilised (a few mK), while the other is used as injection seeder. During measurements, the frequency is stabilised within a small portion of the receiver bandwidth by stabilising the seeder temperature. During receiver response calibration, the seeder frequency is shifted from the reference laser by a known offset in the range of 6 GHz, using the PLL. The ring laser design is based on commercially available components providing the required performances, with margins (Fig. 6.16).

The design of the laser power supplies is based on the ATLID laser-diode power-supply breadboard (Pulse Forming Network), and on the ATLID Q-switch power-supply breadboard (MOSFET switch) (see Fig. 6.18). These two breadboards are fully representative in terms of electrical design and have been successfully submitted to performance, thermal and EMC tests.

Receiver

The Mie channel is based on a Fizeau interferometer, made of two plates separated by a Zerodur spacer. A tilt of $4.3 \mu\text{rad}$ is introduced between the plates to provide a linear spectral dispersion. In the Mie receiver, the received laser signal produces a linear fringe whose position is directly linked to the wind velocity. The resolution of the Fizeau interferometer is 100 MHz (equivalent to 18 m/s). The wind value is determined by the fringe centroid position to better than a tenth of the resolution, as tested by Monte-Carlo simulation.

The Rayleigh channel is based on a double Fabry-Perot etalon with a 2 GHz resolution and 5 GHz spacing. The etalon is split in two zones, which are imaged separately on the detector. The wind velocity is proportional to the relative flux difference between the two etalons.

Both types of filters have actually been realised and their optical performances and thermal stability have been verified (Fig. 6.22).

Interference filters and a low-resolution etalon provide a first blocking of background radiation for both Mie and Rayleigh channels. The resulting equivalent bandwidth for transmission of Earth radiance is about 240 GHz. An additional medium-resolution etalon with a FWHM of 2.4 GHz, further reduces the equivalent bandwidth to 30 GHz in the Mie receiver.

The medium-resolution filter is also used for spectral separation of the two channels. The linear polarisation of the beam from the telescope is transformed into a circular polarisation by a quarter-wave plate. The central part of the spectrum, containing the Mie return line, is transmitted through the medium-resolution etalon while the wings are reflected with an opposite polarisation. Upon transmission through the $\lambda/4$ plate, the reflected beam assumes a linear polarisation, perpendicular to the incoming polarisation, which allows its separation and routing to the Rayleigh receiver.

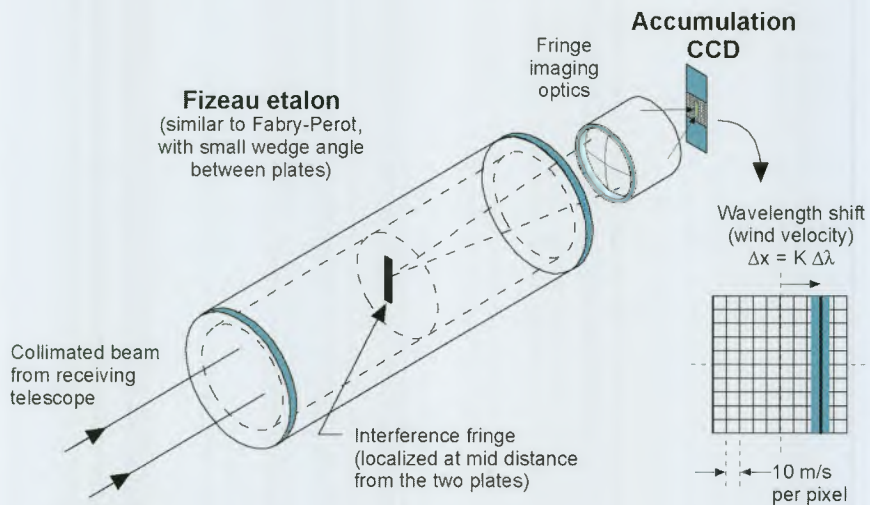
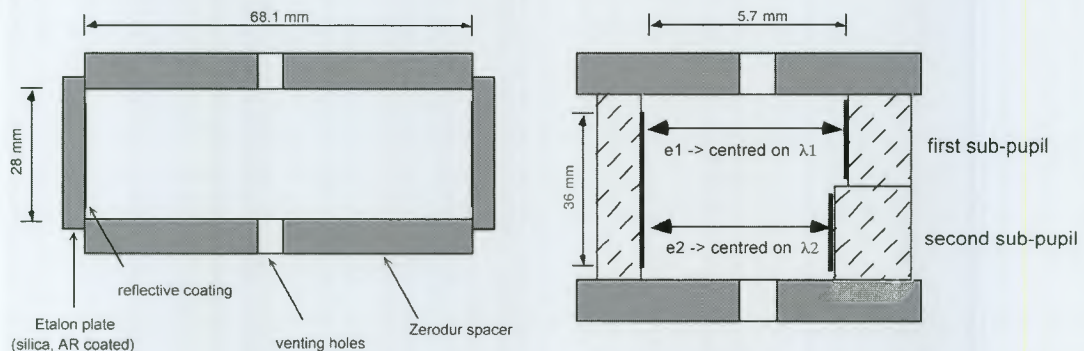


Figure 6.19. Mie receiver principle: Fizeau interferometer and CCD detector.



Fizeau (Mie Channel)

Double Fabry-Perot (Rayleigh Channel)

Figure 6.20. High resolution filters.

Two identical detector modules are implemented for the Mie and the Rayleigh channels. This significantly simplifies the development approach for the detection

assembly. The detector baseline is an accumulation CCD (Fig. 6.23), which allows one to accumulate laser shots on the chip while retaining the altitude information. Because of the small number of read-outs, this technique allows the use of a thinned, back-side-illuminated Si-CCD with a high quantum efficiency in a quasi-photon counting mode. The detector is moderately cooled (-30°C) by a Peltier element to limit the dark current noise. Only the read-out mode differs for the Mie and Rayleigh channels, providing respectively sixteen and two outputs.

Two analogue chains are used for each channel, one measuring the atmospheric wind profile and ground echo and the second one for laser calibration. The CCD sequencing is programmable, allowing in-flight modification of the vertical and horizontal resolution of the wind measurements, giving flexibility in the partition between analogue on-chip accumulation and numerical integration.

The Mie receiver can be taken as an example to illustrate the operation of the accumulation CDD. The linear fringes are imaged in the image zone (Fig. 6.23). After integration over a time corresponding to the vertical resolution, the lines of the image zone are added together in the first line of memory zone 1 and clocked one line down. After repetition of this procedure for each time bin of one echo, the fringe profile is contained in memory zone 1, each line corresponding to one temporal bin. The fringe profile is then transferred rapidly into memory zone 2 via register 2.

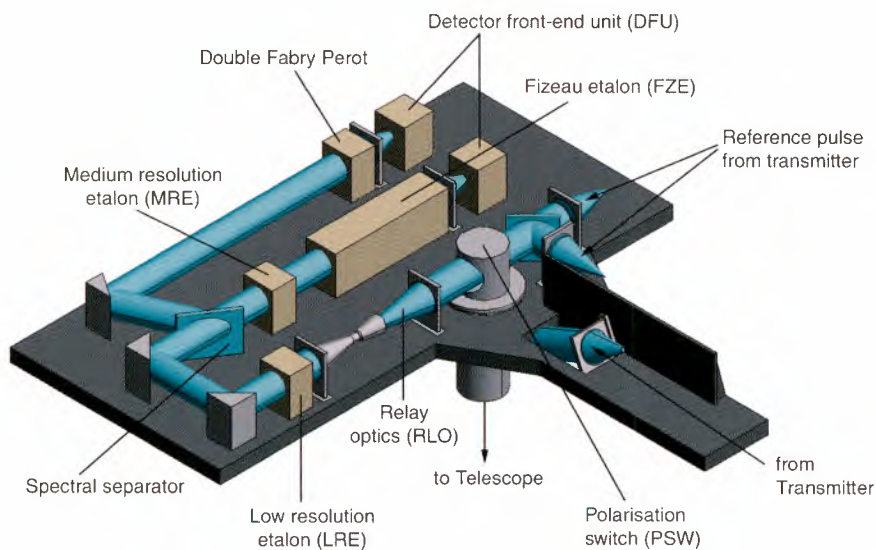


Figure 6.21. Receiver optical bench.

During the next laser shot, the bins of the stored profile are sequentially transferred, via register 1, to the first line of image zone 1, where its content is added to the sum of the fringes of the image zone. Repetition of this sequence allows one to co-add on-

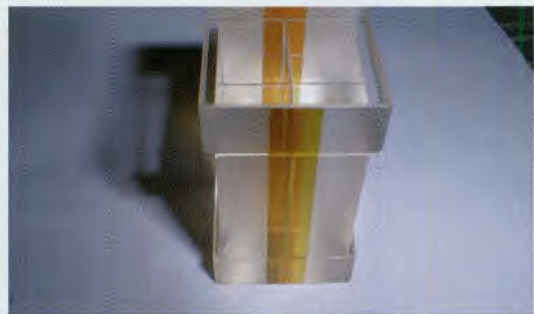
chip ('accumulate') fringe profiles from successive laser shots. The image and memory zones and the registers are cleared to eliminate stray charges, each time their content has been fully transferred to the next zone. At the end of the accumulation sequence, the fringe profile is finally read out via register 2.

This operation mode in which the charges are always moved in the same direction through the CCD has been chosen to avoid pollution of the fringe profile by charges left behind by the potentially larger ground echo.

At laser emission, a part of the beam is injected into the receivers. The image zone is immediately read out during the time-of-flight of the laser pulse, allowing laser frequency jitter to be monitored on a pulse-to-pulse basis.



Fizeau Etalon (MMS)



Double Fabry-Perot Etalon (CNRS)

Figure 6.22. Etalon breadboards (design reference).

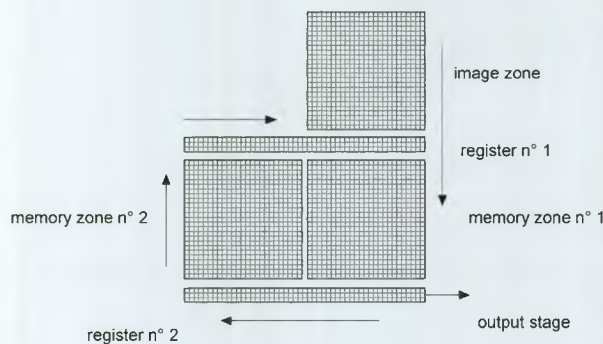


Figure 6.23. Accumulation CCD principle.



Detector Technology Reference

Figure 6.24. GOMOS thinned MPP CCD.

Opto-Mechanical and Thermal Design

The opto-mechanical part of the instrument is composed of the following parts:

- *Telescope:* Primary mirror + mounts, secondary mirror, tripod and primary structure
- *Optical bench:* Transmitter / receiver optics, detector modules, cover
- *Laser:* Power laser head, reference laser head and heat pipes
- *Star Trackers*

The telescope is an isothermal design (mirror + structure) with its primary structure designed as a very stiff pentagonal SiC plate, which acts as the primary structure of the instrument core (Fig. 6.25). This structure supports the secondary mirror assembly (M2+tripod), the optical bench and the laser head. The telescope tripod is linked to the M1 mirror with a diameter of 1.1 m and to the isostatic mounts, in a similar manner as proposed for the FIRST telescope design in SiC (Fig. 6.26). This provides almost zero focus sensitivity with respect to the absolute temperature variation. Only the telescope thermal gradient between the two mirrors needs to be controlled. This is achieved using the internal baffle temperature, ensuring the required focus stability with a factor of two margin.

The telescope is used for both laser emission and backscatter light reception. Optical isolation between the emitted laser beam and the receiver is provided by a proper scattering structure inserted at M2 apex level. The isolation requirement is not very stringent and is achieved with a two orders of magnitude safety margin.

The optical bench is mounted onto the primary structure by means of quasi-isostatic mounts, which limit bench distortions, and hence transmit/receive optics misalignments. Thanks to the use of the monostatic telescope, the required alignment tolerance is relatively loose and the thermal stability is good enough to avoid the need to implement a co-alignment mechanism. The Fizeau and Fabry-Perot etalon temperatures are accurately stabilised ($\pm 0.3^\circ\text{C}$ typically) over the measurement and the orbital periods to obtain a stable spectral response, such that receiver-induced biases are kept to a negligible level. The comprehensive in-flight calibration procedure implies that no accurate long-term thermal stabilisation is required. The optical bench is protected by a light carbon-fibre cover, which provides both optical and thermal isolation from the instrument environment.

The laser head is mounted onto the primary structure, and not onto the optical bench, in order to limit the mechanical and thermal loads on the bench. This architecture is feasible since the laser head alignment tolerance is relatively loose (50 μrad typically) due to the beam expander magnification ratio.



Figure 6.25. *Opto-mechanical architecture of instrument core (star tracker not shown)*

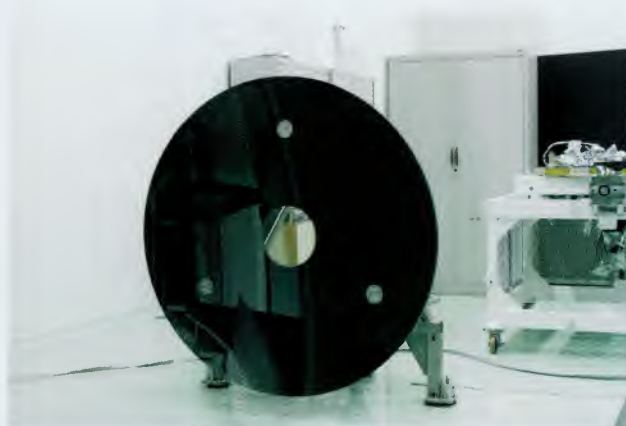


Figure 6.26. *FIRST demonstrator SiC mirror (1.3 m diameter).*

The star trackers are mounted on the primary structure, in order to minimise the misalignment between their optical axis and the telescope's line-of-sight. Only short term stability is required as the sensors are used for attitude-variation restitution between observations of ground echoes.

The opto-mechanical part of the instrument interfaces with the satellite by means of three bipods linked to the main satellite cone structure. The complete instrument first Eigen modes and stresses have been analysed for this configuration, yielding almost a factor of two margin with respect to the satellite and launcher constraints.

Performances & Calibration

The combined Mie and Rayleigh receiver allows one to cover the whole altitude range specified for the wind measurements. Both receivers are employed simultaneously, using a spectral separation between the two channels.

The wind performance discussed in the following is the SNR (instrument) contribution to the system error in nominal conditions (daytime, aerosol median model). As discussed later, this error largely determines the overall mission performance. It is expressed in terms of LOS wind accuracy for a 50 km sample, assuming an on-chip accumulation over 3.5 km and numerical integration by on-ground processing over 50 km (Fig. 6.27).

The two channels are complementary in terms of performances. When the aerosol density increases (strong layers or thin clouds) the low-altitude performance threshold of the Rayleigh channel is higher, but is compensated by the accurate measurements made using the Mie channel.

The Earth and satellite Doppler shifts are compensated at system level by the yaw steering of the platform. The transmitter laser thus always emits at a fixed frequency. This allows the optimisation of the receiver stability, and hence accuracy, by using fixed-space etalons.

Various calibration procedures are implemented to obtain optimum accuracy and stability performances:

- At each shot, part of the emitted beam is injected into the receivers. This allows one to monitor the jitter of the laser frequency and to measure the difference in frequency measurement between receivers.
- Ground echoes are used to remove biases in frequency measurements. This is very accurate only for the Mie receiver. The offsets in the Rayleigh channel are compensated by using the cross-calibration provided by the shot-to-shot laser measurements.

- On-board sensor data (star trackers, gyroscopes, GPS) are used to estimate the satellite and Earth Doppler shifts and compensate biases in the absence of ground echo. These on-board estimates are reset each time a ground echo is available.
- The frequency response of both receivers is periodically calibrated by scanning the laser transmitter over the dynamic range.

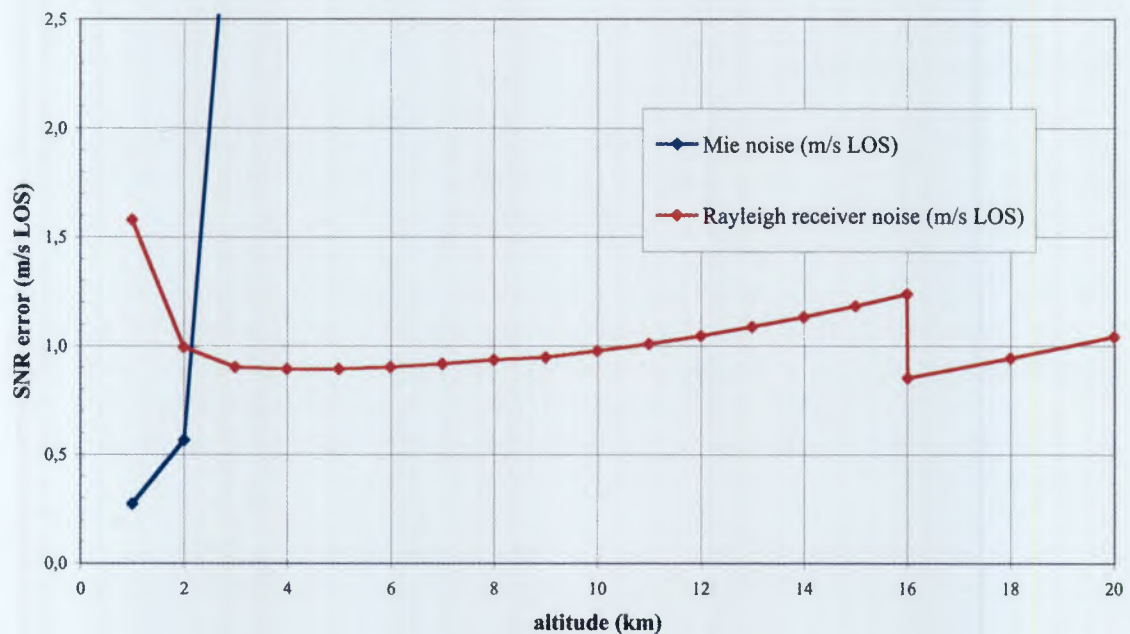


Figure 6.27. SNR performances of Mie + Rayleigh ADM LIDAR in nominal conditions (clear atmosphere, median atmospheric model, daytime, 3.5 km on-chip accumulation and 50 km numerical integration (700 shots)). The change in performance at 16 km is due to the change in vertical resolution. The performances have been predicted by Monte-Carlo simulations.

Overall Performance Budget

Though the main contributor to the error budget is the signal-to-noise of the receiver measurement, various other sources of errors originate from the instrument design itself or from the processing and calibration operations. In addition, when no ground echo is available, the attitude and velocity restitution errors must also be added.

The main contributors to the overall system error include the following:

- The *SNR error* relates to the effect of detection noise statistic and wind retrieval algorithm. This is by far the biggest contributor to the overall error budget.
- *Medium-Resolution etalon stability* relates to distortion induced by any medium-resolution etalon spectral transmission decentre on the molecular return spectral shape. It affects the molecular channel only.
- The *Rayleigh spectrum shape* affects the molecular channel response through spectrum width variation due to probed air volume temperature and spectrum shape distortion due to the Brillouin effect.
- The *Background processing* relates to the after post-processing residual error induced by the Medium-Resolution etalon on the spectral shape of the background light. It affects the aerosol channel only.
- The *Mie signal contamination* models the residual aerosol return entering the molecular channel. It affects the molecular channel only.
- *Ground echo accuracy* relates to the calibration of the ‘zero wind’ using the aerosol channel and the ground return.
- *Internal calibration accuracy* refers to the ‘zero’ inter-channel calibration error using a laser pulse emitted internally on both channels.
- *Response calibration accuracy* refers to the error on the spectral calibration using an internal laser pulse swept in frequency over the useful spectral range of both channels.
- The *Sensor/LOS alignment stability* refers to the determination of LOS Earth and satellite Doppler shifts extrapolated from onboard sensor data and used when the ground echo is not available. Thermo-elastic behaviour of the instrument structure as well as attitude restitution stability, over half an orbit in the worst case, are at the origin of this contributor.

The system performance presented below includes all of the errors described above. This performance considers the SNR error for each channel at the indicated altitude range. Systematic bias errors (correlated errors between profiles) are also considered. The calculations are based on the pointing performances described in Section 6.4.4.

	Mie channel @ 2 km	Rayleigh channel @ 10 km
Measurement accuracy (noise + bias)	0.67 m/s	1.05 m/s

Table 6.5. Instrument overall LOS performance (with ground echo).

When no ground echo is retrieved, the measurement bias is not cancelled and the total measurement error is slightly deteriorated (Table 6.6). However, this worst case is based on the assumption that ground echoes are only available twice per orbit. This is very unlikely to happen and will not significantly influence the mission performance.

	Mie channel @ 2 km	Rayleigh channel @ 10 km
Measurement accuracy (noise + bias)	0.85 m/s	1.23 m/s

Table 6.6. Instrument overall LOS performance (without ground echo).

For the Mie channel, the LOS wind error is below the requirement of 0.6 m/s from 0 to 2 km height. The reliability is around 100% in the same altitude region. For the Rayleigh channel, the LOS wind error is below the requirement, except for a marginal performance around the height of 16 km (leading to a slight exceeding of the requirements in one altitude layer, which is not considered critical to overall mission performance).

As explained in 6.2.2, the orbit height has an impact on the overall system performance. There is however considerable system margin that would allow the performance to be improved by e.g. reducing the orbit altitude. The fuel assumed in the system budget would allow the spacecraft to fly at 360 km altitude. This altitude would provide a potential improvement in the range of 0.2 m/s in the HLOS velocity error.

Flexibility

Thanks to the implementation of a programmable sequencer for the detector, the altitude vertical resolution and range can be changed in-flight during the course of the mission. The vertical resolution can be varied from 100 m to 2 km or more and there is no limitation on the altitude range. The horizontal accumulation length can also be changed during the mission. This length can be varied from 500 m (Mie or Rayleigh) to 50 km without performance degradation for the required horizontal integration length of 50 km. The lower value of the accumulation length is mainly limited by the CCD read-out noise. This capability will be used to implement the processing strategy outlined in Section 7.2.

Instrument Resource Budget Estimates

The overall mass of the instrument concept (instrument core + top panel electronics) is 263 kg, which includes design margins according to the maturity of the components. The average power consumption is 304 W average (with 25% laser duty cycle, assuming full heater power). The main contributor to the power budget is the laser.

The data rate is very low (11 kbps in the most demanding case) due to the optical accumulation principle of the receiver. The overall instrument envelope fits within various launcher fairings, with several hundred millimetres margin at the baffle level.

6.4 The Satellite

6.4.1 Satellite Configuration

Derived Requirements

The main system demands on the satellite are to fly in a Sun-synchronous dawn-dusk orbit of 400 km altitude, and to carry a continuously operated lidar instrument (ALADIN) whose main field of view is 35° off nadir to the anti-Sun side of the satellite track.

The performance requirements of the instrument mean that an optical aperture of 1.1 m is needed, resulting in an outer diameter for the protecting baffle of about 1.2 m diameter, which dictates to some extent the dimensions of other satellite elements. A further consequence of the measurement performance requirements is the need to provide an excellent thermal stability, which affects the distribution of the units in the satellite.

An important factor in the satellite layout is the desire to minimise drag at the altitude chosen, in order to minimise fuel consumption for orbit maintenance (Section 6.2.2). The whole concept must also be capable of being launched by the smallest/cheapest practical launcher.

Description of Selected Concept

A baseline configuration has been selected after an extensive analysis and trade-off of several candidates. The design features of the selected baseline concept are shown in Figure 6.28. The satellite consists of a bus as a conventional box structure with central cone (Fig. 6.30), upon which the instrument is mounted via the three isostatic mounts (bipods). This assembly is flown with the instrument pointing down in a plane perpendicular to the flight path and 35 degrees offset from nadir in the anti-Sun direction (see Fig. 6.1). Since the satellite is flown in a dawn-dusk orbit, the y-side always faces away from the Sun, and the solar arrays can be wings, one forward and one aft of the bus (with reference to the flight direction), fixed in orientation.

The advantages from the thermal design point of view are significant, since this ensures that no direct sunlight enters the instrument baffle under operational conditions, assisting in instrument stability. The thermal conditions are effectively

stable for the whole mission lifetime, especially as there are eclipses only for a period of about 4 months.

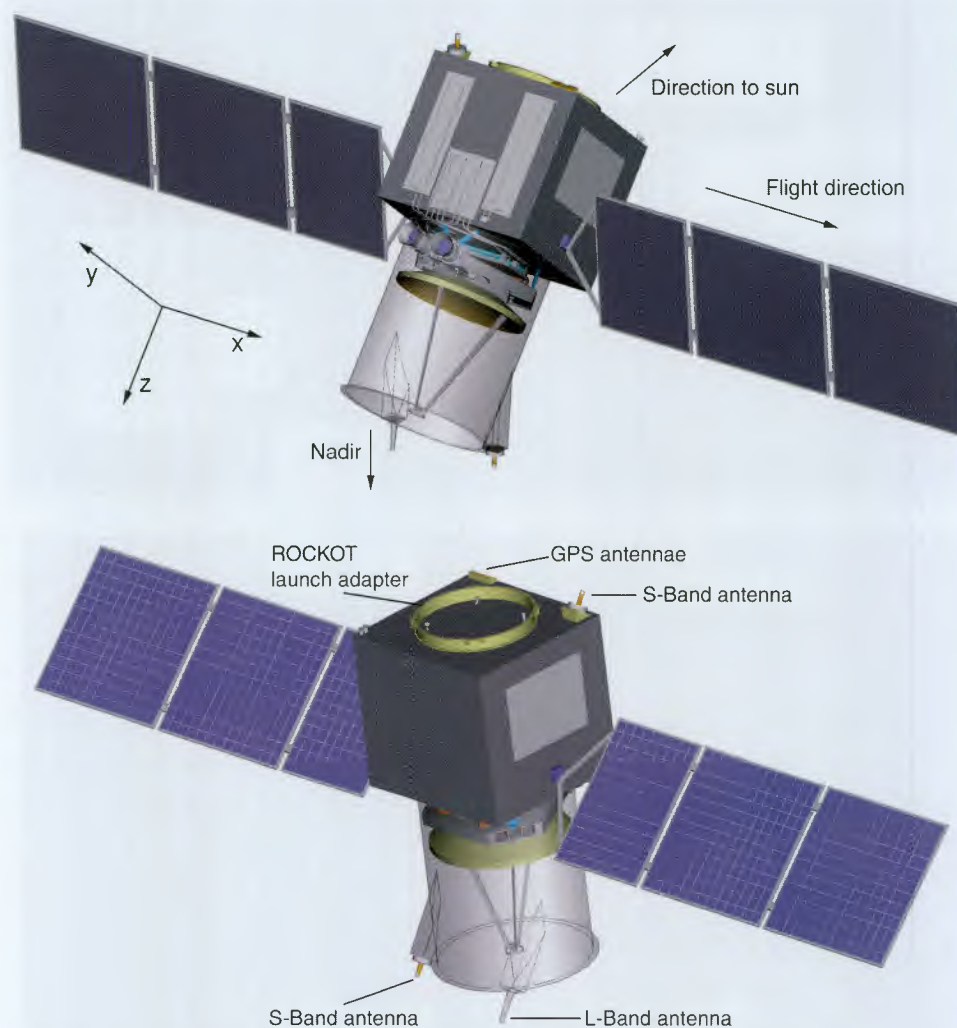


Figure 6.28. Deployed satellite configuration of selected baseline.

The anti-Sun face of the satellite can be dedicated to the instrument radiators, relieving the baffle of additional structural demands. The use of this bus panel has been made possible by arranging the bus electronic units on the inside of the flight and anti-flight faces of the bus. These latter two faces can also form all the radiative surfaces where necessary for the bus electric units. With the (in-flight) lower face of the bus carrying the instrument, the opposite face can easily accommodate the launcher attachment interface. This establishes an easy and optimum load path from the instrument isostatic mounts through the central structural tube to the launcher. The resulting configuration is shown in the views presented in Figure 6.29.

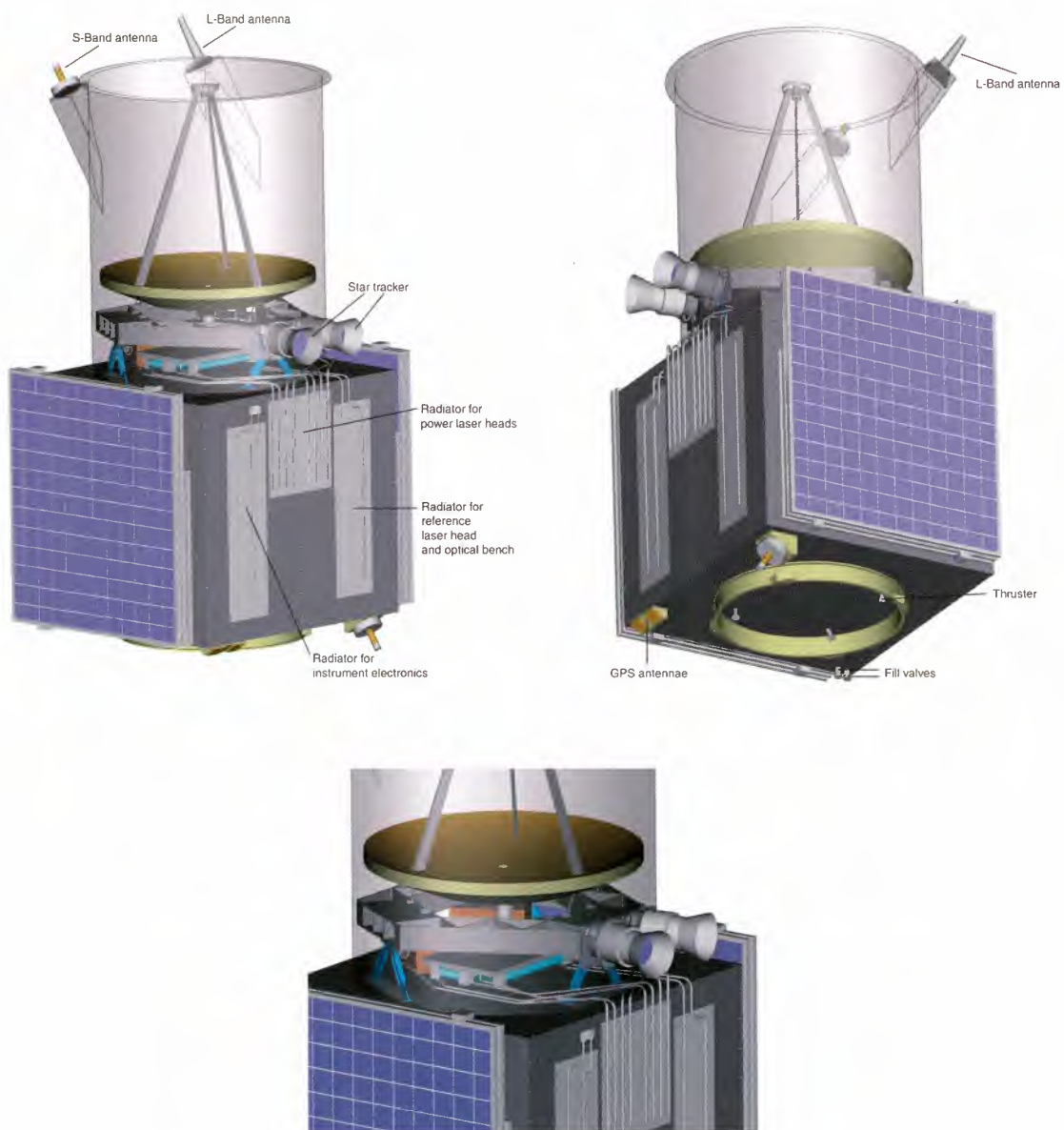


Figure 6.29. Different views of baseline configuration.

Structure

The selected bus structure design consists of a central cone, feeding the launch loads of the instrument directly to the launch adapter on the bottom. Four side walls are attached to the cone by flat shear walls. This design makes it possible to mount all electronics boxes of the bus and associated satellite equipment onto only two side panels. In addition, these +x and -x panels serve directly as radiators for dissipating the heat of the bus equipment.

The +y and -y panels do not carry internally mounted equipment, thus offering easy access during satellite assembly and test. All structural elements are made of aluminium honeycomb.

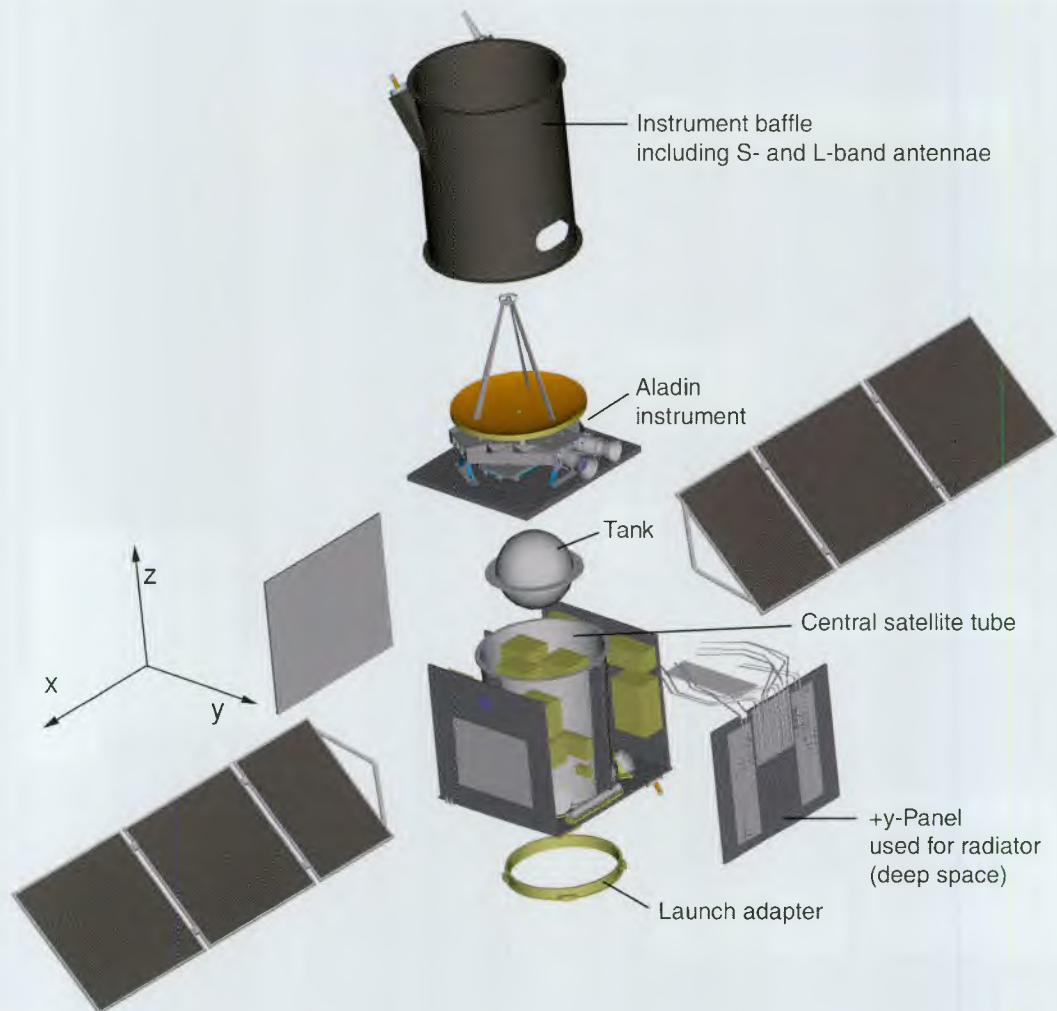


Figure 6.30. Main satellite components.

Subsystem Layout

As depicted in Figure 6.31, the units mounted internally on the bus are generally grouped on the flight and anti-flight walls of the bus (+/-x). This enables the centre of gravity to be easily placed near the launcher axis of symmetry. Exceptions to this are the instrument electronics, the thrusters and the reaction wheels. The star trackers are directly mounted on the primary structure close to the instrument optics.

To limit the cable length, the instrument electronics are mounted close to the instrument on the inside of the top face (+z) of the bus and on the upper parts of the

+/-x panels. This aspect must be closely controlled, as space is at a premium, the intention being to minimise the bus volume to reduce drag cross-section.

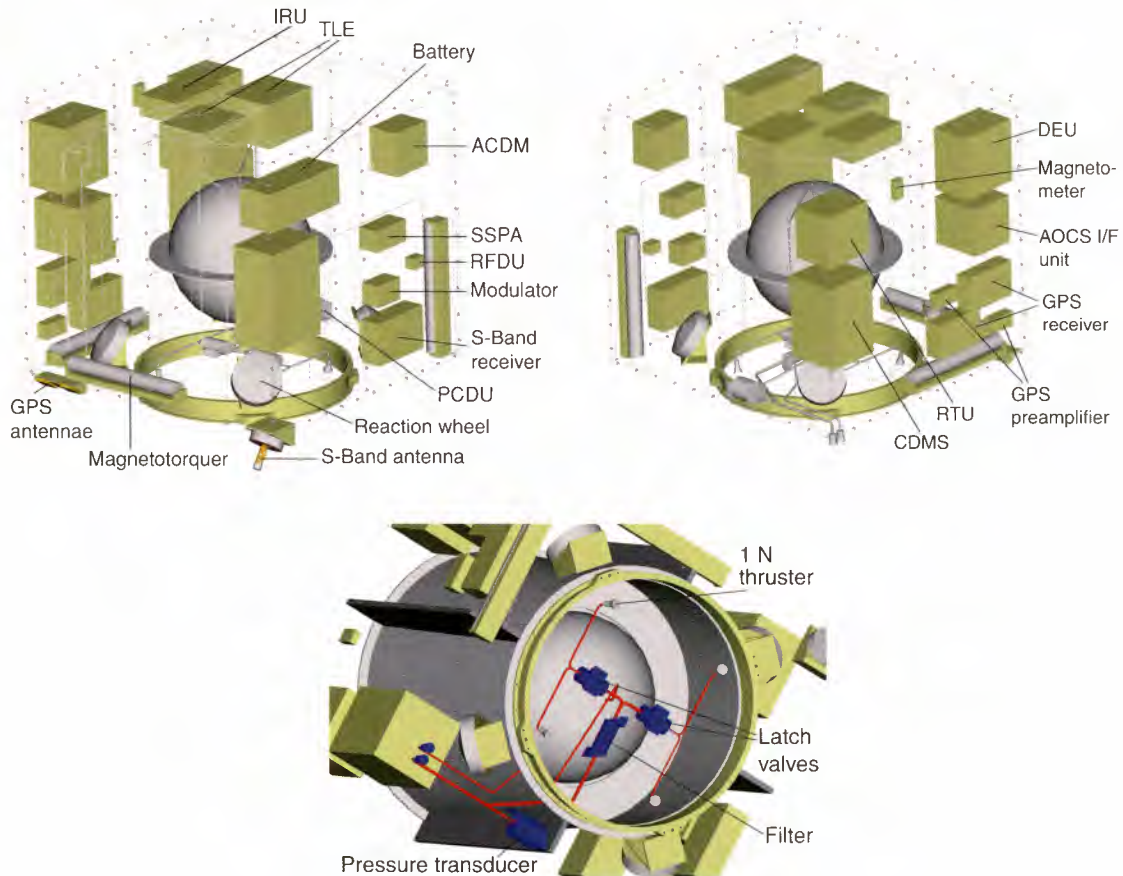


Figure 6.31. Unit layout of the satellite bus panels.

The propulsion equipment can be completely accommodated inside the central tube. The tank will be situated as near as possible to the CoG and mounted directly on the tube walls. The thruster group can be placed inside the launcher adapter ring on the lower face (-z) of the bus. The maximum capacity of the tank is bigger than needed for the approximately 60 kg of fuel required.

The four reaction wheels are mounted directly on the lower face of the bus, outside the central tube area, at angles suitable to the optimisation of the AOCS function.

Because of the dawn-dusk orbit, the solar arrays will have a fixed orientation when deployed. No tracking mechanism is required, as justified in 6.2.4. The deployment mechanism will be designed to ensure orientation of the arrays at 10° to the orbital plane.

The L-band data link antenna is a design derived from the high-resolution picture transmission standard (HRPT) defined for METOP. This requires an antenna which is nadir pointing, with a field of view cone up to 70 degrees from nadir. The optimum place for the antenna is on the bottom lip of the instrument baffle, mounted in a way which minimises stray-light reflections into the baffle. The lower S-band TT&C antenna must also have a field of view covering the lower hemisphere, i.e. its boresight has to point near to nadir. By placing the antennas on either side of the baffle, both antennas can be adequately installed.

The upper S-band TT&C antenna is correspondingly tilted in boresight to cover the other hemisphere, so it must be placed on the opposite upper corner of the bus. The GPS antennas, being patch antennas, can be mounted on the upper edge of the bus. The antenna locations can be seen in Figure 6.28.

The design of the satellite has not conflicted with the demands of the launcher envelope of the baselined Rockot launcher candidate. Consequently, for convenience of design and sizing of the bus central tube, the 'standard' interface diameter of 937 mm has been chosen, allowing a significant degree of alternative launcher choice without the need to rethink the satellite concept.

6.4.2 Thermal Architecture

Overall Thermal Architecture and Constraints

The overall thermal architecture is based on the definition of a simple thermal interface between instrument and bus, with no heat flux between instrument and bus through the structure. As shown in Figure 6.30, the bus incorporates on the +/-x panels the radiators for the bus electronic boxes, including a separate radiator for the battery. In addition to the bus components, the bus houses the instrument electronic boxes and the relevant radiator, located on the +y panel. The radiators of the power laser head and a common radiator for the optical bench and the reference and seed laser head are also located on the +y panel. The dissipation heat of all these instrument components is transported to the radiators via heat pipes.

The temperatures of all sensitive components are stabilised with dedicated small heater systems, consisting of heaters, thermistors and electronic control. Where necessary, these components are insulated against their support structures and internal surroundings.

Instrument

Because of the required temperature stability in some instrument components, the whole radiator area foreseen for the instrument is located on the +y side, which always

views deep space and offers a relatively constant heat-sink temperature. These radiators are located on the bus panel in order to save weight and to minimise the thermal impact on the baffle internal gradient. The baffle employs a segmented heater system to meet the required temperature stability. The heat generated within the baffle is radiated directly through its insulation.

The instrument boxes are fixed to the optical bench or the primary structure. They are all thermally insulated against the support structure and its surrounding. Their dissipation heat is transported via L-shaped heat pipes to the three +y radiator panels. The expected thermal dissipations at the element groups are summarised in Table 6.7. The overall required dissipation heat is 294 W and as the +y panel is able to dissipate on its 1.7 m² surface about 540 W so that this panel is partially insulated with MLI sheets. For the power laser head boxes, a cold-redundancy concept will be applied. Both boxes are combined to the same radiator so that the active box is dissipating to the radiator and some heat is fed back to the inactive box via reverse working heat pipes to hold this box at the required temperature level.

Item	Power [W]
Radiator for instrument electronic boxes	157
Radiator for Power Laser Head (PLH)	125
Radiator for optical bench and seed laser boxes	12
Total	294

Table 6.7. *Thermal dissipation of instrument components.*

The dissipation heat of the optical bench and the reference laser head, mentioned above, also includes the heat produced by the small auxiliary heater system, which helps stabilise the temperature of these components. The thermal design allows analysis and testing of the individual boxes without having to account for any impact from the overall environment and structure.

Satellite Bus

The overall heat dissipation of the bus is about 215 W including the battery heat dissipation. As the bus electronics are not very sensitive to temperature stability, the heat of the bus will be radiated via the +/-x panels. These two panels, each with a 1.7 m² surface area, are able to dissipate much more heat than required (considering also an albedo effect and a seasonal solar incidence angle of up to 30°) and are partially covered with MLI, allowing in addition final adjustments during system tests.

All bus boxes are directly fixed to the inner side of these +/- x panels so that their dissipation heat can be conducted through the panel and radiated on this opposite side.

The battery will be accommodated on a thermally but not mechanically de-coupled radiator panel due to its lower operation temperature. Thus, the thermal design of the bus is based on standard tools and hardware without special risks or development requirements.

6.4.3 Electrical Architecture

The overall electrical architecture of the ADM satellite as shown in Figure 6.32 is composed of the avionics subsystem, the electrical power subsystem (EPS) with solar generators and interconnecting harness, the telemetry, tracking and command subsystem (TT&C), the payload data transmission subsystem (PDT), and finally the thermal-control electrical equipment.

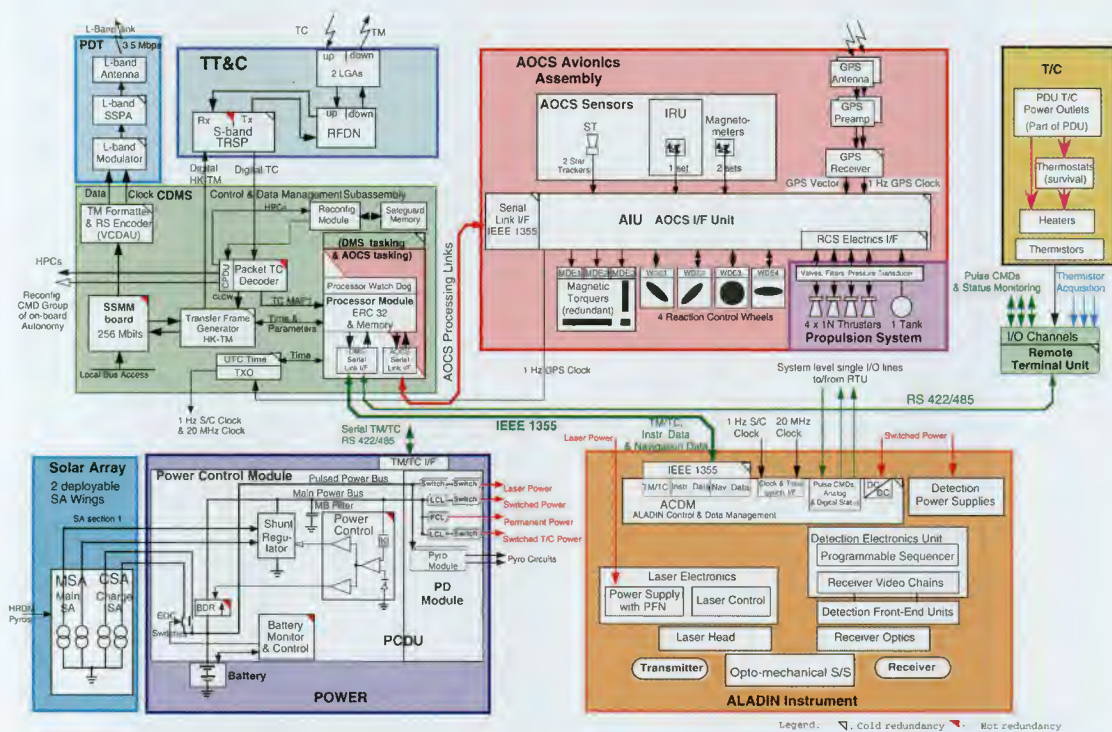


Figure 6.32. Overall electrical functional block diagram.

The avionics subsystem includes classical control & data management system (CDMS) and the attitude and orbit control system (AOCSS) assembly with all sensors and actuators. The avionics assembly has an integrated avionics processor system sharing the processor for the CDMS and the AOCSS tasks.

Dedicated internal functional/electrical interfaces to the satellite bus equipment and the ALADIN instrument are controlled by the CDMS via serial links. A limited number channels as pulse commands and analogue and digital inputs will be required according to the need of the units.

The Electrical Power Subsystem (EPS) is realised by the Power Control and Distribution Unit (PCDU), a NiCd battery and the solar array. The PCDU and solar array are designed for the selected hybrid power subsystem design.

The telemetry, telecommand and tracking (TT&C) subsystem is a standard S-band system with two transponders, two low gain antennas providing omnidirectional coverage, and a Radio Frequency Distribution Unit (RFDU). The payload data transmission subsystem (PDTS) will transmit the science data in L-band.

Electrical equipment for thermal control are heater mats, thermistors, thermal-control power outlets in the PCDU and thermostats for survival heater power switching. Nominally the temperature control is performed via software-controlled circuits.

Avionics Subsystem

The avionics architecture is defined in Figure 6.33 and represents a subsection of the overall electrical architecture. The major elements, their functions and implementations are summarised below.

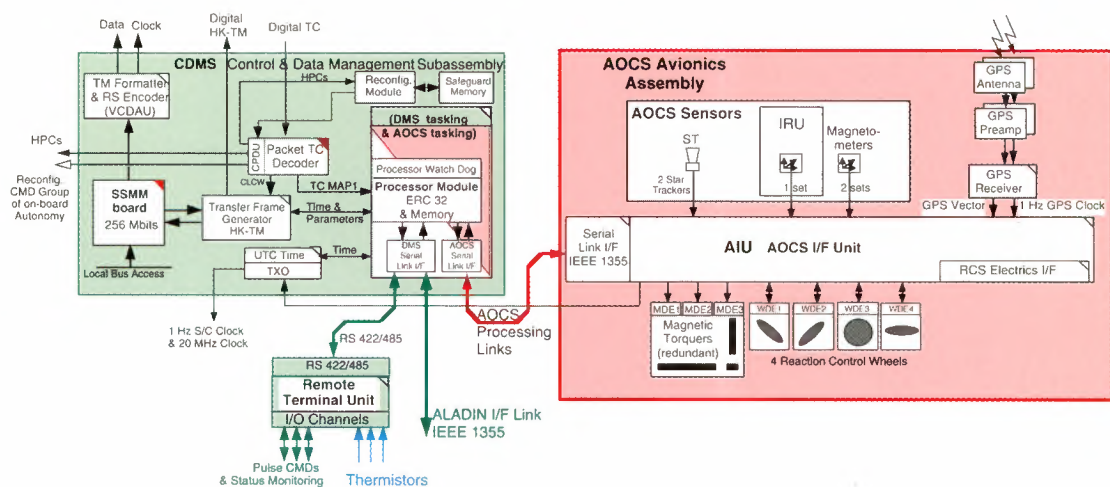


Figure 6.33. Avionics architecture.

The CDMS consists of one redundant ERC 32 Processor (SPARC) with Packet TC Decoder, Transfer Frame Generator (Packet TM), Reconfiguration Module and Safeguard Memory, System Clock, and Solid State Mass Memory (SSMM) for instrument data storage. The functions to be provided are command, telemetry, overall spacecraft control, and timing facilities, dedicated AOCS/RCS control-law implementation, and required data storage during all phases of the mission.

The software will consist of the real-time operating system software (VxWorks as baseline) and dedicated application software, in charge of data management and AOCS tasking. The SSMM will be implemented as 256 Mbit RAM, with direct access to the bus of the CDMS.

Serial end-to-end links are selected for the interface: IEEE 1355 links to the AOCS Interface Unit (AIU) and the instrument, RS 422 to the non-intelligent users like the Electrical Power Subsystem and the RTU. A standard RTU will provide limited pulse commands distribution and analogue and digital status acquisition.

Direct clock and time-reference distribution to the ALADIN Instrument will be provided and implemented as 1 Hz clock with UTC datation and a 20 MHz clock in the instrument.

The AOCS assembly comprises all relevant sensors and actuators with their respective interfaces. These interfaces are connected to the common AIU with autonomous switching capabilities for primary power and elementary failure handling functions. The AOCS application software (e.g. control laws) will be running in the CDMS processor.

Electrical Power Subsystem (EPS)

The EPS design is mainly driven by the laser pulse power and the instrument detector requirements. The laser needs 100 Hz peaks in the kW range, for periods of 7 s and about 1 s for warming up. The power subsystem must comply with laser power for pulsed, diode-pumped solid-state laser technology. The detector power supply has to be free of ripples.

The dawn-dusk orbit determines the battery layout by the worst-case eclipses in summer solstice.

The EPS and solar generator interface architecture as depicted in Figure 6.34 is selected as a baseline. It includes an hybrid power bus mainly because of EMC reasons offering a regulated primary power bus and a direct battery buffered outlet for the laser pulse power. The main characteristics of the elements of the EPS are listed in Table 6.8. All power units are based on existing designs, with flight-proven technologies.

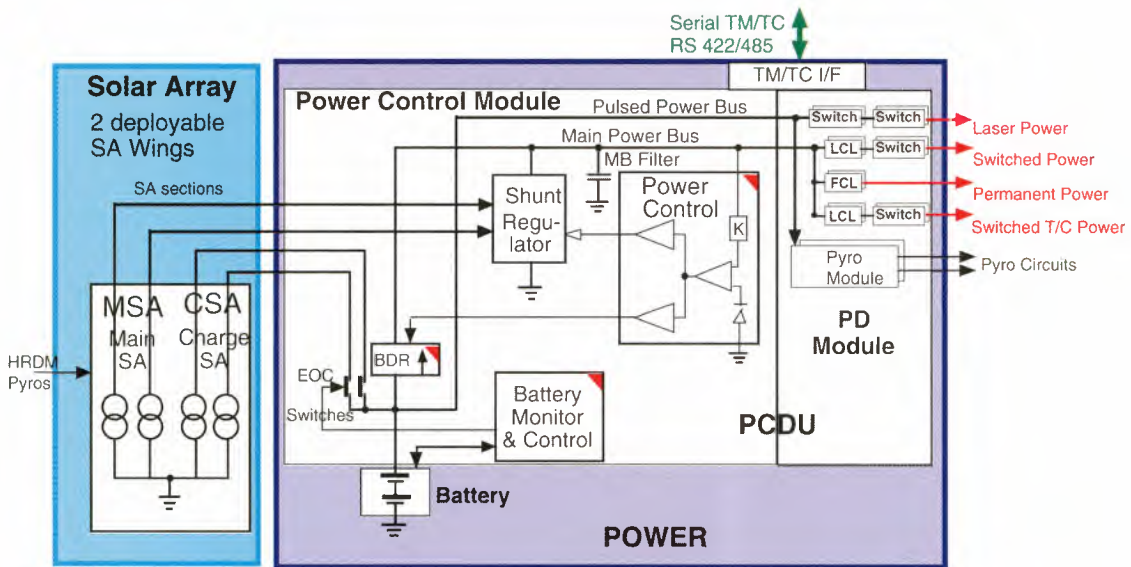


Figure 6.34. Baseline for Electrical Power Subsystem (EPS).

<p>Solar Array</p>	<ul style="list-style-type: none"> • Fixed wings; parallel strings connected to sections • 12 main power bus sections + one section for redundancy • 8 battery charge sections + one section for redundancy • 920 W EOL • Si-BSFR cells, 8.4 m² total wing area • 2 x 10 kg
<p>Power Conditioning and Distribution Unit (PCDU)</p>	<ul style="list-style-type: none"> • Power control module for hybrid power bus concept with S³R for main bus power <ul style="list-style-type: none"> - Separate switches for battery charging, controlled by battery charge status - Battery discharge regulation in eclipse - Power of charge array sections can be switched directly on to the main power bus - PCDU power bus recovers automatically from any shutdown transition if the cause of it is disappeared • Power distribution module including <ul style="list-style-type: none"> - Pyro module - Latching current limiters in line with the protective switches
<p>One NiCd Battery</p>	<ul style="list-style-type: none"> • 28 cells in line • 18 Ah • 25.5 kg • The battery layout is mainly for LEOP power service and for high current flow for the laser peak power • The eclipse power DOD is < 40%.

Table 6.8. Main characteristics of the Electrical Power Subsystem (EPS).

Tracking, Telemetry and Command (TT&C) Subsystem

The TT&C subsystem consists of all elements for RF reception, demodulation, modulation and transmission. The fundamental functions are to receive up-link signals for telecommand purposes, and to transmit down-link telemetry signals. In addition, ground tracking is supported.

The RF-subsystem comprises two low-gain antennas (for omni-directional coverage), an RF-distribution network (RFDN), consisting of two transfer switches and RF-harness, and two S-band transponders, each consisting of a receiver, a transmitter and a diplexer. The block diagram shown in Figure 6.35 illustrates the subsystem configuration, implemented with off-the-shelf hardware.

The max. 64 kbps downlink rate can be handled with a link margin here of more than 4 dB. The required RF power is minimal (3 mW). For the telecommand channel of 2 kbps the link margin is bigger than 50 dB.

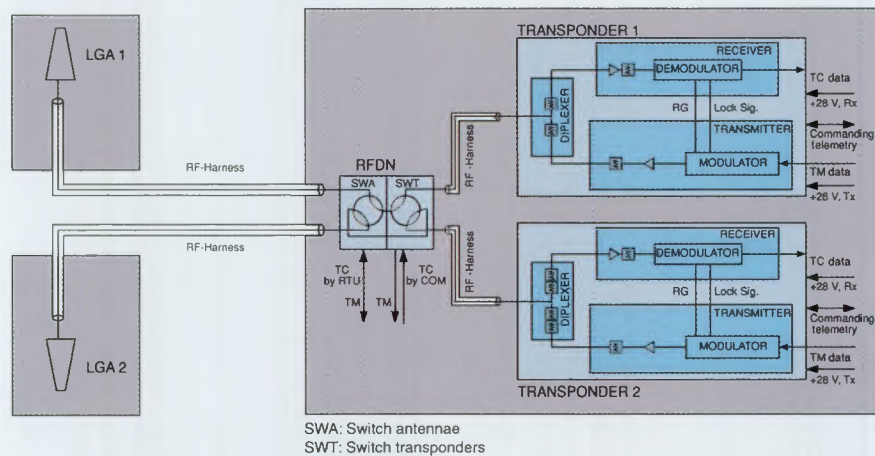


Figure 6.35. TT&C subsystem functional configuration.

Payload Data Transmission Subsystem (PDT)

In order to benefit from existing ground and on-board terminals, the L-band link – as used for HRPT of METOP – has been selected for PDT.

The PDT consists of two transmit chains in cold redundancy configuration composed of an internally redundant modulator assembly containing an encoder section, a pulse-shaping filter, a modulation section and an up-conversion section, an L-band solid-state power amplifier (SSPA). A switch connects the active chain to the filter and the

antenna. The passive chain is nominally unpowered. Each chain supports a data rate of 3.5 Mbps (4.66 Mbps after encoding). The link margin with 5.6 W RF power is 6.5 dB, assuming an on-board and ground equipment quasi-identical to the HRPT equipment of METOP. A block diagram of the PDT is shown in Figure 6.36.

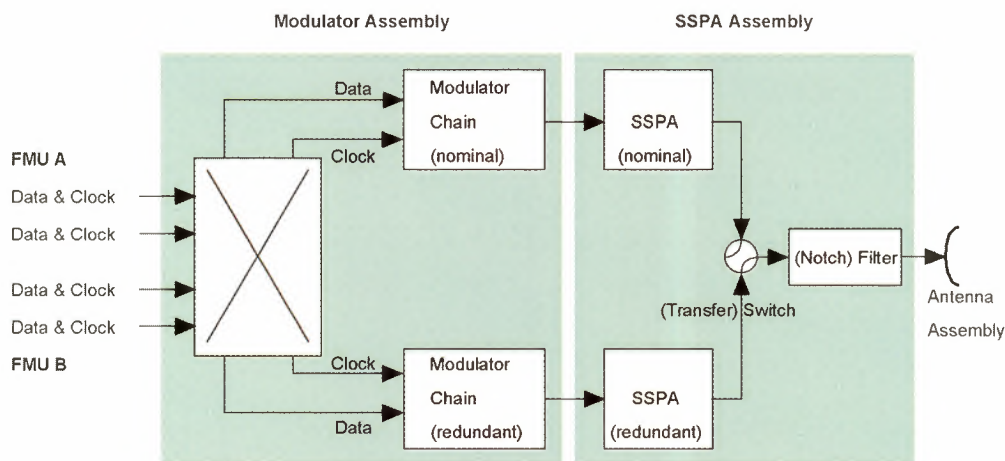


Figure 6.36. Architecture of the Payload Data Transmission Subsystem (PDT).

6.4.4 Attitude and Orbit Control

AOCS Performance Requirements

The AOCS requirements are summarised in Table 6.9. These requirements lead to a high-accuracy measurement system, involving an accurate inertial measurement unit and star trackers.

The requirement on the absolute attitude restitution is driven by the height assignment accuracy of the measurements. It does not have a direct impact on the accuracy of the measurement. The relative accuracy of the attitude measurement, however, directly influences the accuracy of measurements with no calibration information (i.e. between ground echoes). A worst case for this is the availability of ground echoes only over the poles, which leads to a requirement of ~50 minutes stability. In the case of the eclipse period, this is augmented by the thermoelastic alignment error between the sensors and the LOS of the instrument.

	Xo	Yo	Zo
Attitude (in μrad rms)			
Control			
Pointing	520	520	520
Stability over 3 ms	0.5	0.33	0.33
Stability over 0.5 s	–	2	2
Stability over 7 s	300	2	2
Restitution			
Absolute	130	–	–
Relative	10	10	10
Orbit (rms)			
Restitution			
Position (in m)	20	20	20
Velocity (in m/s)	0.067	0.067	0.067

Table 6.9. *AOCS performance requirements summary.*

AOCS Modes

The AOCS modes and their transitions are simplified to minimise the operational complexity. These modes, depicted in Figure 6.37, are the same as considered in the Leostar avionics development and have already been validated in a multi-mission framework. Detailed simulations with existing development tools have shown that the ADM can be handled within the existing hardware and software, which gives a high level of confidence in the results presented below.

The Idle mode is used during ground integration and during the launch. After launcher separation, the launcher induced altitude rates are damped in less than 15 minutes by a standard rate reduction mode, using only a magnetometer, the wheels and the thrusters for a fast convergence. Afterwards, the solar arrays will be deployed.

The satellite then enters its Acquisition and Safe Hold (ASH) mode. The ASH is used for initial attitude acquisition. The ASH uses the minimum possible hardware, avoiding in particular gyroscopes and thrusters, which gives a particularly simple, robust and autonomous mode. Moreover, this mode does not use consumables, is not time-limited, and does not disturb the orbit. In this mode, the satellite is oriented in such a way that the solar arrays points towards the orbit normal, i.e. near the Sun direction, and slowly rotates around this axis. The ASH is also used in the case of emergency.

After ground authorisation, the transition mode is entered. In this mode, the fine attitude sensors, which consist of gyros and star trackers and the onboard navigator, will be initialised on the basis of ground data. After attitude-estimation convergence, the satellite will autonomously point to the Earth. It then initiates the GPS receiver in very secure conditions. At the end of this mode, the satellite is Earth-pointing and can enter the normal mode.

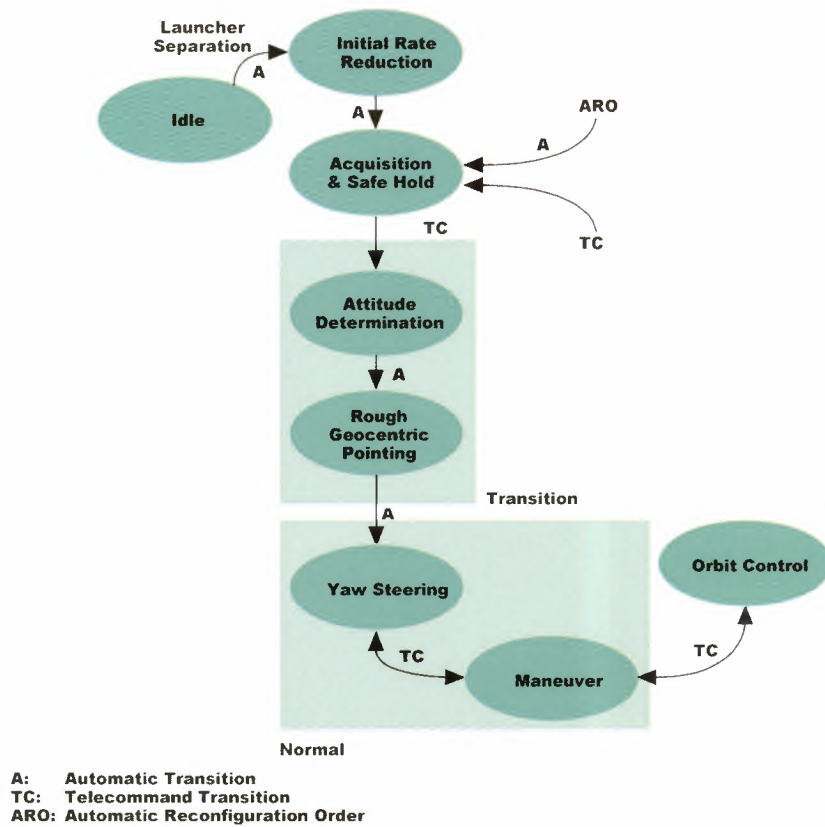


Figure 6.37. AOCS modes and transitions.

The normal mode is the mode in which the satellite will spend its operational life. During this mode, the satellite points its Z_0 axis towards the Earth. The X_0 axis points to the satellite velocity direction and modulated with the required yaw steering angle. In this mode the satellite is controlled by the reaction wheels, which are periodically off-loaded by the magnetic torquers.

The orbit-control mode is used to control and adjust the orbit. In this mode, the satellite is controlled as in normal mode, but the thrusters are used to provide the required boost.

Table 6.10 shows the hardware used in the different modes. The selected off-the-shelf available AOCS equipment consists of redundant sensors and actuators. The magnetometer and the fine sensors are in cold redundancy. The inertial reference unit is internally redundant with an additional gyroscope and processing units in cold redundancy. Four wheels are used, and the magnetic torquers are made of a redundant winding.

Mode	Sub-Mode	Magn.	GPS	Star-Tr.	IRU	Wheels	Mag.Tor.	Propuls.
Initial Rate Reduction		X				X		X
Acqu. & Safe Hold		X				X	X	
Transition	Attitude Determ.	X		X	X	X	X	
	Rough Geoc. Pointing		X	X	X	X	X	
Normal	Yaw Steering		X	X	X	X	X	
	Manoeuvre		X	X	X	X	X	
Orbit Control			X	X	X	X	X	X

Table 6.10. AOCS hardware per mode.

Equipment Sizing

The equipment sizing has been verified by detailed analysis and validated by simulation. The magnetic torquers are sized by the ASH convergence time and the disturbing torques. 100 Am² torquers are sufficient to counteract the disturbances, and to make the satellite converge in ASH mode. This sizing also fulfils the normal mode requirements for off-loading the wheels.

The wheel momentum is sized by the capacity required in normal mode to counteract the non-periodic external disturbances applied to the satellite. The main contributors to this disturbance budget are the air-drag torque and the magnetic torque. Analyses and simulations showed that 5 Nms for each wheel would already be sufficient for the disturbance control. However, considering the current state of the satellite design, 10 Nms wheels are selected at this stage.

The wheel torque is sized by the time required to perform a 90° rotation prior to orbit maintenance. A 0.1 Nm torque for each wheel is sufficient to reach the 90° orientation in 2 minutes, even after a wheel failure. This performance allows one to keep a very simple thruster layout, and to limit operation interruption due to orbit control to a few minutes.

The thruster configuration, consisting of four 1 N thrusters, is adapted to a single-direction boost for orbit control. They are placed on the -z panel of the satellite and

used only for orbit maintenance in nominal operations. However, it is possible to produce the torques required for rate reduction after launch by actuating them in pairs.

AOCS Performances

The AOCS performance is mainly a function of the sensors, and at a lower level of the wheel vibrations. The pointing control performance, as simulated for the 400 km orbit, easily fulfils the requirements, mainly because the sensors are mounted on the instrument, thus minimising their relative thermal distortion. The stability over 7 s will easily be fulfilled, because it is applicable only to non-zero variations over this time period, i.e. to frequencies lower than 0.2 Hz involving only a part of the gyro-star-tracker noise and GPS filtered noise. The same is true for the 0.5 s requirement, which involves only frequencies lower than 1 Hz and a small part of the gyro-star-tracker noise.

The stability requirement over 3 ms applies only to high frequencies and therefore only to wheel vibration. A first worst-case computation has shown that if the wheel unbalance is in the range of 0.1 g·cm and the harmonics stay at a similar magnitude, the requirement of 0.33 μ rad can be met.

The attitude-restitution requirements are the main drivers. The absolute attitude-restitution requirement is applicable around the satellite roll axis and can marginally be met. The remaining biases, caused by thermal and mechanical distortions between the star tracker and the instrument LOS, are the main contributors to the resulting performance.

The attitude-restitution requirements over 50 minutes can be met, because the attitude propagation is very accurate due to the high-performance characteristics of the inertial unit. The worst-case calculation has shown that the requirements can be fulfilled also in the case of eclipses.

The orbit-restitution requirements will also be easily fulfilled with standard equipment and adequate filter algorithms.

Comparing Table 6.11 and Table 6.9 shows that the AOCS requirements are met. The absolute restitution in roll requirement is marginal and leads to a slightly higher height assignment error. However, this is still judged to be sufficient to achieve the mission objectives. The worst case for the relative restitution is non-compliant. However, this situation is judged to be very unlikely (half an orbit without any ground echo) and can only occur in the three months around the summer solstice, where the thermal distortion effects are maximal due to the eclipse.

	X ₀	Y ₀	Z ₀	Errors type
Attitude (in μrad rms)				
Control				
Pointing	190	230	210	All
Stability over 3 ms	< 0.3*	< 0.3*	< 0.3*	Noise
Stability over 0.5 s for frequencies lower than 2 Hz	0.2	0.2	0.2	Noise
Stability over 7 s for frequencies lower than 0.2 Hz**	2.0	2.0	2.0	Noise
Restitution				
Absolute restitution without eclipse	160	210	180	All
Absolute restitution with eclipse	190	220	210	All
Relative restitution over 2 min	0.9	0.9	0.9	Noise
Relative restitution over 50 min out of eclipse	18	21	20	Thermal + noise***
Relative restitution over 50 min with eclipse orbit	46	34	41	Thermal + noise***
Orbit (rms)				
Restitution				
Position (in m)	20	20	20	Noise
Velocity (in m/s)	0.033	0.033	0.033	Noise

* with wheels balanced to about 0.1 g·cm and equivalent other harmonics

** with control bandwidth greater than 0.2 Hz

*** The values include the misalignment between the sensors and the LOS (compatible with the assumptions in Section 6.3.2).

Table 6.11. AOCs performance summary.

Type	Equipment	Nbr	Main Characteristics	Technology	Redundancy
Sensors	Magnetometer	2	3-axis	Fluxgate	Cold Redundancy
	GPS Antennas & pre-amps	2	Half-space coverage	Patch Antenna	Cold Redundancy
	GPS Receiver	2	C/A GPS Receiver	RF ASIC and μ Proc	Cold Redundancy
	Star Tracker	2	Large Field of View	CCD	Cold Redundancy
	Inertial Reference Unit	1	3 measurement axes	HRG	Internal
Actuators	Reaction Wheels	4	10 Nms / 0.1 Nm	Ball Bearings	3 among 4
	Magnetic Torquers	3	100 Am ²	Windings	Cold Redundancy

Table 6.12. AOCs hardware and redundancy matrix.

6.4.5 Satellite Budgets

Table 6.13 shows a launch mass of the ADM satellite of 785 kg, which is fully compatible with the baseline launcher Rockot for the selected 400 km Sun-synchronous orbit. This figure already includes 100 kg of fuel for a mission lifetime of 3 years plus one additional year for consumables. In addition, the budget includes the standard maturity factors for the selected equipment, depending on their design status.

On top a 10 % system margin has been applied taking into account the present status of the overall design.

The power budget shows the power demand during sunlight and eclipse phases. The total energy demand is 219 Wh.

	Mass [kg]	Power Demand [W] *)
Instrument	263	304
Structure, Balance Mass and Harness	118	
Thermal Control	26	15
Power	97	23
AOCS and RCS	86	115
CDMS	26	43
Communication	17	12
Satellite Mass	633	
Satellite Power		512
System Margin 10%	63	51
Consumables	100	
Total Launch Mass	796	
Total Power Demand		563

*) average during normal operation

Table 6.13. Overall mass and power budget.

6.5 The Launcher

The main characteristics of potential launch vehicles are summarised in Table 6.14. These launchers include European as well as non-European alternatives. Those not included in this table either do not meet performance or size requirements, or are assumed to have performances, and also prices significantly in excess of requirements.

Payload capability is quoted in the table for 800 km altitude, but can be assumed to be about 20% more for a 400 km orbit.

The reference chosen for the Phase-A of this mission is the Rockot launcher, with Taurus as a second choice, and Athena as a third choice.

Accommodation of the satellite in Rockot is shown in Figure 6.38, and demonstrates that there is a lot of flexibility available for the overall satellite dimensions.

Launcher	Fairing			Performance Mass to 800 km Sun-sync. [kg]
	Diameter [m]	Cylindrical height [m]	Total height [m] if > cyl. ht	
Taurus XLS	2055	3357	5738	950
Athena 2/120	2743	3307	6187	1090
Athena 2/141	3276	4529	8017	1090
Athena 3	3276	4529	8017	2200
Rockot	2260	2813	4017	800
M5	2270	3315	5355	n/a
PSLV	2900	4250		1000*
Kosmos	2200	1809		1100

Table 6.14. Potential alternative launchers for the ADM satellite.

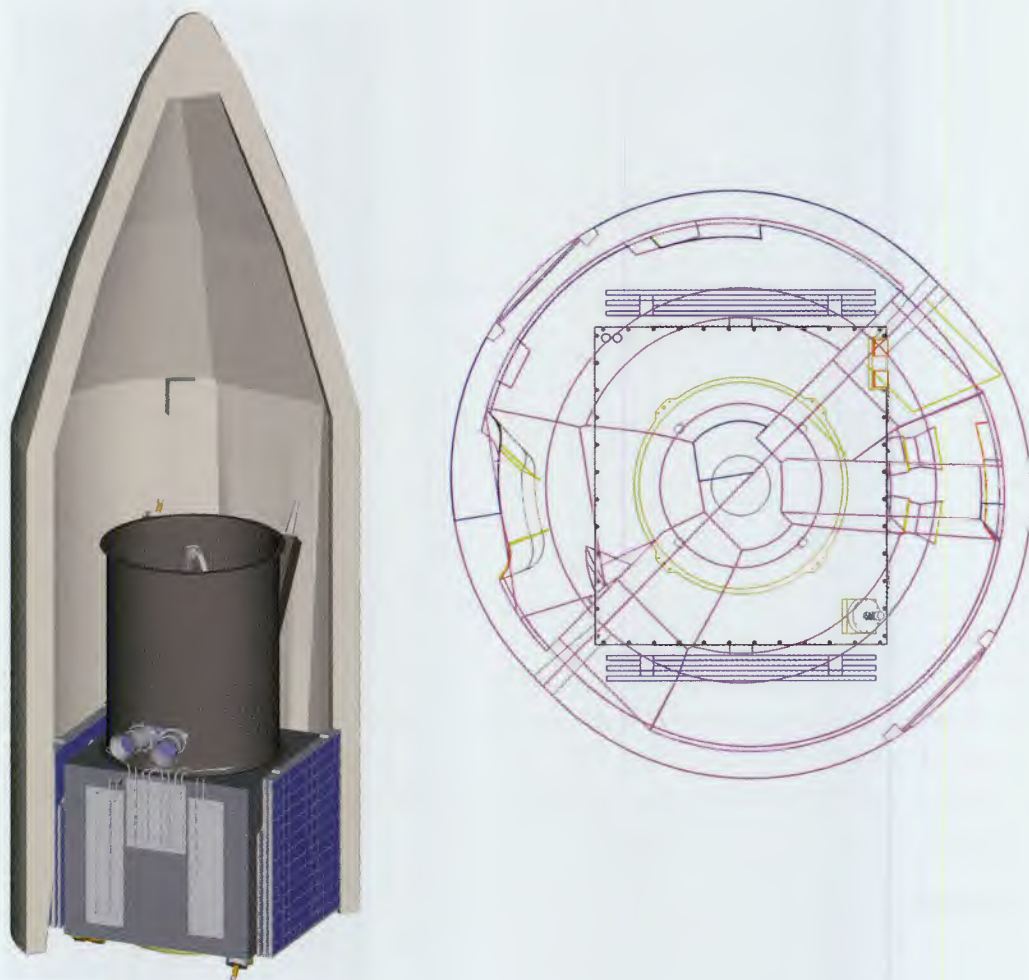


Figure 6.38. ADM satellite stowed in Rockot launcher.

The launch related activities begin with the pre-launch phase, where the satellite will be shipped to the launch site in Plesetsk, mated to the launch vehicle, followed by a final pre-launch check-out. The launch campaign will last about one month.

The ensuing Launch and Early Orbit Phase (LEOP) is divided into the launch and the acquisition phase (initial rate reduction phase and Sun-pointing phase). The countdown and launch sub-phase lasts from the start of the countdown, through the lift-off, and until the separation of the satellite from the launch vehicle. The upper stage of the Rockot launcher, the so-called Breeze stage, can provide any required payload attitude. The specified 3σ attitude error along each spacecraft axis, as well as the angular velocity after separation, are specified and well within the capabilities of the selected AOCS.

Directly after separation, the initial rate reduction starts, using the magnetometer as sensor and possibly the thrusters as actuators, in order to reduce the angular velocity for safe solar-array deployment. This is followed by the solar-array deployment and initialisation of the ASH mode.

6.6 The Ground Segment

6.6.1 Ground Segment Design Guides

The major functions of the ground segment are to:

- monitor and control the satellite, including the payload and the ground-segment elements
- receive the instrument data from the satellite, and
- process, disseminate and archive the data and products, and provide for their retrieval.

The key requirements state that the Level 1 products shall be available at the Science Data Processing Centre within 3 hours of observation, with a reliability of 95%. This Science Data Processing Centre will produce the Level 2 products and the associated processor software, and disseminate this through a network to the meteorological as well as other scientific users. The delivery of Level 1 products for other users will be done upon request. There will be the possibility to order these archived products via the Internet.

6.6.2 Ground Stations

To meet the timeliness requirements for the selected orbit, the following two data reception stations have been selected (Fig. 6.39):

- Kiruna (67.88N, 20,25E)
- Barrow (71.3N, 156.7 W).

Table 6.15 gives an overview of the attainable contacts for the baseline and an alternative ground station combination. With the baseline combination, for any orbit visible from Kiruna, the data will be dumped to Kiruna. Only for orbits not visible from Kiruna will the data be dumped via Barrow. The nominal TT&C station will be located in Kiruna.

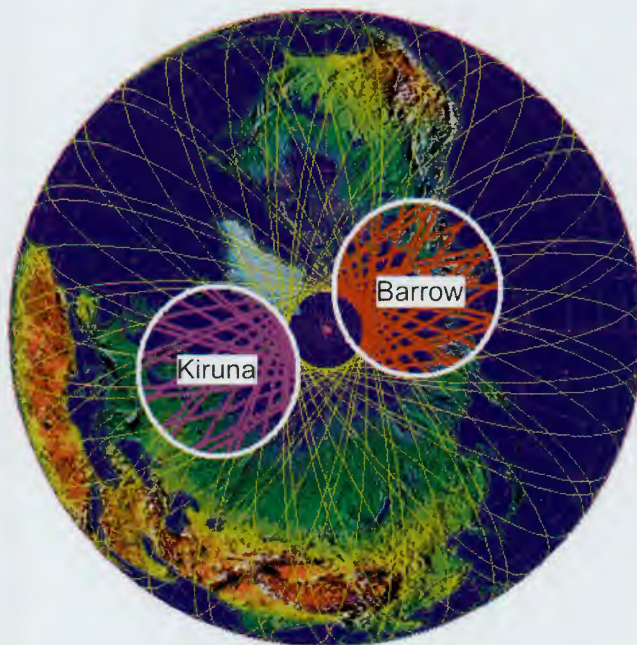


Figure 6.39. Ground-station visibility from Kiruna and Barrow for 400 km orbit.

Combination	Total Coverage		Single-Coverage Characteristics		
	Percentage	Coverage per week	Minimum	Average	Maximum
Kiruna / Barrow	8.5%	14h 17min 07s	1min 37s	6min	7min 55s
Svalbard /Tiksi	9.51%	15h 58min 26s	1min 33s	8min 30s	14min 17s

Table 6.15. Data-reception coverage characteristics.

6.6.3 Ground-Segment Architecture

The Figure 6.40 shows the functional architecture of the ground segment, which consists of the following entities:

- Mission Operations and Satellite Control Element (MSCE)
- Command and Data Acquisition Element (CDAE)
- Processing and Archiving Element (PAE).

The Science Data Processing Centre (SDPC) is directly located on the user site and will be built up at a dedicated meteorological centre, performing the interface between the ADM system and the various users. The different ground-segment elements are inter-linked by existing networks. The external entities are connected via standard public networks.

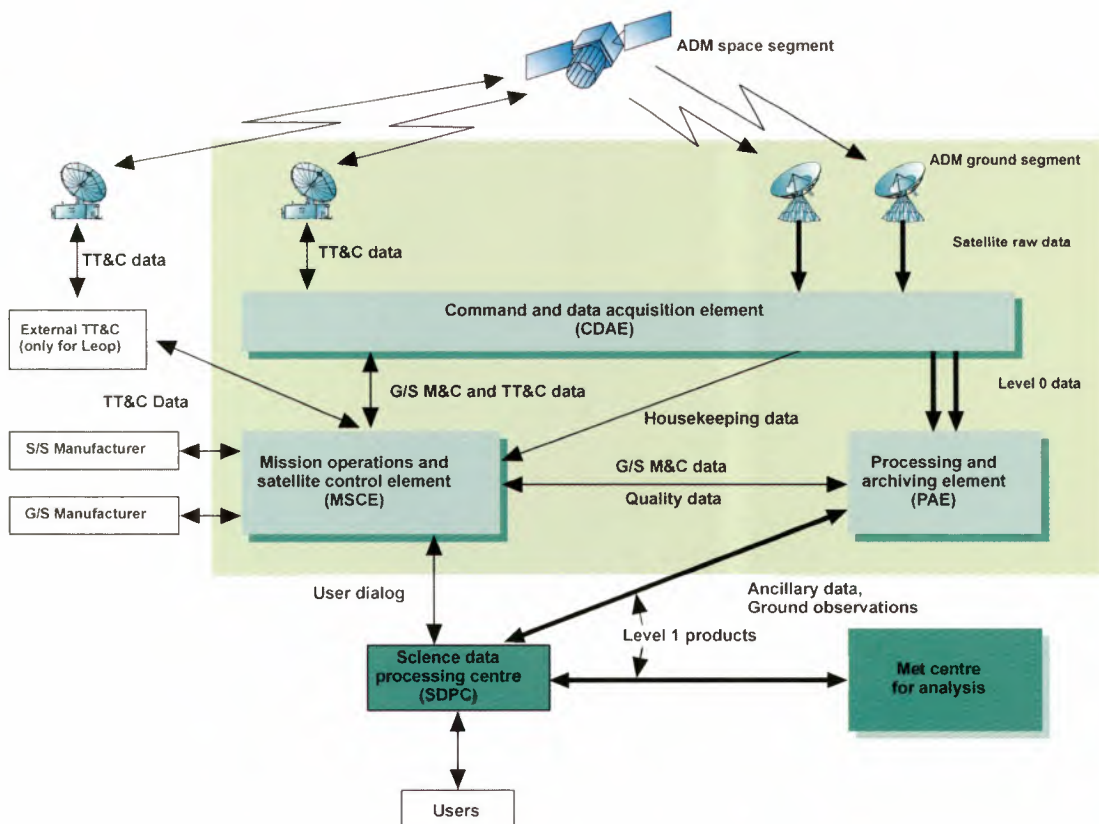


Figure 6.40. Functional architecture of the ground segment.

Mission Operations and Satellite Control Element (MSCE)

The MSCE is the core of the ADM ground segment. Its task is to operate the space segment and the ground segment. Among others, it performs the following functions:

- Mission Operations
- Satellite Operation, Monitoring and Control
- On-Board Software Maintenance, and
- System Performance Evaluation.

It is planned that the MSCE will be realised and operated at ESOC in Darmstadt. ESOC will have available all tools required to execute the tasks mentioned above. For flight dynamics, the Orbit Attitude Operations System called ORATOS will be used, which has already been employed for a number of different missions. For all other tasks mentioned above, the SCOS 2000 system is presently being developed and will be operational before the end of 1999.

Command and Data Acquisition Element (CDAE)

The CDAE is divided into the:

- TT&C station, and
- data-acquisition stations.

The TT&C station is the interface between the satellite and the ground segment for the exchange of satellite housekeeping data and the uplinking of telecommands including software upgrades to the satellite. For nominal operation, the housekeeping telemetry reception and the telecommand transmissions will be achieved on a 24 hour cycle. In order to meet the required 72 h autonomy the satellite will be pre-programmed accordingly. For contingency cases the data exchange is possible during more than 68% (11 out of 16 orbits) of the orbits. For nominal operations, the ESOC TT&C station at Kiruna is selected. As backup, other ESA TT&C stations can be used.

The data-acquisition stations have the task of acquiring the global data stream, containing the space segment housekeeping data and the instrument observation data, and forwarding them all to the PAE and the housekeeping data to the MSCE.

For the down-linking of the instrument observation data, an L-band link offering a data rate of 3.5 Mb/s has been selected. It has been designed to be compatible with the L-band HRPT facility, presently under development in the frame of the EPS programme (METOP ground segment). The HRPT facilities are small remotely

controlled stations, characterised by a parabolic tracking antenna with a 2.4 m reflector and a G/T better than 6 dB/K. The electronics is implemented in a 19 inch rack system, controlled by a PC with a GPS time and frequency reference system. In addition, the station comprises an integrated link quality-assurance system. These stations are expected to be available in 2002 for METOP and can directly be installed at the Kiruna and Barrow sites.

The data and processing flow for the observation data and the centres where the processing will be performed is depicted in Figure 6.41. All raw data, extended by annotation data describing the restituted orbit and pointing parameters, will be archived. The Level 1 products, characterised as geocoded wind component vectors including quality-control information will be delivered not later than 3 hours after observation to the science data-processing centre.

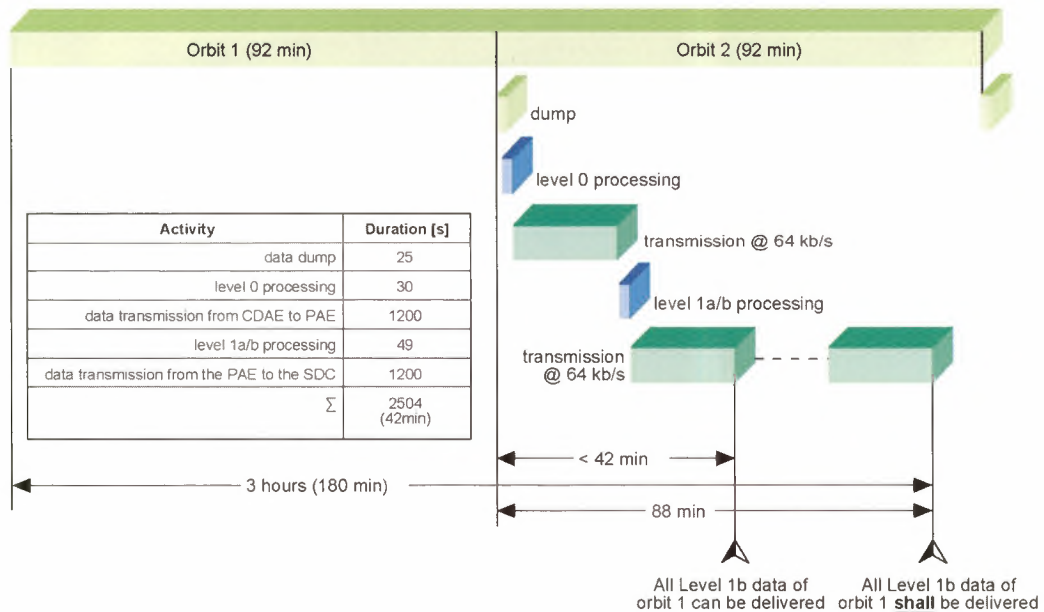


Figure 6.41. *Timelining of data transmission and processing.*

6.6.4 Networks

For communications between the different elements of the ground segment and with external entities, a range of networks will be exploited, as shown in Figure 6.42. It shows the architecture of the ADM ground segment together with the communication networks.

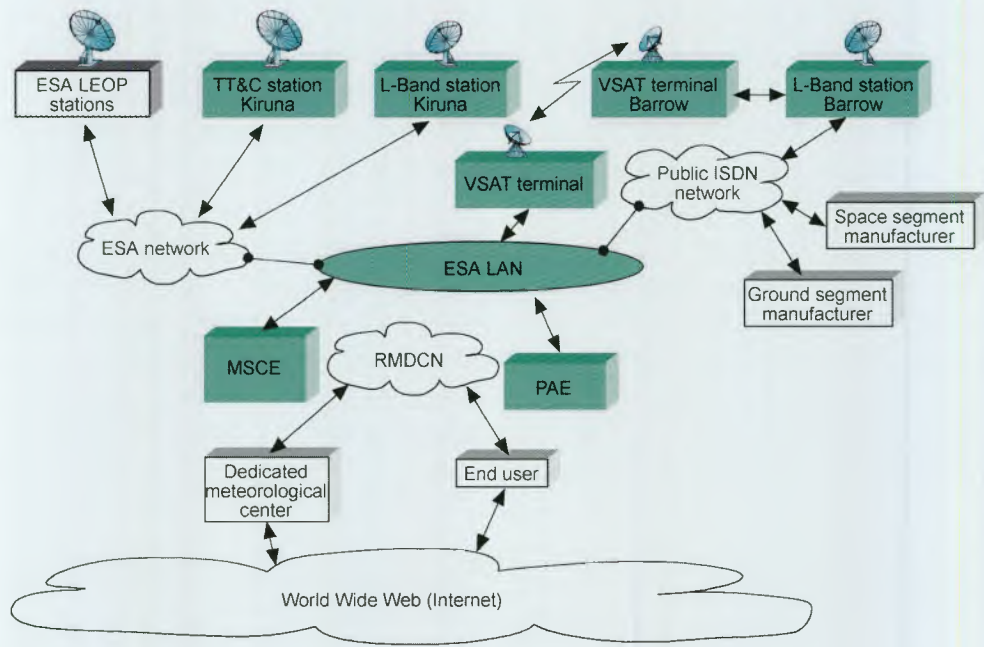


Figure 6.42. Ground-segment architecture with networks.

7 Data Processing and Validation

7.1 Introduction

From Raw Data to Mission Parameter

The instrument transmits raw data to the ground segment consisting of the accumulated spectra from the Mie receiver and the flux intensities from the Rayleigh receiver. These data are provided every 3.5 km length (nominal). Alternatively, the instruments can provide data every 1 km for dedicated areas when required, and for each altitude bin (-1 km to 16.5 km height for the Mie channel, 0.5 km to 26.5 km for the Rayleigh channel). In addition to these data, laser internal calibration and the attitude data are transmitted, as well as the receiver response calibration data.

Prior to integrating data over the 50 km length, cloud detection is performed in order to segregate the samples of clear air and those affected by cloud to control the processing in the presence of scattered cloud (see Section 7.4). Even in such a case the wind profile above the cloud is still obtained. Ground (or sea) echo is also searched in order to calibrate the ‘zero wind’ when possible. If there is no echo, satellite sensor data will be used to reconstitute Doppler shift variations due to the attitude of the satellite.

In order to transform raw data into wind measurements processing has to be performed for Mie and Rayleigh channels. This requires taking the radiance background and the spectrometer spectral response, as well as calibration data, into account. The decision to use Mie or Rayleigh channel data can be based on a signal-to-noise ratio threshold. Finally, each wind measurement for each altitude layer is located in an Earth reference frame, using satellite sensor data.

A schematic flow diagram for the data processing, calibration and validation, and information dissemination for the spaceborne Doppler wind lidar is shown in Figure 7.1. The various elements of this are discussed in the following subchapters, as indicated by the numbers shown to the right of each item. The particular tasks of the data pre-processing centre are shown in Figure 7.2, explaining the various processing steps.

Wind analyses from a dedicated meteorological centre are the final product of the ADM and will be distributed to the atmospheric research community at large. However, relevant Level 0, 1, and 2 processing and products will also be generated, distributed, and archived during the ADM. The data-processing levels have been defined by the Committee on Earth Observing Satellites (CEOS). Their definitions are shown in Table 7.1.

Level	CEOS Level Definition
raw data	Data in their original packets, as received from the satellite.
0	Reconstructed, unprocessed instrument data at full space-time resolution with all available supplemental information to be used in subsequent processing, e.g. ephemeris, health and safety appended.
1a	Unpacked, reformatted Level 0 data at full space-time resolution with all supplemental information to be used in subsequent processing appended.
1b	Radiometrically corrected and calibrated data in physical units at full instrument resolution as acquired.
2	Retrieved environmental variables at the same resolution and location as Level 1 source data.

Table 7.1. Data-processing level definitions (after CEOS).

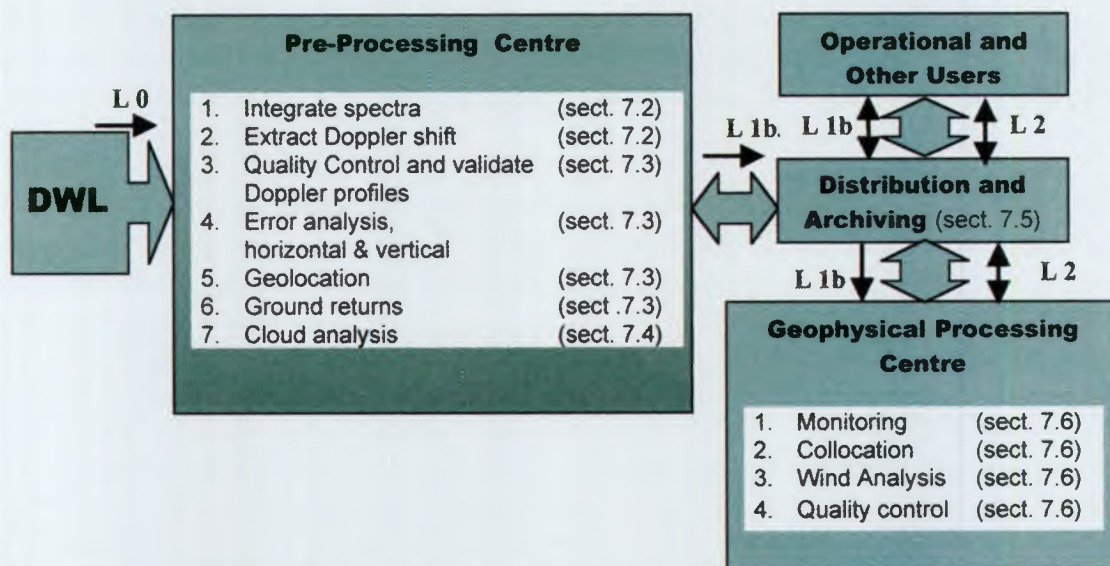


Figure 7.1. Schematic flow diagram for the data processing, validation and calibration of the information from a spaceborne DWL.

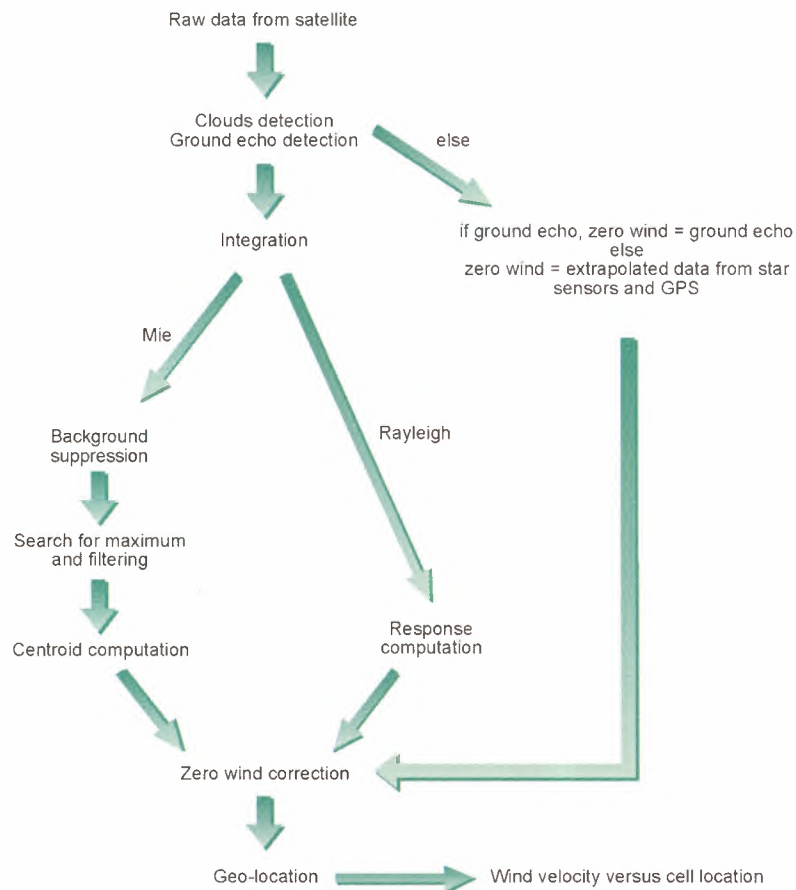


Figure 7.2. *The tasks of the data pre-processing centre.*

The Earth Explorer ADM is a demonstration mission in several respects. Although the ground processing is not very complicated, there are several aspects of the processing that will be developed during the demonstration mission by the lidar scientific community. The most important of these are discussed in this chapter.

7.2 Spectra and Doppler Frequencies

The information at Level 0 shown in Figures 7.1 and 7.2 will include all the spectral and lidar data, as well as necessary calibration and telemetry data. The spectral data basic accumulation on a shot-to-shot basis must take place in the primary detectors of the lidar. However, at each altitude the cloud and clear-air returns will be mixed. For example, an accumulation of 200 independent shots in an air layer with only 1% cloud cover gives a probability of a cloud-contaminated recording of $\sim 87\%$. Since convective clouds are broken and associated with large wind variability, it is therefore preferable to accumulate fewer shots at lidar detector level at one time, rapidly read this out for processing, and then repeat the sequence of short accumulations for

eventual computation of one wind profile by integration of several accumulation profiles.

By applying a criterion to reject primary cloud-contaminated data, the probability of clear-air returns is increased. Additional information about the atmospheric characteristics in the clear (Rayleigh) and cloudy (Mie) air can be inferred from the raw primary data, and better wind-profile estimates can result from this. Primary accumulation over 3.5 km (at 2 Hz rate) is the nominal baseline, but accumulation over shorter distances will be investigated for further optimisation during the mission.

In this case a 50% cloud cover will generally result in only slightly over 50% cloud-contaminated primary recordings at the cloud level, which can be identified from the estimated Mie and Rayleigh SNR values. Cloud occurrence results in a somewhat degraded Rayleigh performance over the 50 km integration length, but on the other hand the Mie recordings for the ~ 50% of cloudy returns can potentially improve the mean wind estimate at the cloud level, if both integrated detector readouts are combined in the processing.

Extraction of Doppler frequencies from integrated spectra and recordings in ground processing will be carried out using already prototyped software. They are based on algorithms taking theoretical evaluation and practical experience into account. These require modest levels of computing power, will be extremely rapid and provide processed data (Level 1) in essentially real time. The basic outputs of such spectral processing will include Doppler frequency shift, strength of aerosol signal, strength of molecular signal, strength of noise background, assessment of statistical error, assessment of systematic or bias error, proportion of cloud contaminated data and proportion of null results.

7.3 Quality Control

7.3.1 Validation and Errors

With respect to the validation of Doppler frequencies and the associated error assessment, two aspects need to be considered, namely statistical and systematic errors.

The main statistical error arises from the fluctuating photon-count numbers in the accumulated recordings. This can be dealt with in terms of the modelling and algorithms of performance that will be developed. In particular, for the aerosol system these essentially random statistical errors will be mainly dependent on the strength of the primary back-scattered signal. The quality-control algorithms will provide guidance on the reliability as well as on the purely statistical errors in individual measurements.

On the other hand, systematic errors in derivation of the wind velocity component and height assignment can arise in a number of ways. Vertical error correlation and profile bias can be introduced by moving particles at one altitude providing an apparent signal at another altitude. This may be due to the timing inaccuracies in the lidar, but also to the combination of strong aerosol stratification and the laser pulse shape. These effects have been investigated by Vaughan and Willetts (1998) for the case of typical carbon-dioxide pulse lasers. These effects are limited with short laser-pulses and a precisely calibrated system. In addition, the assessment of aerosol signal strength and warning of severe stratification will provide a valuable safeguard against faulty assignment of altitude.

Another source of this error arises from any inaccuracies in the spacecraft pointing and velocity restitution. The smaller the temporal scale of the random variations, the more damaging its effect will be. For the ADM, the effect has been reduced by appropriate selection of the instrument configuration and LOS. A good restitution of the LOS reduces the potentially large systematic HLOS wind errors. Additionally, a calibration will be performed on the ground return over land and sea.

In any case, if the cloud top height is well measured then the wind-component profile above this cloud level, measured relative to the motion of the cloud level, can be assimilated in principle. This will work well for stratiform clouds that have relatively small cloud dynamics and are rather uniform in cloud top height. In the case of convective clouds, the cloud dynamics can be substantial and the cloud top wind may not be representative of the mean flow. However, in these situations the atmosphere is usually unstable and the clouds broken, so that for multiple shots there is a large probability of them reaching the Earth's surface.

For validation and error assessment, it is planned to make use of aircraft observations. In addition, collocated radiosonde stations will be used to provide reference observations, a method also applied for the validation of cloud-motion winds.

7.3.2 Geolocation and Ground Returns

As emphasised above, precise knowledge of spacecraft pointing, position and velocity will be important in minimising systematic and bias errors in the derivation of measured winds. This has been discussed in Chapter 6, where detailed error budgets are given.

However, such returns must be considered with care. For example, signals from vegetation – crops, trees etc. – are likely to be considerably broadened by local movement, while those from moving targets will clearly give bias errors. The sea surface is the most obvious example, in which the wave spectra develop until the most dominant waves have the same speed as the local mean wind. Obviously the most reliable ground returns come from bare mountain, desert and snow-field type surfaces.

Obstruction of the Earth's surface by cloud and the subsequent absence of a ground return are additional limitations because reliable ground-truth returns may not always be as frequent as desired. The resulting errors have been taken into account in the error analyses and have been demonstrated to remain within acceptable limits. Additionally, even in the absence of a ground return, wind-shear profiles can be assimilated rather than absolute wind profiles. As mentioned in Chapter 4, this will only slightly reduce performance since effectively only one vertical level is lost.

Returns from the Earth's surface will be used to provide 'ground truth' for calibration and validation of the wind-profile observations.

7.4 Importance of Clouds

The impact of clouds on measurement capability deserves closer examination. Atmospheric transmission is hindered by the presence of cloud for all the DWL concepts that were considered. However, cloud top returns are generally bright, since clouds are effective scatterers. Nevertheless, the interpretation of this clear signal is complicated due to the cloud dynamics. In stratiform clouds the internal dynamics are mainly isotropic and small in magnitude, i.e. with an RMS variability of only a few tenths of a ms^{-1} . In convective clouds, however, cloud dynamics are anisotropic and much larger in amplitude. Here, the vertical wind-speed distribution is very skew (log-normal) and can locally be as large as 20 ms^{-1} (Lorenc et al, 1992). Returns from convective cloud tops will thus be difficult to interpret and give a biased estimate of the mean flow.

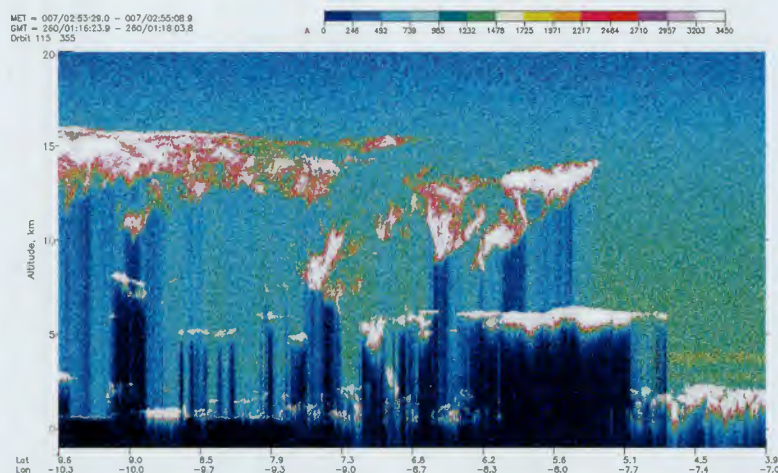


Figure 7.3. Lidar measurements in a tropical storm complex from LITE at a wavelength of 355 nm providing some insight into the cloud penetration and DWL processing properties in extremely cloudy and dynamic situations (Courtesy, NASA).

To facilitate the derivation of a volume-mean vector wind Stoffelen and Marseille (1998) suggest separating cloud from clear-air returns in the processing. Then, within a 50 km integration cluster, cases with anomalously large LOS wind or signal-to-noise ratio variability can be detected and assigned for dedicated processing or even rejection. Research and development will be needed to develop algorithms that effectively extract the useful information content of the measurements in these cases.

An example of lidar measurements from LITE in a tropical storm complex shows that even in cases of deep convection some cloud penetration is still possible (see Fig. 7.3).

7.5 Distribution and Archiving

Part of the distribution and archiving function of the ADM ground segment is described in Chapter 6; the PAE will archive the Level 1 data obtained from the DWL. Level 1 data will be processed to produce Level 2 data, which will be assimilated in a meteorological analysis. Since the volume of Level 1 data is small and the processing from Level 1 to 2 not very involved, it is most probable that Level 1 data will be distributed (together with a reference processing package as is common practice) to enable Level 2 processing at the user site. This it is already common practice for many operational meteorological satellite instruments.

The processing centre should have the responsibility for running this reference package, including the functions described previously, but also for developing, maintaining and supporting this package for other users, according to the recommendations of the lidar science community. The Level 1 to 2 processing package will be distributed through the distribution and archiving function described here.

The assimilation of Level 2 data (i.e. HLOS component winds with specified error properties) is straightforward (Chapter 4). Since the final product of the ADM is an improved meteorological analysis, these analyses are provided by dedicated meteorological centres and are distributed and archived. If major updates to the ground processing are implemented, re-analyses of the period with DWL observations should be performed, archived, and distributed. Current efforts on atmospheric re-analysis for use in climate-related studies indicate this as a likely evolution of the ADM.

7.6 Geophysical Processing Centre

The role of the Geophysical Processing Centre (Fig. 7.1) could be taken over by a meteorological centre. They have a great capability to calibrate, validate, and monitor observing systems (see e.g., Stoffelen, 1998, for the ERS scatterometer). The heterogeneous data of the GOS is assimilated in such a way into a meteorological model (as depicted in Fig. 4.1) that an almost uniform quality is achieved. The error

characteristics of the meteorological model are monitored closely by comparing it against the observations of the GOS, and are therefore well known. As such, the meteorological model state can be compared to any DWL profile and within a few hours sufficient statistics can be gathered to make judgements on the characteristics of the DWL measurements. From that moment on, useful calibration, validation, and monitoring activities can be started at the meteorological centre, assuming a stable system. For this purpose, the DWL data are collocated in near-real-time with the meteorological model, but also with other observations of related quantities (i.e. radiosonde, scatterometer, cloud motion winds, and aircraft reports in the case of a DWL).

When the calibration, validation, quality assessment, and monitoring activities are fully in place, the meteorological centre will embark on meteorological analysis and forecasts which will include DWL data, in parallel with the reference operational suite where DWL profiles are not used (control). The first-guess field incorporating past DWL observations will then be compared to the most recent observations in the GOS, in parallel with similar comparisons of the control first-guess. Thus, an assessment will be made of the improvement in the first guess due to the DWL data. A similar validation will be performed on the DWL and control forecasts.

If the DWL data prove beneficial for the analyses and forecasts, they will be incorporated into the operational suite. Obviously, monitoring activities will be crucial at this point, because a corruption of the analyses and forecasts due to an instrument failure has to be avoided. The operational use of the data signifies the most successful demonstration of the ADM, since forecast impact is generally only achieved after an improvement in the meteorological analyses.

The processing centre will use the collocated-observation and field products from the meteorological centre in order to validate and improve the processing. This will necessitate ancillary information, present at the meteorological centre, to be transferred in near-real-time to the processing centre. In turn, the improvements in the processing or quality assessment will benefit the assimilation at the meteorological centre.

In any case, the meteorological centre will eventually produce analyses in which the DWL profile data are incorporated. The scientific community at large will use these analyses to perform atmospheric circulation or tracer advection studies. The distribution and archiving centre will distribute the analysed atmospheric fields for further study.

7.7 Conclusions

The data processing and validation concept presented in this chapter is the most effective means of implementing the processing of the DWL observations. It relies on the infrastructure already in place at major meteorological centres. This is expected to be the most efficient way of establishing the required means for the end-to-end processing (including quality control and validation) of the ADM. The ADM will accelerate the development of tailor-made processing algorithms and would considerably enhance the feasibility-assessment of a full-scale DWL system measuring three-dimensional winds in order to better determine atmospheric dynamics.

8 Mission Performance

8.1 Introduction

Performance has been an important driver for the selection of the incoherent ultra-violet (UV) wavelength concept over the other concepts that were considered during the Phase-A of the ADM. The option to fly a DWL on the International Space Station, ISS, was rigorously evaluated and discarded because of inadequate performance. Only the free-flyer concept as proposed for the ADM will be discussed here. Profile reliability and accuracy, as well as performance in the upper troposphere and lower stratosphere, were the most important considerations in the concept selection.

Chapter 4 provides a detailed derivation of the requirements for the demonstration of a DWL in space as envisaged in the ADM. Feasible concepts now exist that can demonstrate the potential of a spaceborne DWL. In this chapter an assessment is presented of the performance of the system concept as proposed in Chapter 6, taking into account the processing described in Chapter 7. The principal performance assessment is the subject of Section 8.2. Table 8.1 puts the requirements of the ADM (see Table 4.3) into perspective and shows that these are closely met.

Passive meteorological sensors of temperature and humidity profiles have great limitations in cloudy conditions. On the other hand, active sensors are sensitive to cloud as well, but here strong signals with well-determined Doppler shift will be obtained from cloud tops, and above the cloud the principal performance is met. Below an optically thick and fully closed cloud layer, no wind-profile information will be obtainable. In Section 8.3 it is shown that this situation occurs infrequently. There is generally sufficient cloud porosity to obtain a useful performance in cloudy conditions, as demonstrated, for example, in the LITE mission (Winker and Emmitt, 1998) as shown in Section 7.4.

NWP performance is related to the observation of areas with meteorological instability. Wind shear is a pre-cursor of meteorological instability and an important issue is the correlation of wind-shear occurrence and cloud cover. Studies have shown that the detectability of wind-shear regions from space under cloudy conditions is still very satisfactory (Stoffelen and Marseille, 1998 and 1999). Section 8.4 discusses NWP performance and wind-shear detectability more in detail.

Moisture fluxes are of major importance for the tropical energy balance, and it is generally expected that large moisture fluxes are associated with cloud. Simulations confirm that areas with large humidity fluxes are encountered slightly more often in cloudy than in clear areas. Earlier studies reported some difficulties in the detection of humidity fluxes with earlier Doppler wind lidar concepts (Lorenc et al., 1992). Recently, it has been shown that they are generally detectable (Stoffelen and Marseille, 1998 and 1999). Section 8.5 discusses in more detail the tropical energy

balance and the detectability of humidity fluxes. Section 8.6 summarises the potential spin-offs from the ADM and Section 8.7 presents the main conclusions of this chapter.

		ADM Observational Requirements			ADM Performances		
		PBL	Troposph.	Stratosph.	PBL	Troposph.	Stratosph.
Vertical Domain	[km]	0-2	2-16	16-20	0-2.5 ¹	2.5 ¹ -16.5 ²	16.5 ² -26.5 ³
Vertical Resolution	[km]	0.5	1.0	2.0	0.5	1.0	2.0
Horizontal Domain		global			80S-85N ⁴		
Number of Profiles	[hour ⁻¹]	100			100		
Profile Separation	[km]	> 200			> 200		
Temporal Sampling	[hour]	12			12		
Accuracy (Component)	[ms ⁻¹]	2	2-3	3	2	2-3	3
Horizontal Integration	[km]	50			50		
Error Correlation		0.01			0.01		
Reliability	[%]	95			> 95		
Timeliness	[hour]	3			3		
Length of Observational Data Set	[yr]	3			3		

Table 8.1. ADM observational requirements and ADM mission performances.

Notes:

- 1) The performance required for the PBL will be available up to 2.5 km.
- 2) The performance required for the troposphere will be available up to 16.5 km.
- 3) The chosen concept will provide wind profiles with an accuracy of 3 ms⁻¹ up to 26.5 km. The instrument concept allows an extension to 30 km.
- 4) The limitation to 85°N and 80°S is not considered critical from a requirements point-of-view but simplifies satellite design.

8.2 Performance in Clear Air

The instrument's clear-air performance depends mainly on the molecular scattering signal strength and is easy to predict. The Mie channel will provide a good signal in the lower troposphere and for clouds. The number of levels in the troposphere that can be measured depends on the aerosol loading.

Figure 8.1 shows the expected mean clear-air performance provided by the UV concept, where at each individual level the better of the molecular and aerosol return is chosen for the observation of the Doppler shift (Stoffelen and Marseille, 1999). The aerosol loading of the atmosphere was chosen randomly, such as to represent the statistical aerosol-distribution characteristics of the real atmosphere at 355 nm (Vaughan et al, 1999). During the mission, a combined processing in the lower troposphere is expected to increase the actual performance above that predicted.

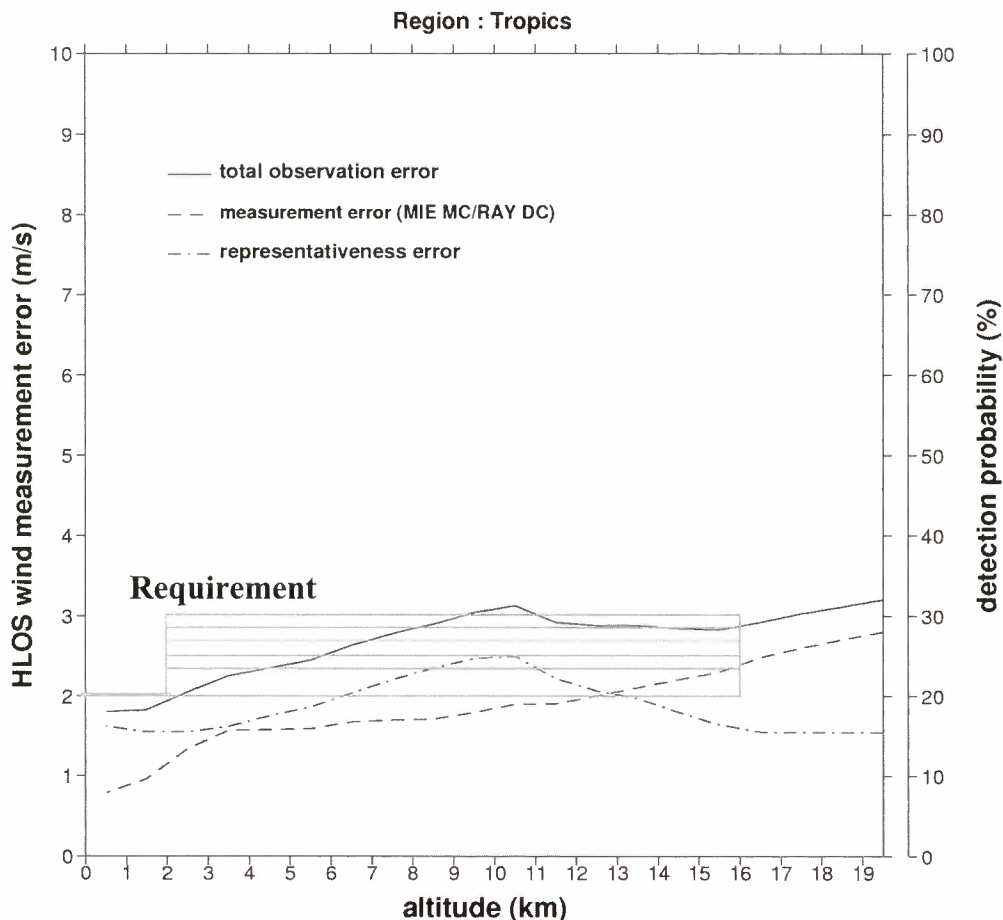


Figure 8.1. Simulated performance of HLOS winds for the ADM DWL concept at a vertical resolution of 1 km. A spatial representativeness error variability is added for the HLOS component winds to represent a volume-mean quantity (see text). In clear air the observation requirements are closely met (requirement is added for reference).

Atmospheric analyses resolve volume-mean quantities as described in Chapter 4. As such, the ADM DWL observations will not have the perfect spatial representation for the analysis, and so a spatial representativeness error variability must be added to the detection error variability, as is common practise in meteorological data assimilation. Figure 8.1 demonstrates that in clear air the useful wind-profile quality specification as recalled in Table 8.1 is closely met.

The allocation of the detected signal to the appropriate height level is crucial. Error sources may lie in, for example, laser frequency drifts, detector drifts or blurring. An additional effect arises from multiple scattering: if the light path perpendicular to the LOS is substantial, the assigned altitude will be lower than the real altitude. However, the calibration scheme for the laser frequency and detector frequency response, as well as the narrow FOV, basically eliminate the negative effects of these potential error sources.

In some cases, atmospheric spatial variability effects (shear, cloud, and aerosol), encountered during shot accumulation, could cause vertical error correlation after the data processing. Such effects will be investigated in the development of the wind-profile retrieval or DWL observation operator. Along the line of accumulation or integration in useful signal conditions, it will be possible to estimate the atmospheric wind or the signal-to-noise ratio variability. This would be useful not only for quality control, but also a useful by-product to determine areas with atmospheric turbulence and cloud.

8.3 The Impact of Clouds

Atmospheric transmission is hindered by the presence of cloud, potentially posing a problem for a spaceborne DWL. Wind profile information below thick cloud is not achievable. On the one hand, clouds around the tropopause are usually transparent and a signal from below the cloud can be obtained. The backscattered signal from the cloud is generally very strong and will result in a good determination of the Doppler shift. On the other hand, clouds in the lower troposphere are thick and do obstruct the lower part of the profile.

Table 8.2 shows the cloud-cover figures in the atmospheric database that was used in the simulation of the ADM DWL by geographical area. These values have to be interpreted carefully, due to the fact that where clouds are present, they are often broken, still permitting the measurement of a wind profile when using multiple-shot wind-profile observations. Winker and Emmitt (1998) report on the cloud porosity in case of the LITE mission, confirming the beneficial effect of multiple shots in the lower troposphere. For example, a cloud cover of 0.99 and 700 shots provides only a probability of 0.09% that all shots encounter cloud.

Region	Polar	Storm T.	Subtrop.	Tropics	Subtrop.	Storm T.	Polar
Latitudes	> 60S	60S-40S	40S-20S	20S-20N	20N-40N	40N-60N	>60N
% Clear	37	27	32	18	40	31	34

Table 8.2. *Percentage of clear-air scenes by geographical area of the atmospheric database that is used in the simulation of the ADM DWL (February).*

Obviously, the expected amount of energy reaching the lowest levels of the troposphere is dependent on the total cloud cover aloft. If clear air resides below the cloud layer, a strong aerosol loading is needed to get a good-quality wind-profile retrieval using a (much) reduced number of shots. Close to the surface the aerosol loading will generally be sufficient. A cloud cover of 75% aloft will cause only a quarter of the shots to contribute to a wind observation at a particular vertical level. This leads, for the molecular return, to a decrease in the RMS accuracy of the wind observation by roughly a factor of two with respect to the clear-air performance at that same level.

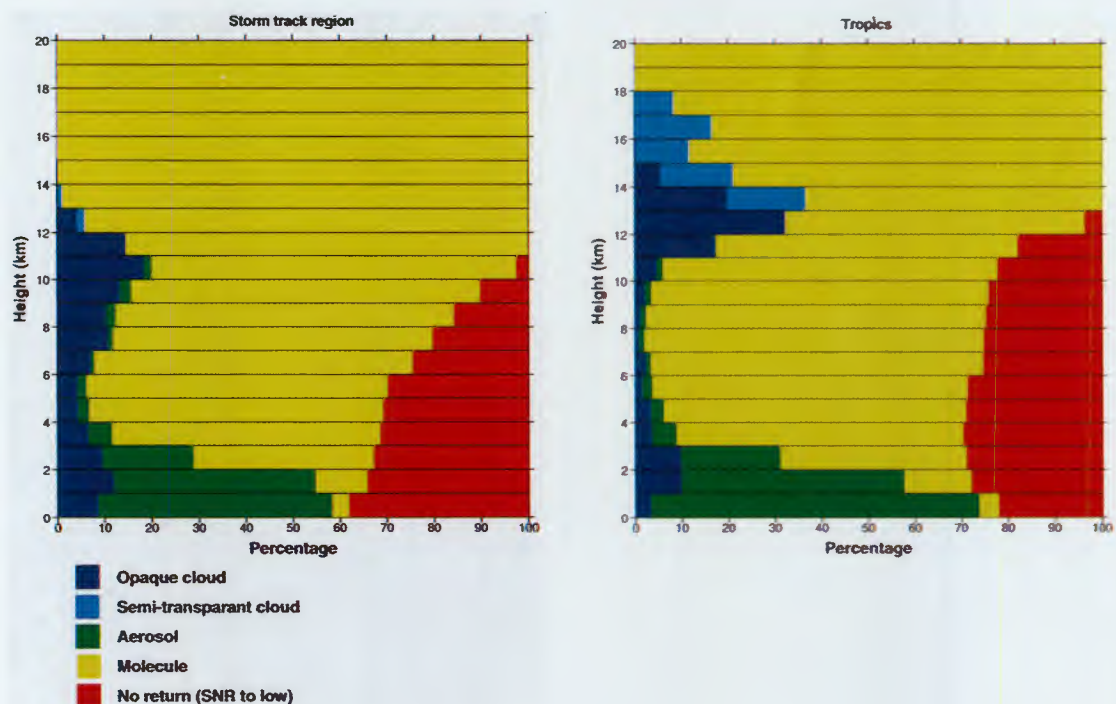
A statistical analysis of the performance of the proposed DWL in cloudy air has been performed. The DWL system has been simulated in an environment where the clouds were provided from a realistic meteorological model (Stoffelen and Marseille, 1998 and 1999). Figure 8.2 depicts the signal return and wind HLOS quality as obtained in the two cloudiest regions of the world. Below an altitude of 13 km ‘no returns’ occur, due to obstruction by thick cloud, whereas in the tropics above this level mainly transparent clouds are present. Though few, aerosol returns occur up to 10 km height. In these regions cloud obscuration is most significant in the lower troposphere, at about 30%. Signal quality reduction takes place in several profiles due to the presence of cloud aloft. Cloud attenuation and obstruction are most substantial in the tropics and in the lower troposphere in the storm track region.

A large amount of shots penetrate the lower troposphere, contributing to very good quality winds, due to the aerosol signal detected by the Mie channel. Broken stratiform cloud in the lowest few km of the troposphere, which is quite common, may be easily penetrated and measurements are then possible due to the strong aerosol signal close to the Earth’s surface. The presence of cloud is most critical around the tropopause and the cloud cover in the tropics is the most extensive according to Table 8.2. Since high-level clouds tend to overlap with lower-level clouds, below the tropopause level in the tropics cloud obstruction is relatively constant at 25%, indicating that in about 75% of cases a complete profile is obtained. This would result in about 100 profiles per hour classified here as good or very good, fulfilling the requirement of Table 4.1.

The number of cloud-top-dominated returns is most important around the tropical tropopause (35%), and less important around the storm-track region tropopause (less than 20%). Even though the returned Mie signal is high here, it is not clear that the observed LOS wind is always representative of the mean flow. The cloud facet that returns the signal may be in a very turbulent region due to cloud dynamics. Little is known about the detectability of strong vertical motions from a spaceborne DWL. However, vertical airborne DWL measurements over convective cloud systems seem to indicate that strong vertical cloud movements often occur below the cloud top at the tropopause, enabling good measurements to be made at the cloud top level. Further analysis in this area is needed.

The proposed scheme of a smaller accumulation length within a larger integration length, permits the rejection of returns on dynamic clouds. In case of broken cloud the multiple accumulations in the integration area will not all have cloud-top returns, but only a fraction of them. This fraction is close to the cloud-cover fraction when the number of accumulations in the integration is large, or in other words, when the accumulation length is small compared to the integration length. By segregating the cloud-dominated and clear signals in the processing by signal-to-noise ratio, one can reduce the contamination by the cloud dynamics by applying a quality control or improved wind retrieval (see Chapter 7). It has been demonstrated (Stoffelen and Marseille, 1998) that (for a coherent DWL concept) in about 50% of the scenes with clouds, it is still possible to retrieve winds from the clear-air return. Their performances were about 1.6 times worse than the requirement for clear air. However, this is still useful.

a)



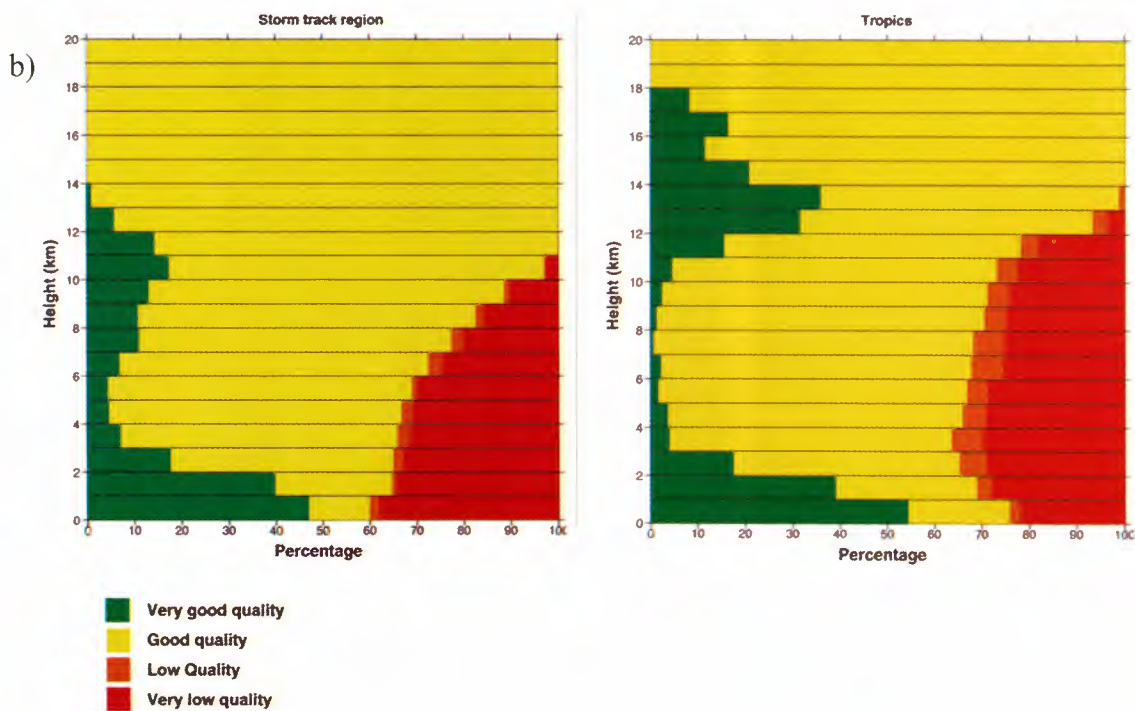


Figure 8.2. Simulated ADM DWL performances for cloudy atmospheres – The left panels are for the storm-track region, whereas the right ones are for the tropical region, i.e. both relatively cloudy regions. The top panels (a) classify the signal return and the lower panels (b) the normalised HLOS accuracy compared with the representativeness error at the different vertical levels.

8.4 Usefulness for NWP

As already demonstrated with OSEs and OSSE (see Section 2.3), the impact of wind profiles on numerical weather prediction is very important. An additional aspect to be considered are precursor features, such as divergence or vorticity. Atmospheric structures that are precursors to the development of extra-tropical cyclones can often be identified before cyclogenesis takes place. In the preparation of the ADM, vertical wind shear has been studied as relevant example. Mid-latitude weather systems are believed to have their origin in processes encapsulated in the theory of baroclinic instability. A suitable measure of the baroclinicity is provided by the Eady growth rate maximum (e.g. Hoskins et al., 1978; Hoskins and Valdes, 1990) in which the vertical wind-shear is the main variable.

To study the impact of clouds on the detectability of vertical wind-shear, the DWL signal return and HLOS wind quality for cases with strong wind-shear have been investigated. As illustrated in figure 8.3, the signal strength and the corresponding wind quality are quite similar in the upper troposphere to cases without strong vertical

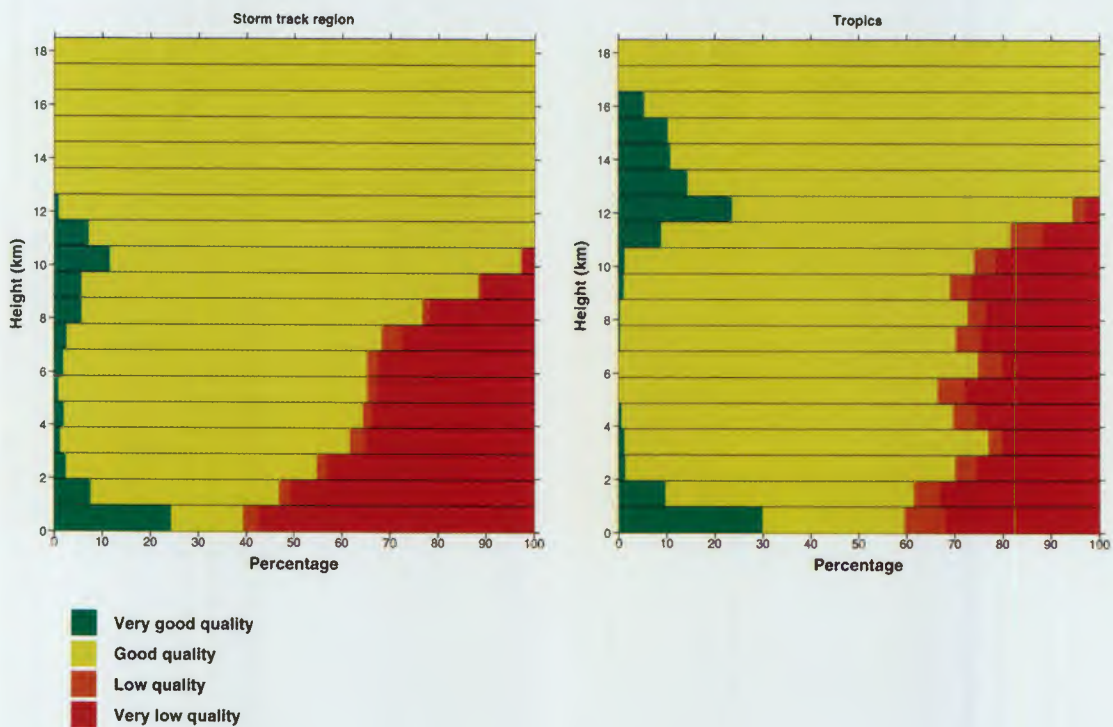


Figure 8.3. Simulated ADM DWL performances for vertical wind-shear - detectability in the storm-track region (left) and in the tropics (right). Wind-shear detectability is only weakly correlated with the occurrence of cloud.

wind-shear, and, as such, the occurrences of shear and cloud are not very correlated (see Fig. 8.2). It has to be noted that relatively few cloud returns (very good quality) appear when strong shear is measured. Only in the lowest few km of the troposphere in the storm-track region is a reduced detectability of wind shear observed, despite the occurrence of aerosol returns at this level. Therefore, the ADM will generally have the ability to observe vertical wind-shear in broken-cloud conditions, with a possibly slightly reduced capability close to the surface in the storm-track regions.

Beyond this, the ADM will have a major impact on wind-profile analysis. In particular, better wind profiles will be available in data-sparse regions like the Southern Hemisphere or over the oceans. The ADM will not replace, but be an extremely useful complement to the existing elements of the GOS (e.g. the global radiosonde network) by providing more frequent, more reliable and global observations of the wind fields in the Earth's atmosphere.

8.5 Usefulness for Climate Studies

A proper analysis of atmospheric transport properties is fundamental for studying the Earth's climate system on several spatial and temporal scales, as outlined in Chapters 2

and 3. Atmospheric analyses are increasingly used to study the complex climate system, and re-analysis projects aim at providing consistent long-term series (ERA15, ERA40). Wind fields are important as background fields in climate models. Although many aspects of the atmospheric circulation could be studied, the ADM's usefulness for climate studies is illustrated here mainly for humidity transport.

Important variables in the hydrological cycle and the tropical circulation are heat and humidity transport. Stoffelen and Marseille (1998, 1999) studied the detectability of tropical fluxes of heat and humidity in cloudy areas. Obviously, processes of humidity transport, condensation and precipitation are often associated with cloud. On the other hand, multiple shots in case of cloud porosity (Winker and Emmitt, 1998) can enhance the detectability of atmospheric heat and humidity fluxes in cloudy conditions as discussed in Section 8.2.

As an example of the usefulness of the ADM DWL for studying atmospheric processes associated with the energy balance, Figure 8.4 shows the quality of the wind observation in the tropics and storm-track region for those meridional moisture fluxes that are larger than the mean plus one standard deviation of the flux variability at the level considered. Comparing these type of histograms with the corresponding histograms of performance classification for all flux conditions (similar to Fig. 8.2), it can be concluded that

- many returns from cloud appear in moist air at all geographical locations
- at altitudes in the middle and lower troposphere cloud obstruction of the moisture flux is most substantial
- for the lowest altitudes, aerosol scattering generally provides an improved performance in moist conditions with respect to the molecular scattering signal.

Thus, assuming that the horizontal line-of-sight winds observed at cloud top height are representative for the general flow, a DWL in space provides essential information on the tropical circulation in the upper troposphere. On the other hand, clouds obscure the detectability of moisture fluxes in the middle troposphere, in particular in the tropics. Due to the Mie system, the near-surface moisture flux is well visible in the majority of cases.

The ADM will meet the user requirements. Even in areas with high cloud cover, unfavourable for DWL wind-profiling, the ADM will provide useful information to study important circulation and transport properties of the atmosphere that are relevant to study our climate system, and which are outlined in Chapters 2 and 3. The mission will provide new insights into the distribution of kinetic energy in the Earth's atmosphere.

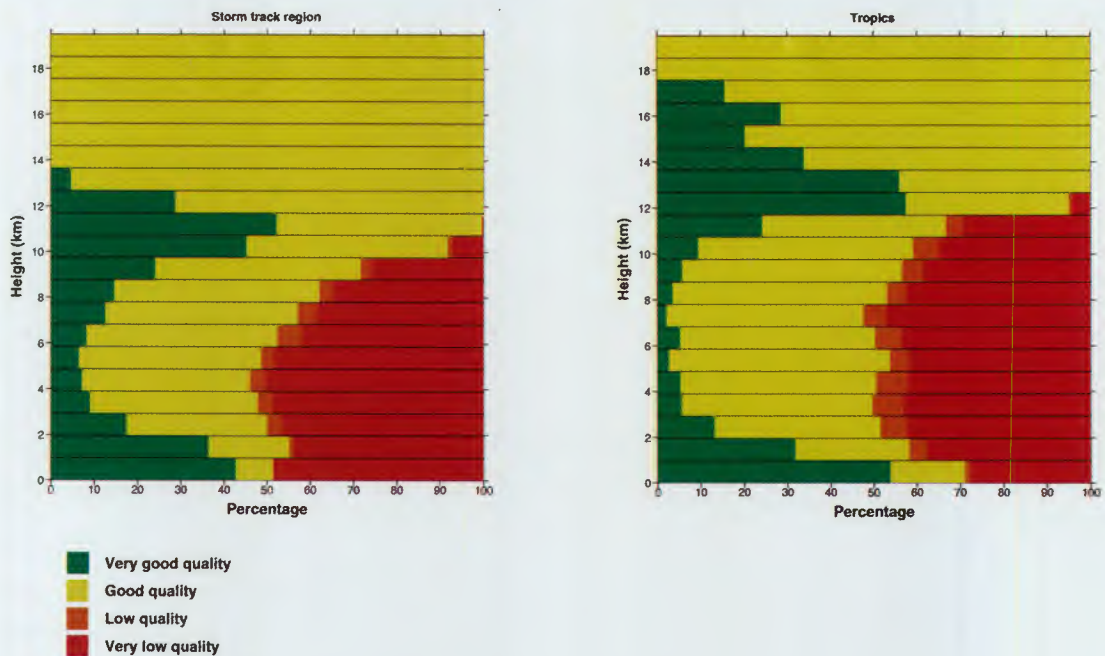


Figure 8.4. Simulated ADM DWL performances for meridional humidity-transport - detectability in the storm-track region (left) and tropics (right) (similar to Fig. 8.2a).

8.6 Other Elements Provided by the ADM

In addition to line-of-sight velocity measurements, the ADM space-based DWL will be able to provide information on cloud characteristics over the depth of the atmosphere, as well as aerosol measurements in the troposphere. These include:

- cloud top height (notably cirrus top and base)
- cloud cover
- cloud and aerosol extinction and optical thickness
- identification of multi-layer clouds
- a measure of clear-air turbulence or other wind variability
- lower-troposphere aerosol stratification
- the height of the tropopause
- the height of the planetary boundary layer (PBL).

The properties of these secondary products are determined by the requirements for the wind-profile product. The vertical resolution of the secondary products is the same as the one used for the velocity measurements. The horizontal resolution of the information is locally enhanced, depending on the shot-accumulation strategy. Since priority has been given to the LOS wind measurement, only a small effort has so far

been put into the retrieval of the secondary products, so that the above list needs to be further explored.

Cloud properties are prognostic variables in some atmospheric models now and will be even more so in the future. In a four-dimensional data-assimilation scheme, some of the DWL cloud products may be assimilated directly in the atmospheric analysis. The cloud information is relevant for radiative-transfer calculations in the model. Tropopause and PBL height may also be validated against forecast and general circulation models. Moreover, DWL cloud top winds are a unique validation of geostationary cloud-motion winds. Many atmospheric circulation models currently use a fixed aerosol profile. The tropospheric aerosol products may be inserted as tracers in the data-assimilation system, again to benefit radiative-transfer calculations, but also chemistry computations. This in turn may be helpful for the ADM data processing.

8.7 Conclusions

The ADM will meet the scientific objectives outlined in Chapters 2 and 3. It will meet the observational requirements tabled in Chapter 4. The ultraviolet concept presented in Chapter 6 has the potential to meet the ideal user requirements (as tabled in Section 4.1) which will provide an increased beneficial impact from spaceborne wind profile measurements in atmospheric analyses, modelling, and prediction. The proposed demonstration ADM will pave the way to future operational wind-profiling missions.

The expected accuracy of the measured DWL HLOS winds in clear air is very similar to conventional meteorological wind-profile observations. However, the DWL wind profiles result in a much more uniform sampling over the globe. They cover the oceans with a density similar to the mean density of the ground-based wind profiles over land in the Northern Hemisphere.

As shown in Chapter 2, although distributed very irregularly, the conventional wind-profiling network is of key importance to atmospheric analyses and weather forecasts. The proposed wind-profiling complement is, therefore, expected to be very beneficial.

The impact of cloud on the DWL performance is very important. Although lidar signals are able to penetrate thin clouds (e.g. cirrus) to a certain extent, opaque clouds obscure the underlying atmosphere. It is shown that multiple shots are a good strategy for deeper atmospheric penetration in case of broken cloud. As such, the DWL provides good detectability of the near-surface moisture flux due to aerosol detection, which is important for climate studies. The impact of multiple shots is most substantial in the tropics.

The improved analyses will be of benefit for both tropical and extra-tropical weather forecasts. Improved information on transport and circulation will be beneficial for

climate studies as detailed in Chapter 2. In particular, improved advection of tracers, like ozone, aerosol, or other species, would benefit the atmospheric-chemistry community, and enable enhanced analysis of humidity convergence.

The Atmospheric Dynamics Mission will make a unique contribution to atmospheric modelling and research by providing, for the first time, one of the key parameters, i.e. the atmospheric wind, directly and globally. The mission is therefore a true exploratory mission.

9 Programmatic

9.1 Development Approach

The development plan proposed by the industrial team at the end of Phase-A is shown in Figure 9.1. It leads to a launch at the end of 2004. Phase-B is assumed to start in July 2000. Also shown are the ongoing breadboard activities. A gap is included between Phase-B and C/D to allow for proposal negotiation. The schedule is tight, but for the challenging units appropriate risk-reduction measures in the form of breadboarding activities have been initiated and will allow the 2004 launch date to be met.

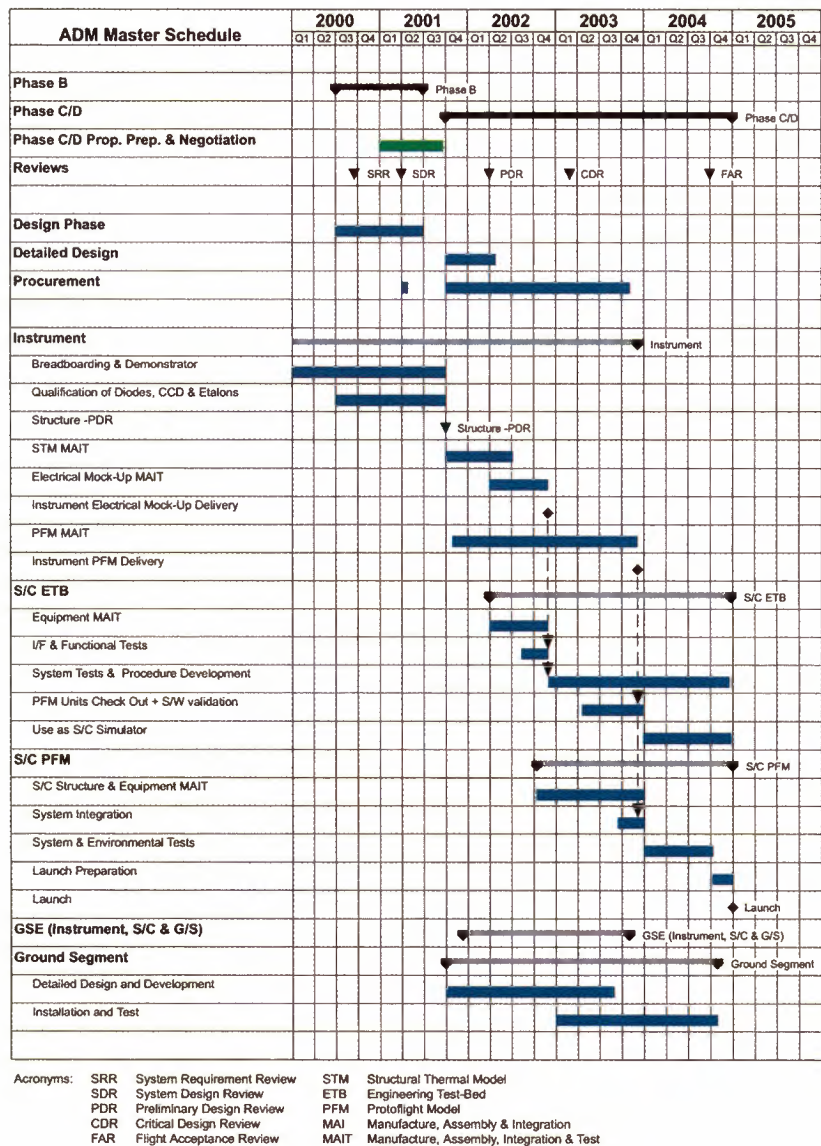


Figure 9.1. Development plan.

The model philosophy and the development flow are shown in Figure 9.2. A distinction is made between the instrument and the platform equipment. For the instrument, a structural-thermal model (STM) is proposed consisting of the opto-mechanical and thermal subsystem and dummies of the other elements. For the transmitter and receiver subsystems, it is proposed to build-up breadboards, at qualification-model level for key elements. Subsequently, this breadboard will be completed on an EM level to an electrical mock-up used for electrical and functional testing at instrument level. For interface and functional system tests, this mock-up will then be connected to an engineering test bed (ETB).

Concerning the spacecraft equipment, engineering/qualification models are proposed to perform delta qualifications for the power control and distribution unit (PCDU) and the CDMS described in Section 6.5.3. For these units, qualified designs already exist at board level and therefore structural and thermal qualification will be done with proto-flight models. Only flight models are procured for all other platform units. The spacecraft is also functionally tested in the ETB.

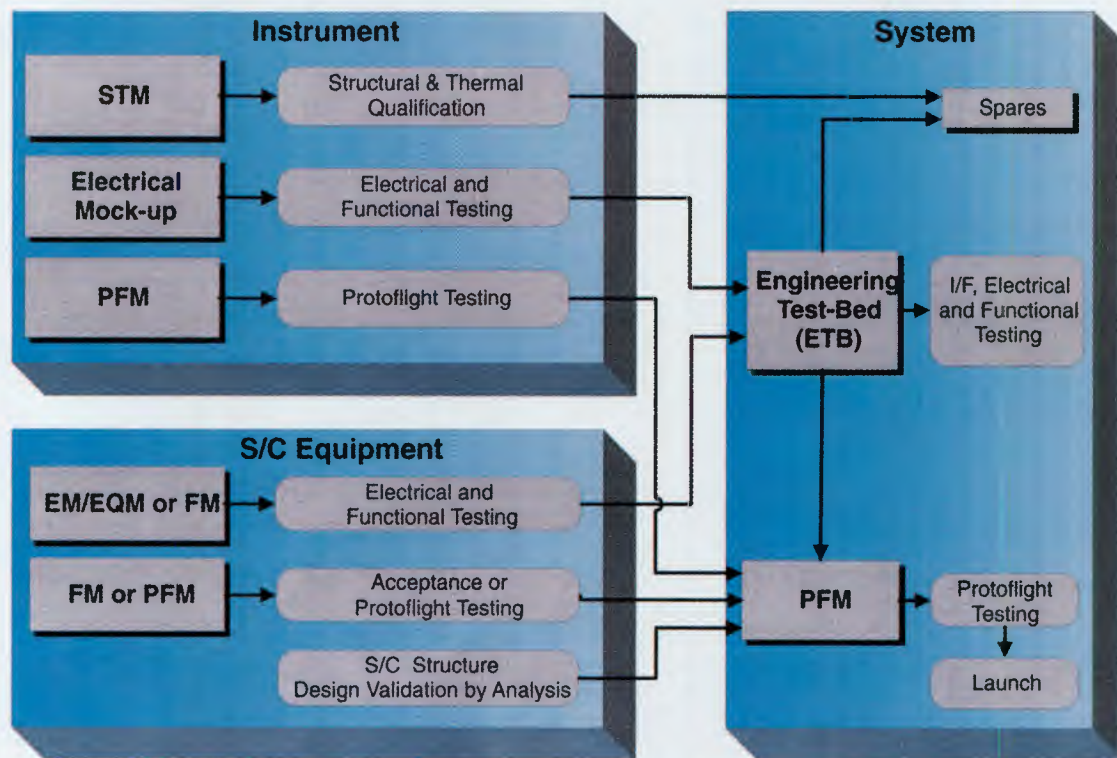


Figure 9.2. Model philosophy and development flow.

9.2 Heritage, Critical Areas and Risks

Table 9.1 shows the implementation and heritage for the ADM space and ground segment. The large heritage at platform level and the pre-development activities for the instrument are to be noted.

		Implementation	Heritage
ALADIN Instrument			
Transmitter	Concept	Frequency tripled Nd:YAG, 130 mJ 100 Hz	
	Medium Power Oscillator	Q-switched diode pumped Nd:YAG 130 mJ @ 1.06 μm	Based on existing ground based military application designs
	Power Amplifier	Diode pumped Nd:YAG 350-400 mJ @ 1.06 μm	Based on existing ground based military application designs
	Frequency Tripler	KD*P or LBO nonlinear crystals, efficiency >30%	Efficiencies demonstrated in various applications, dedicated test program conducted in Phase-A
	Q-Switch	KD*P design with dedicated high voltage electronics	Identical unit developed and successfully tested in frame of ATLID breadboarding activities
	Pump Diodes	1 kW stack or autostack diodes	Commercial products from European suppliers; life test data available
	Pump Diode Electronics	Current pulses of 150 μs with 85 A at 192 V	Representative BB developed and successfully tested in frame of ATLID
	Reference and Seed Laser with Drive Electronics	Low power CW diode pumped non-planar ring lasers	Available as commercial product from European supplier
	Thermal Control	Heat pipe	Standard space product
Receiver	Rayleigh Receiver	Double edge Fabry Perot	Already manufactured and tested by Service d' Aéronomie-CNRS; space qualified technologies are used
	Mie Receiver	Fizeau interferometer	A B/B is already manufactured and tested (IDWL study). Space qualified technologies are used (molecular bonding)
	Detector	Thinned back illuminated CCD in accumulation mode	All technologies are validated on GOMOS spectrometer. Performance and operation concept will be validated on prototype to be tested before end of 1999
	Filters	Interference and Fabry Perot filters	Based on existing designs
	Detection Chain Architecture and Operation		Partly validated during IDWL
Telescope	Primary Mirror and Structure	1.1m diameter F/0.9 aperture All SiC design	Derived from FIRST and OSIRIS development activities
Core Instrument Structure		All SiC design	FIRST, OSIRIS structural and flight models, early breadboarding

		Implementation	Heritage
Platform			
Configuration		Integrated satellite design directly serving required instrument accommodation	Offered by most LEO spacecrafts, e.g. Flexbus, Leostar, Proteus, etc..
Structure		Box type structure with central cone based on aluminium honeycomb elements	Very large heritage in numerous ESA programmes by use of standard material and technology
Thermal		Conventional passive design with heat pipes, heaters, radiators, thermistors, ...	Very large heritage in numerous ESA EO and science missions
AOCS	Attitude	3-axis controlled off-nadir across track pointing with yaw steering	Can directly be implemented by most LEO platforms
	Sensors	Star tracker, 3-axis magnetometer, inertial reference unit (IRU)	Off-the shelf equipment
	Actuators	4 ball bearing reaction wheels + 3 magnetotorquers	Off-the shelf equipment
	Positioning	GPS receiver equipment	Off-the shelf equipment
	Propulsion	4 x 1N Hydrazine thrusters and 100 kg fuel and tank	Off-the shelf equipment
Data Handling	Concept	Integrated data management system	Heritage from small satellites e.g. Leostar, Flexbus, Proteus
	Data Bus	IEEE 1355 for intelligent users, RS 422/485 for non-intelligent users	Standard, parts are available
	Computer	Data management based on single platform computer, centralised avionics S/W for satellite command & control, AOCS, thermal, etc	Based on ERC 32 processor development
	Data Storage	256 Mbit memory unit	Reuse of already existing design, e.g. Cluster
Comm's	TT&C	Standard S-Band transponder, 2 kbps uplink, 64 kbps downlink	Off-the shelf equipment
	Payload Data Transmission	Instrument data downlink via meteorological L-Band with 3.5 Mbps	Reuse of existing hardware as presently in development for Metop
Power	Solar Array	8.4 m ² in 2 fixed wings, based on Si-BFSR cells	Reuse of Globalstar design, several potential suppliers for cells
	Battery	NiCd battery with 18 Ah	Off-the shelf equipment
	Regulation	Hybrid power bus design, unregulated for instrument, regulated for all other	Large heritage for both, regulated and unregulated bus technology
Launcher		Rocket	SS19, Breeze on Proton, two demo flights in 1999

Ground Segment			
Ground Segment Elements	CDAE	Data dump every orbit required, hence two near-polar L-band stations necessary	L-band receiving station already in development for METOP ground segment
	MSCE	Standard mission operations and control	Large heritage, e.g. at ESOC
	PAE	Data processing and archiving up to Level 1, data distribution to Science Data Processing Centre	Large heritage, e.g. at Eumetsat

Table 9.1. Implementation and heritage.

Table 9.2 shows the critical areas identified at the end of Phase-A and the proposed risk-reduction measures. Critical areas concern only the instrument, where criticality is low to moderate. The key elements exist already, which allows us to be confident regarding the technology. It is necessary, however, to verify the end-to-end performance of all elements integrated and to demonstrate the flight compatibility. This is achieved by proposing early breadboard and qualification activities, partially started already, and establishing the appropriate model philosophy as defined in Section 9.1.

		Critical Areas	Risk Reduction
ALADIN Instrument			
Transmitter	Lasers	End-to-end performance in terms of pulse energy, beam profile and qualification	Dedicated transmitter BB initiated
	Pump Diodes	Formal space qualification	Dedicated lifetime verification programme initiated
Receiver	CCD	Charge transfer efficiency	Dedicated test programme initiated
	Combined Mie and Rayleigh Receiver	Proper function of combined receiver	Performance verification in frame of IDWL running.

Table 9.2. Critical areas and risk-reduction measures.

No critical areas have been identified in the platform and the ground segment. For the launcher, there are alternatives to Rockot.

In summary, the proposed implementation concept has a few areas of low to moderate criticality at instrument level, related more to ‘putting together’ elements than to technological challenges.

9.3 Related Missions, International Co-operation Possibilities and Timeliness

The NPOESS lists wind profiles as a top priority observation which, however, is not covered by the present NPOESS baseline. In view of the high interest, mission

concepts are being mentioned in the USA (and also in Japan), but no consolidated plans exist at this time. SPARCLE is a NASA experiment consisting of flying a 2 micron system on the Space Shuttle. It is planned for launch in 2001 and to last for the typical duration of a Shuttle flight. It will provide data only for the lowest km of the atmosphere.

Co-operation can be envisaged within Europe with other European international organisations. Eumetsat have shown their interest in the ADM and could participate, e.g. facilitating the archiving and the near-real-time data distribution to operational users. The ECWMF has indicated an interest in becoming the lead centre in assimilating ADM data.

Co-operation could also be sought with NASA / NOAA and consist, as a minimum, of the provision of a high-latitude data-acquisition station, e.g. Barrows in Alaska, to guarantee near-real-time data provision for all orbits.

The ADM is very timely. It will allow to develop all capabilities scientific, technical, technological and operational in time for deployment in a future operational system of the Joint Polar System that includes the American NPOESS and the Eumetsat Polar System (EPS) with the METOP satellites.

9.4 Enhancement of Capabilities and Applications Potential

The expected advances in science have been discussed in previous chapters. This mission is also very relevant to the enhancement of capabilities to enable applications and future operational systems.

The potential for operational application of the ADM observations has been recognised for many years and recalled again recently (WMO,1998). Eumetsat and the meteorological services have also shown an interest in the operational utilisation of wind-profile observations.

The ADM will develop the underlying science, the technology, the observation techniques, the models and the assimilation schemes and operational practices required to provide these applications with operational systems on a routine basis. The ADM science and technology developments will provide almost immediate returns. The need for and usefulness of the ADM are clearly apparent.

The ADM will allow Europe to develop its position in space lasers, a domain in which, despite the investments for more than a decade, the lack of a mission prevents it from being present in this critical technological area.

References

- Atlas, R., 1998: Potential impact of a DWL on weather analyses and forecasts, Zephyr project presentation, <http://zephyr1.gsfc.nasa.gov>.
- Cardinali, C., J. Pailleux and J.N. Thépaut, 1998: Use of simulated satellite doppler wind lidar data in NWP: an impact study, CNRM/GMAP Note No. 6.
- Chanin, M.L. et al., 1994: Recent lidar developments to monitor stratosphere-troposphere exchange, *J. Atmos. Terr. Phys.*, 56, 1073-1081.
- Courtier, P., P. Gauthier and F. Rabier, 1992: Study of preparation for the use of Doppler wind lidar information in meteorological assimilation systems; *ESA-CR(P)-3453*.
- Cress, A., 1999: Impact of wind profile observations on the German Weather Service's NWP system, Arbeitsergebnisse Nr. 56, Geschäftsbereich Forschung und Entwicklung, DWD, Offenbach. ISSN 1430-0281.
- European Space Agency, 1996: Atmospheric Dynamics Mission, *ESA SP-1196 (4)*.
- European Space Agency, 1998: The Science and Research Elements of ESA's Living Planet Programme, *ESA SP-1227*, 105p.
- Flesia, C., and C.L. Korb, 1999: Theory of the Double-edge molecular technique for Doppler Lidar wind measurement, *Appl. Opt.*, 38, 432-440.
- Garnier, A., and M.L. Chanin, , 1992: Description of a Doppler Rayleigh lidar for measuring winds in the middle atmosphere, *Appl. Phys.*, B55, 35-40.
- Hello, G., F. Lalaurette and J. N. Thépaut, 1999: Combined use of sensitivity information and observations to improve meteorological forecasts: the "Christmas storm" case, Accepted in *Quart. J. Roy. Meteor. Soc.*
- Hollingsworth, A. and P. Lönnberg, 1987: The statistical structure of short-range forecast errors as determined from radiosonde data. Part I: The wind field. Part II: The covariance of height and wind error, *Tellus*, 38A, 111-136 and 137-161.
- Hoskins, B. J., and P. J. Valdes, 1990: On the existence of storm tracks, *J. Atmos. Sci.* 47, 1854-1864.
- Hoskins, B. J., I. Draghici, and H. C. Davies, 1978: A new look at the ω -equation, *Quart. J. Roy. Meteor. Soc.*, 104, 31-38.

Ingmann, P., L. Isaksen, A. Stoffelen and G.-J. Marseille, 1999: On the Needs, Requirements and Feasibility of a Space-borne Wind Profiler, Proc. of 'Fourth International Winds Workshop', Eumetsat, *EUMP 24*, 199-206.

Källberg, P., and S. Uppala, 1999: Impact of Cloud Motion Winds in the ECMWF ERA15 Reanalysis, Proc. of 'Fourth International Winds Workshop', Eumetsat, *EUM P 24*, 109-116.

Kelly, G.A., 1997: Influence of observations on the Operational ECMWF System, *WMO Bulletin*, 46, 336-342.

Kelly, G.A., M. Tomassini and M. Matricardi, 1996: Meteosat cloud-cleared radiances for use in three/four dimensional variational data assimilation, Proc. 'Third International Winds Workshop', Eumetsat, *EUMP 18*, 105-116.

Lorenc, A.C., 1986: Analysis methods for numerical weather prediction, *Quart. J. Roy. Meteor. Soc.*, 112, 1177-1194.

Lorenc, A.C., R.J. Graham, I. Dharssi, B. Macpherson, N.B. Ingleby and R.W. Lunn, 1992: Preparation for the use of Doppler wind lidar information in meteorological assimilation systems; *ESA-CR(P)-3454*.

McNally, A.P. and M. Vesperini, 1995: Variational analysis of humidity information from TOVS radiometer, *Eumetsat/ECMWF Fellowship Programme, Research Report No. 1*, ECMWF.

Meteorological Society of Japan, 1997: Special issue of the Journal of the Meteorological Society of Japan documenting the symposium on data assimilation in meteorology and oceanography (Tokyo - 13-17 March 1997). *J. Meteor. Soc. Japan*, 75, No 1B, 111-496.

Peuch, A., J.N. Thépaut and J. Pailleux, 1999: An OSSE using TOVS total ozone data. Proc. 'SODA Workshop on Chemical Data Assimilation', *KNMI TR-189*.

Rabier, F., J.N. Thépaut and P. Courtier, 1998a: Extended assimilation and forecast experiments with a four-dimensional variational assimilation system, *Quart. J. Roy. Meteor. Soc.*, 124, 1861-1887.

Rabier, F., A. McNally, E. Anderson, P. Courtier, P. Uden, J. Eyre, A. Hollingsworth and F. Bouttier, 1998b: The ECMWF implementation of three-dimensional variational assimilation (3D-Var). II: Structure functions. *Quart. J. Roy. Meteor. Soc.*, 124, 1809-1829.

Räisänen, J., 1998: CMIP2 subproject climate change in northern Europe - Plans and first results. Proceedings of 'CMIP Project Workshop', Melbourne, Australia, 14-15 October, 1998.

Rees, D. et al., 1996: The Doppler wind and temperature system of the ALOMAR lidar, *J. Atmos. Terr. Phys.*, 58, 1827-1842.

Stoffelen, A., 1998: Scatterometry, Thesis Utrecht University, ISBN 90-393-1708-9.

Stoffelen, A. and G.J. Marseille, 1998: Study on the utility of doppler wind lidar data for numerical weather prediction and climate, *ESA CR(P)-4198*.

Stoffelen, A., and G.J. Marseille, 1999: Performance analysis of a DWL for the ADM, Project report for LIPAS, ESA Contract No. 3-9132/97.

Stoffelen, A. and H. Eskes (Eds.), 1999: Proceedings of SODA Workshop on Chemical Data Assimilation, *KNMI TR-189*.

Vaughan, M. and D. Willetts, 1998: Influence of atmospheric turbulence, shear, aerosols stratification and cloud motion on space Doppler wind lidar signals, ESTEC Contract No. 12006/96/NL/CN.

Vaughan, M., P. Flamant and C. Flesia, 1999: Scientific concept trade-off, ESA Contract No. 12510/97/NL/RE.

Winker, G.D. and D.M. Emmitt, 1998: Relevance of cloud statistics derived from LITE data to future Doppler wind lidars, Proc. '9th Conference on Coherent Laser Radar', 23-27 June 1997. Linköping, Sweden, p 144-147.

World Meteorological Organisation 1995: Plan for the Global Climate Observing System (GCOS), Version 1, *WMO/TD-No. 681*.

World Meteorological Organisation, 1996: Guide to Meteorological Instruments and Methods of Observation, 6th edition, *WMO-No.8*, Secretariat of the World Meteorological Organisation, Geneva, Switzerland.

World Meteorological Organisation, 1997: Impact of various observing systems on numerical weather prediction. Proceedings of the 'CGC/WMO Workshop' held in Geneva, 7-9 April 1997 (Ed.: J. Pailleux). *WWW Technical Report No 18. WMO/TD No. 868*.

World Meteorological Organisation, 1998: Preliminary Statement of Guidance Regarding How Well Satellite Capabilities Meet WMO User Requirements in Several Application Areas. WMO Satellite Reports SAT-21. *WMO/TD No 913*.

Glossary

ADM	Atmospheric Dynamics Mission
ADMAG	ADM Advisory Group
ADM-FF	ADM Free Flyer
AIREP	WMO Code for Aircraft Report
AIU	AOCS Interface Unit
ALADIN	Atmospheric Laser Doppler Instrument
AOCS	Attitude and Orbit Control System
ARPEGE	Action de Recherche Petite Echelle Grande Echelle (French climate model)
ASH	Acquisition and Safe Hold
ATLID	Atmospheric Lidar
ATOVS	Advanced TOVS
CCD	Charged-coupled Device
CDAE	Command and Data Acquisition Element
CDMS	Control and Data Management System
CDR	Critical Design Review
CEOS	Committee on Earth Observing Satellites
CFRP	Carbon Fibre Reinforced Plastic
CLIVAR	Programme on Climate Variability
CMW	Cloud Motion Wind
COG	Centre of Gravity
CW	Continuous Wave
DE	Double Edge
DOD	Depth of Discharge
DWD	Deutscher Wetterdienst
DWL	Doppler Wind Lidar
ECMWF	European Centre for Medium-range Weather Forecasts
EM	Engineering Model
EMC	Electro-magnetic Compatibility
ENSO	El Niño Southern Oscillation
EPS	Electrical Power Sub-system
ERA	ECMWF Re-analysis
ERS	European Remote-sensing Satellite
ESA	European Space Agency
ESOC	European Space Operations Centre
ETB	Engineering Test-bed
FAR	Flight Acceptance Review
FIRST	Far-infrared Space Telescope
FM	Flight Model
FOV	Field-of-View
FWHM	Full-Width Half-Maximum
GCOS	Global Climate Observing System


GEWEX	Global Energy and Water Cycle Experiment
GMT	Greenwich Mean Time
GNSS	Global Navigation Satellite System
GOS	Global Observing System
GPS	Global Positioning System
HLOS	Horizontal LOS
HRPT	High Resolution Picture Transmission
IASI	Infrared Atmospheric Sounding Interferometer
ISS	International Space Station
ITCZ	Inter-Tropical Convergence Zone
LEOP	Launch and Early Orbit Phase
LIDAR	Light Detection and Ranging
LITE	Lidar-In-space Technology Experiment
LOS	Line of Sight
LTAN	Local Time of Ascending Node
MAI	Manufacture, Assembly and Integration
MAIT	MAI and Test
MC	Multi-Channel
METOP	Future European meteorological polar-orbiting satellite
MLI	Multi-Level Insulation
MMS	Matra Marconi Space
MOSFET	Metal Oxide Semiconductor Field Effect Transistor
MSCE	Mission Operations and Satellite Control Element
MSLP	Mean Sea Level Pressure
NCEP	National Center for Environmental Prediction (USA)
NH	Northern Hemisphere
NOAA	National Oceanic and Atmospheric Administration
NWP	Numerical Weather Prediction
OBDH	On-board Data Handling system
ORATOS	Orbit Attitude Operations System
OSE	Observation System Experiment
OSSE	Observation System Simulation Experiment
PAE	Processing and Archiving Element
PBL	Planetary Boundary Layer
PCDU	Power Control and Distribution Unit
PDF	Probability Density Function
PDR	Preliminary Design Review
PDT	Payload Data Transmission
PDTS	PDT Sub-system
PFM	Protoflight Model
PILOT	WMO Code for Conventional Wind Sounding
PLH	Power Laser Head
PLL	Phase Locked Loop
PRF	Pulse Repetition Frequency
QC	Quality Control

RCS	Reaction Control System
RFDU	Radio Frequency Distribution Unit
RMS	Root Mean Square
Rocket	Russian Launcher
RTU	Remote Terminal Unit
SATOB	WMO Code for CMW Satellite Observation
S/C	Spacecraft
SCOS	Satellite Control Operating System
SDPC	Science Data Processing Centre
SDR	System Design Review
SH	Southern Hemisphere
SNR	Signal-to-Noise Ratio
SOIRD	S/C Operations Interface Requirements Document
SRR	System Requirement Review
SSM/I	Special Sensor Microwave / Imager
SSMM	Solid-State Mass Memory
SSPA	Solid-State Power Amplifier
STM	Structural Thermal Model
TC/TM	Telecommand and Telemetry
TEMP	WMO Code for Conventional Wind, Temperature and Humidity Sounding
TOGA	Tropical Ocean and Global Atmosphere
TOMS	Total Ozone Monitoring Spectrometer
TOVS	TIROS-N Operational Vertical Sounder
TT&C	Telemetry, Tracking and Command
UARS	Upper Atmosphere Research Satellite
UKMO	United Kingdom Meteorological Office
UTC	Universal Time Coordinated
UV	Ultra-Violet
WCRP	World Climate Research Programme
WGS	World Geodetic System
WMO	World Meteorological Organisation
WWB	Westerly Wind Burst
WWE	Westerly Wind Events
WWW	World Weather Watch
4D-Var	Four-dimensional Variational Assimilation

Acknowledgements

We are very grateful for the valuable contributions from A. Culoma, U. Kummer and R. Meynart.

Thanks are also extended to C. Readings, M.L. Reynolds and A. Tobias for their time and effort in reviewing the document, and to D. Reinprecht for preparing the document for publication.



European Space Agency
Agence spatiale européenne

Contact: ESA Publications Division
c/o ESTEC, PO Box 299, 2200 AG Noordwijk, The Netherlands
Tel. (31) 71 565 3400 - Fax (31) 71 565 5433